THE ROLE OF *PLASMODIUM FALCIPARUM* MALARIA IN ENDEMIC BURKITT'S LYMPHOMA PATHOGENESIS

A thesis submitted by

Raka-Larissa Basu

In partial fulfillment of the requirements for the degree of

Doctor of Philosophy

in

Genetics

TUFTS UNIVERSITY

Sackler School of Graduate Biomedical Sciences

August, 2016

Advisor: David Thorley Lawson

Abstract

Endemic Burkitt's lymphoma (eBL) is the most common pediatric cancer in sub-Saharan Africa. BL is a B cell germinal center (GC)-derived lymphoma that is characterized by a reciprocal chromosomal translocation involving the c-myc gene and an immunoglobulin (Ig) locus, resulting in the constitutive activation of the c-myc proto-oncogene. This translocation occurs via the action of the enzyme activation-induced cytidine deaminase (AID). The etiology of eBL has been linked to *Plasmodium* (*P.*) *falciparum* malaria and Epstein-Barr virus (EBV) co-infection. While there has been much progress in explaining the mechanisms linking EBV to lymphoma development, the role of P.*falciparum* malaria in the genesis of eBL is only beginning to be understood. It is known that malaria caused by *P.falciparum* infections has profound effects on the B cell compartment and is immunosuppressive, resulting in an increased viral burden of Epstein-Barr virus (EBV). This results in higher numbers of B cells latently infected with EBV that transit the germinal center. Recently, our laboratory demonstrated that *P.falciparum* is capable of deregulating AID expression in B cells, and this at least in part is triggered by the malarial byproduct hemozoin.

Our hypothesis is that *P.falciparum* heightens AID activity in the GC. This increases the risk of a c-myc translocation occurring in a GC cell latently infected with EBV, which prevents the cell from undergoing apoptosis, and thereby able to tolerate this translocation. This thesis examines the impact of *P.falciparum* malaria on AID expression and activity in human B cell sub-populations.

Levels of AID-induced somatic mutation were compared in c-myc of *ex vivo* human tonsil B cell subsets from a region of holoendemic malaria compared to control cells. No significant parallel was found between higher AID expression and mutation frequencies in tonsil B cell subsets from the malaria-endemic compared to non-malaria regions. *In vitro* studies however yielded novel findings. *P.falciparum* is capable of upregulating AID expression and class switch recombination activity in tonsil B cells, as determined by the measurement of IgG1 switch circle transcript levels. In addition, the *P.falciparum*-specific antigen, PfEMP1 was found to be required for optimal AID induction and the data also suggest its action is via the B cell receptor (BCR). Specific B-cell subsets were probed and the impact of *P.falciparum* on AID activity was found to be specific to the GC and memory B cell compartments. Altogether, these studies shed more light on the induction of AID by *P.falciparum* and its contribution to eBL pathogenesis. This work for the first time correlates augmented AID expression induced specifically by *P.falciparum* with increased enzymatic activity in the site of the eBL lesion and therefore an increased risk for c-myc/Ig translocations.

Acknowledgements

First and foremost, professionally, I am thankful for my supervisor David Thorley-Lawson, his scientific training, constructive editing, and for teaching me to persevere in the toughest of times. I am a much stronger person today thanks to him. My committee members, Erik Selsing, Philip Hinds and John Coffin, for being supportive and pleasant to interact with at my meetings or otherwise. My lab mates, past and present, not only for their scientific support, but also for their company and friendship. Dr. Kirk Deitsch from Weill Cornell Medical College, for taking the time to teach me about culturing *P.falciparum*. Mike Baldwin, from the Chishti lab at Sackler, for also guiding me through and sharing knowledge about culturing parasite. Allen Parmelee and Stephen Kwok of the flow cytometry facility, have not only been the most important technical resource during my time here, but also dear friends. Di Pierce, our program coordinator and the sunshine on my rainy day, always has been there with chocolate and pep talks. Finally, my classmates (the genetics girls) at Tufts, without whom, I would not have made it through my time here. Their camaraderie and sharing all the emotions with me through the ups and downs of this PhD have been enormously important.

I would like to give special thanks to my family. I am thankful for my Baba - Falguni Basu and Ma - Paramita Basu, for their unconditional support and pushing to help me succeed and never give up or get lazy! My education and the person I have become today is all because of them. My Didi, Madhurima Basu-Sajdak for being my very first friend in life, her tough love and always being by my side, all of which kept me going through this whole experience.

I am so incredibly thankful for my husband (Shami), Elton Kong. He has kept me smiling ever since the day he came into my life 8 years ago. Thanks to him for making me so happy, continually noticing the silver linings to everything in life, cooking me delicious dinners, being my biggest cheerleader, and commiserating over tough/failed (~PCR) experiments! Without him, this also would not be possible.

Finally, I dedicate this thesis to my wonderful and happy dog- Gumbo. He is a constant reminder that there is more to life than a PhD, and to always appreciate the simple things. He gives me a reason to come home, always to the most enthusiastic welcome and was a loyal companion during thesis-writing. Thank you to my sweet pup, Gum!

Table of Contents

Abstract ii

Acknowledgements iv

List of Tables x

List of Figures xi

List of Abbreviations xiii

1. Introduction 1

1.1 Burkitt's Lymphoma 1

1.1.1 Characteristics of BL, subtypes and epidemiology 1

1.1.2 eBL etiology 3

1.1.3 Chromosomal translocation in BL 4

1.2 Activation-induced cytidine deaminase (AID) 5

1.2.1 Regulation of AID activity 6

1.2.2 AID function: CSR and SHM 8

1.2.3 Targeting of AID: transcription. 9

1.2.4 AID and the c-myc translocation 10

1.3 c-myc 11

1.3.1 c-myc/IgH translocation in BL 11

1.3.2 c-myc dysregulation in eBL 11

1.3.3 Cell biologic consequences of c-myc dysregulation 13

1.4 EBV 15

1.4.1 EBV and BL 16

1.4.2 EBV and malaria 19

1.5 Malaria 20

1.5.1 *P.falciparum* malaria 20

1.5.2 PfEMP1 21

1.5.3 PfEMP1 and polyclonal B cell activation 24

1.5.4 Malaria transmission and the immune system 25

1.5.5 TLRs, TLR9 26

1.5.6 Hemozoin 27

1.5.7 Malaria and BL 27

1.6 Thesis goal and synopsis 30

1.6.1 Project Rationale 30

1.6.2 Hypothesis and thesis summary 31

2. Materials and Methods 33

2.1 Tonsils 33

2.2 Isolation of tonsillar mononuclear cells and peripheral blood mononuclear cells .. 33

2.2.1 Tonsillar mononuclear cells (MNCs) isolation 33

2.2.2 Peripheral blood mononuclear cells (PBMCs) isolation 34

2.2.3 Purification of PBMC and tonsil B cell sub-populations 34

2.2.4 Extracellular Staining for flow cytometry (MoFlo) 35

2.3 Purification of genomic DNA, PCR and sequencing 35

2.3.1 Proteinase-K digestion of isolated tonsil or PBMC B cells 35

2.3.2 PCR of c-myc exon 1 & 2, β-globin, and IgVH 36

2.3.3 Cloning of PCR products and Sequencing mutation analysis 36

2.4 Plasmodium falciparum extract stimulation assay 37

2.4.1 Maintenance of P.*falciparum* wildtype (3D7) and PfEMP1-null (DC-J) cultures, and preparation of parasite extracts 37

2.4.2 Determination of PfEMP1 expression in P.*falciparum* strains 38

2.4.3 Stimulation Assay 39

2.5 Purification of RNA, RT-PCR, and quantitative real time PCR (qRT-PCR) 40

2.5.1. RNA extraction, cDNA synthesis 40

2.5.2 qRT PCR using Taqman assays 40

2.6 Statistical Analysis 41

3. Results 42

3.1 Assessing AID-induced mutation frequency in Boston and Ghana human B cells 42

3.2 P.falciparum induces AID in human B cells in vitro potentially using PfEMP1 47

3.2.1 *P.falciparum* 3D7 strain induces AID in B cells *in vitro* 47

3.2.2 Studying PfEMP1 49

3.2.3 PfEMP1 is required for P.*falciparum* to maximally induce AID *in vitro* 51

3.3. PfEMP1 likely uses surface-Ig crosslinking to induce AID 57

3.3.1 Anti-Ig complements DC-J and CpG 57

3.4 P.falciparum-induced AID is active/ capable of class switch recombination 61

3.4.1. Is *P.falciparum*- induced AID active? 61

3.4.2 *P.falciparum* extracts targeting specific B cell subpopulations 65

3.4.3 *P.falciparum* extracts impact non-naïve B cells for AID induction 67

3.4.4 Parasite extracts cause CSR in GC and memory B cells 70

3.5. Summary of key findings 73

4. Discussion and Future Directions 74

4.1 AID-induced mutation frequency in Ghana vs. Boston do not correlate to in vivo levels of AID mRNA expression in GC B cells. 74

4.2. P.falciparum induces active AID at least in part via PfEMP1 79

4.3. P.falciparum induces active AID in the GC and memory B-cell compartments 84

5. Appendix 91

Disovering incorrect switch circle assay design- 2015 93

Chromosomal damage and/or rearrangements in P.falciparum-stimulated B cells in vitro 95

6. References 97

List of Tables

Table 1. Characteristics of BL subtypes……. 2

Table 2. Mutation analysis of AID-induced mutations……. 46

Appendix Tables

Table A1. List of extracellular antibody staining antibodies…… 91

Table A2. List of primers and PCR conditions for PCR……... 91

Table A3. List of probes or assays for qRT-PCR……. 92

List of Figures

Figure 1. Co-incidence of lymphoma belt and holoendemic malaria transmission…… 3

Figure 2. Model of AID-induced somatic hypermutation…….. 6

Figure 3. Breakpoints and mutations in c-myc/Ig translocations of eBL……. 13

Figure 4. Summary of cell biologic effects of c-myc overexpression…….. 14

Figure 5. Current model of eBL pathogenesis…….. 18

Figure 6. PfEMP1 mediates adhesion in infected RBCs…….. 22

Figure 7. Tonsil Naïve and GC B cells express AID at different levels……... 43

Figure 8. *P.falciparum* extract stimulation of AID mRNA in normal tonsil B cells…… 48

Figure 9. 3D7 and DC-J strains express or do not express PfEMP1…… 50

Figure 10. *P.falciparum* and DC-J parasite extract stimulation of AID mRNA in normal tonsil B cells…….. 52

Figure 11. Parasite extract (*P.falciparum* 3D7 and DC-J) concentration titration in stimulating AID mRNA in normal tonsil B cells……. 54

Figure 12. Overall comparison of 3D7 and DC-J extract stimulation of AID mRNA in normal tonsil B cells……. 56

Figure 13. *P.falciparum* 3D7 and DC-J parasite extract complementation by anti-Ig and stimulation of AID mRNA in normal tonsil B cells……. 58

Figure 14. *P.falciparum* strains: 3D7 and DC-J complementation by anti-Ig…….. 60

Figure 15. IgG1 switch circle assay design…….. 62

Figure 16. Parasite stimulation of AID and IgG1 switch circle mRNA in whole tonsil MNCs…… 64

Figure 17. Parasite stimulation of AID and IgG1 switch circle mRNA in naïve B cells. 66

Figure 18. Extracellular staining MoFlo purity check of CD10/CD27 positive selection…….68

Figure 19. Parasite stimulation of AID and IgG1 switch circle mRNA in naïve and GC/memory B cells……... 69

Figure 20. Extracellular staining MoFlo purity check of separate CD10 and CD27 positive selection……71

Figure 21. *P.falciparum* extract stimulation of AID and IgG1 switch circle mRNA in whole tonsil MNCs, GC, or memory B cells……72

Figure 22. AID mRNA expression in GC B cells from malaria-endemic region (Ghana) and non-malaria region (Boston)…….. 75

Figure 23. Overall AID mRNA expression in Boston and Ghana tonsil GC B cells……75

Figure 24. Model: How *P.falciparum* increases the risk of eBL……...90

Appendix Figures

Figure A1. IgM transcript expression in Boston PBMC and tonsil B cells……...94

Figure A2. Karyotype of Giemsa-stained RAJI cells……96

List of Abbreviations

AID	Activation induced cytidine deaminase
APOBEC	Apoliprotein B mRNA editing enzyme, catalytic peptide like
BCR	B cell receptor
BIM	Bcl-2-like protein II, Bcl-2-like interacting mediator of apoptosis
BL	Burkitt's lymphoma
bp	Base pair
CD40L	Cluster of differentiation 40 ligand
CFSE	Carboxyfluoorescien diacetate succinimidyl ester
CIDRI-α	Cysteine interdomain region-1α
CQ	Chloroquine
CSR	Class switch recombination
DSB	Double stranded break
eBL	Endemic Burkitt's lymphoma
EBNA	EBV encoded nuclear antigen
EBV	Epstein-Barr virus
GC	Germinal center
HIV-BL	HIV-related Burkitt's lymphoma
Ig	Immunoglobulin
IL4	Interleukin 4
MNC	Mononuclear cell

MyD88	Myeloid differentiation factor 88
NFκB	Nuclear factor kappa-light-chain enhancer of activated B cells
PBMC	Peripheral blood mononuclear cell
P.falciparum	*Plasmodium falciparum*
PfEMP1	*Plasmodium falciparum* erythrocyte membrane protein 1
PKA	Protein kinase A
PolII	RNA Polymerase II
RBC	Red blood cell
RPA	Replication Protein-A
SHM	Somatic hypermutation
SBL	Sporadic Burkitt's lymphoma
ssDNA	Single stranded DNA
TGF-β	Transforming growth factor-beta
TLR	Toll-like receptor
UNG	Uracil-DNA glycosylase

1. Introduction

1.1 Burkitt's Lymphoma

1.1.1 Characteristics of BL, subtypes and epidemiology

Burkitt's lymphoma (BL) is a rapidly proliferating B cell tumor characterized by a translocation of the c-myc oncogene to an Ig locus, resulting in deregulation of c-myc. There are three subtypes of BL: endemic (eBL), sporadic (sBL) and HIV-associated (HIV-BL). *Table 1* presents an overview of the characteristics of all three subtypes of BL. In short, sBL is predominantly found in the US and Europe primarily in teenagers and young adults; HIV-BL is found globally in HIV+ individuals; finally, eBL is found in tropical zones where malaria is holoendemic, almost exclusively in children, and almost always infected with EBV. BL often presents itself in the jaw in the endemic form (Burkitt, 1958; Burkitt, 1972), and the rapid proliferative index (ki67 score > 95%, associated with a cell doubling time of 24 hours) quickly leads to tumors that are fatal within 6 months if untreated (Chene et al., 2009). BL is the most prevalent childhood cancer in equatorial Africa, accounting for 74% of all pediatric cancers (Parkin et al., 2014) (Morrow, 1985).

	eBL	**sBL**	**HIV-BL**
Incidence	1-20/100,000	0.01/100,000	Variable
Geography affected	Equatorial Africa, Papua New Guinea	United States, Europe	Worldwide
Cofactors	EBV, malaria	Unknown	HIV infection
EBV found in tumors	>95%	<20%	~30%
Ig breakpoint locus	VDJ region	Switch regions	Switch regions
Age range	2-16 years	All ages	All ages

Table 1. Characteristics of BL subtypes. Adapted from (Rochford et al., 2005; Thorley-Lawson and Allday, 2008).

Epidemiological evidence points strongly to the etiology of eBL being closely linked to EBV, and *P.falciparum* malaria co-infection. eBL occurs predominantly in the equatorial region of Africa ('lymphoma belt') which closely matches the distribution of holoendemic malaria (Morrow, 1985) (*see Figure 1*). Almost 100% of BL in sub-Saharan Africa carries EBV and the tumor cells are latently infected, carrying the viral genome as a clonal extra-chromosomal episome (Magrath, 1990; Thorley-Lawson and Allday, 2008; Wright, 1971).

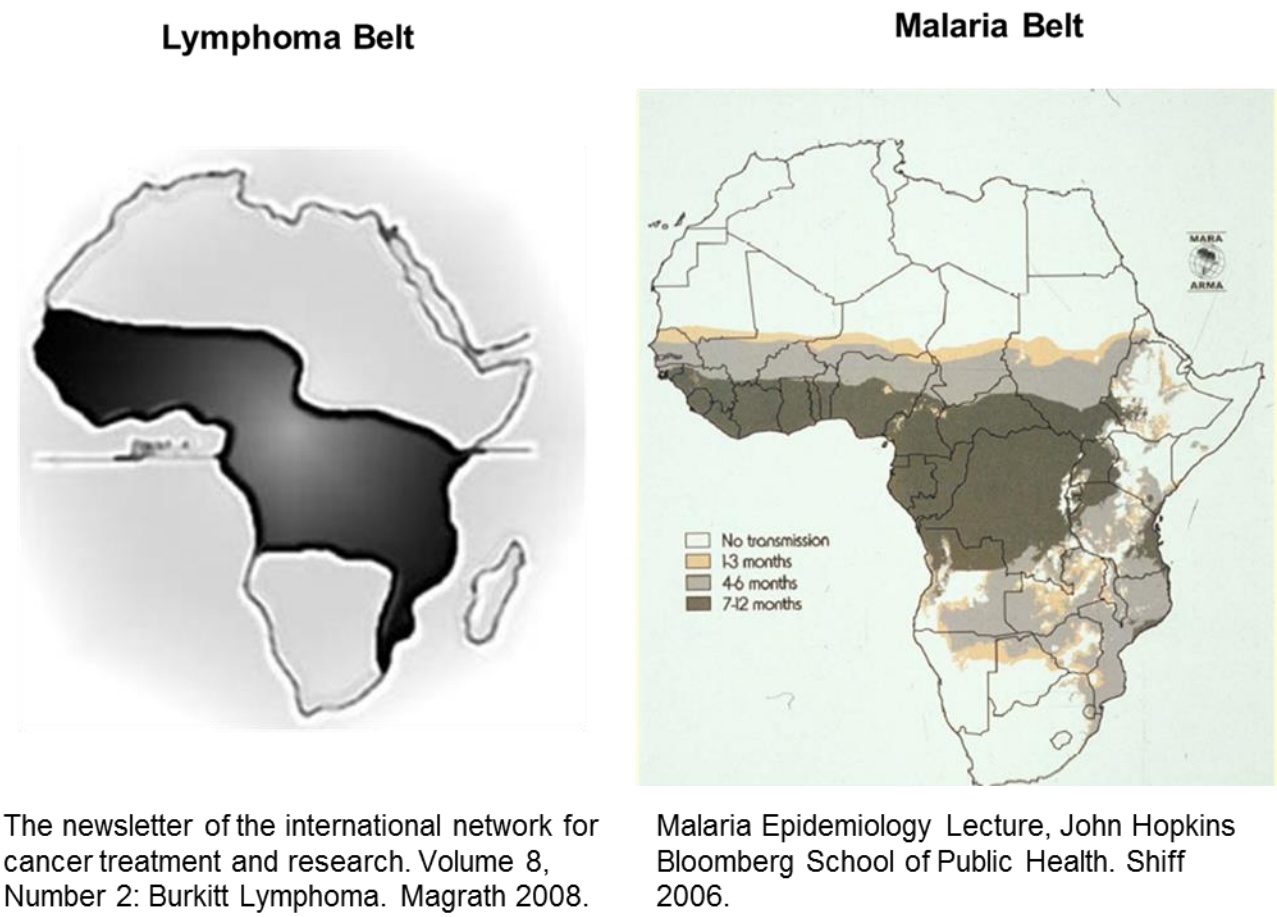

Figure 1. Co-incidence of lymphoma/BL belt and the malaria endemic regions of Africa. BL is mostly found in the lymphoma belt of sub-Saharan Africa (left panel), which also coincides with the hyperendemic and holoendemic malaria region of Africa (right panel).

1.1.2 eBL etiology

The endemic form of BL was first clinically described in 1958 by Denis Burkitt while working in Uganda (Burkitt, 1972). Soon after, Burkitt and his colleagues underwent a 16,000 km research travel expedition referred to as the 'lymphoma safari', during which they assessed the geographical distribution and the incidence of BL. They found that the presence of eBL was closely correlated with the same temperature and rainfall zones as malaria (Burkitt, 1962). Since then, the striking association with malaria has been

confirmed in multiple studies. In the lowlands of Kenya, there is a high transmission of malaria and lymphomas, whereas the children of the same ethnic group living in urban areas or the highlands have a much lower incidence of malaria and lymphoma (Omukunda et al., 2013). This original link between eBL and malaria suggested the occurrence of lymphoma to be linked with an infectious agent carried by mosquitoes. Soon after however, EBV was discovered in cultures of the tumor (Epstein et al., 1964). Since then, EBV has been found in virtually every eBL tumor, although the transforming proteins are not expressed in these tumors.

1.1.3 Chromosomal translocation in BL

Subsequently after the discovery of EBV in BL tumors, it was shown that the consistent molecular hallmark is a chromosomal translocation involving c-myc and one of the Ig loci, juxtaposing the c-myc oncogene downstream of Ig enhancer elements, resulting in its constitutive activation and uncontrolled growth of the cell. The c-myc translocation that characterizes all BL is facilitated by the DNA mutating enzyme AID (Ramiro et al., 2004). AID is almost exclusively expressed in GC cells undergoing SHM and/or CSR. Thus, B cells undergoing the GC reaction are most likely the progenitor cells for BL (Thorley-Lawson and Allday, 2008). The breakpoints in the t(8;14) chromosomal translocation for c-myc differs between the BL subtypes, which has led to the suggestion that perhaps different mechanisms might account for the different subtypes of BL (*see Figure 3*). Somatic hypermutation (SHM), class switch recombination (CSR) and V(D)J recombination have all been proposed as possible mechanisms which might produce the

c-myc/Ig translocation. (*Discussed in more detail in AID and c-myc subsections of this introduction*).

Although it has been well established that malaria and EBV are cofactors of eBL, the most current knowledge of which is described in depth below, the precise mechanisms of the combined effect is yet to be fully understood.

1.2 Activation-induced cytidine deaminase (AID)

AID is a 24kDa member of the APOBEC family of DNA mutators (Conticello, 2008; Muramatsu et al., 1999). AID is primarily expressed in GC B cells and is the key deaminating enzyme for antigen-dependent antibody diversification through SHM and CSR. AID mutant mice and humans with deficiencies in functional AID show profound defects in SHM and CSR and suffer from hyper-IgM syndrome (Muramatsu et al., 2000). AID deaminates cytidine residues in single-stranded DNA (ssDNA) thereby generating uracil:guanine mismatches in the target DNA. The uracil can be processed in various ways: DNA replication produces C-> T transition mutations, whereas base excision or mismatch repair (via DNA repair molecules UNG or MSH2, respectively) of uracil lesions generates point mutations in SHM or double stranded breaks in CSR (*see Figure 2*). Induction of AID is possible through CD40 engagement and stimulation through IL4 (Muramatsu et al., 1999). Expression of AID in GC cells is further enhanced by signals provided through the B cell receptor (BCR) and Toll like receptor 9 (TLR9) (Bernasconi et al., 2003). AID expression, B cell proliferation and CSR are also induced and/or enhanced by CpG DNA which activates the TLR9 pathway (He et al., 2004). It is highly likely that *in vivo* there is collaboration between the signal transduction pathways of the

TLRs with pathways activated in B cells by the host immune system (CD40-ligand (CD40L) and IL4), that will induce optimal AID expression to generate a robust immune response (Xu et al., 2007).

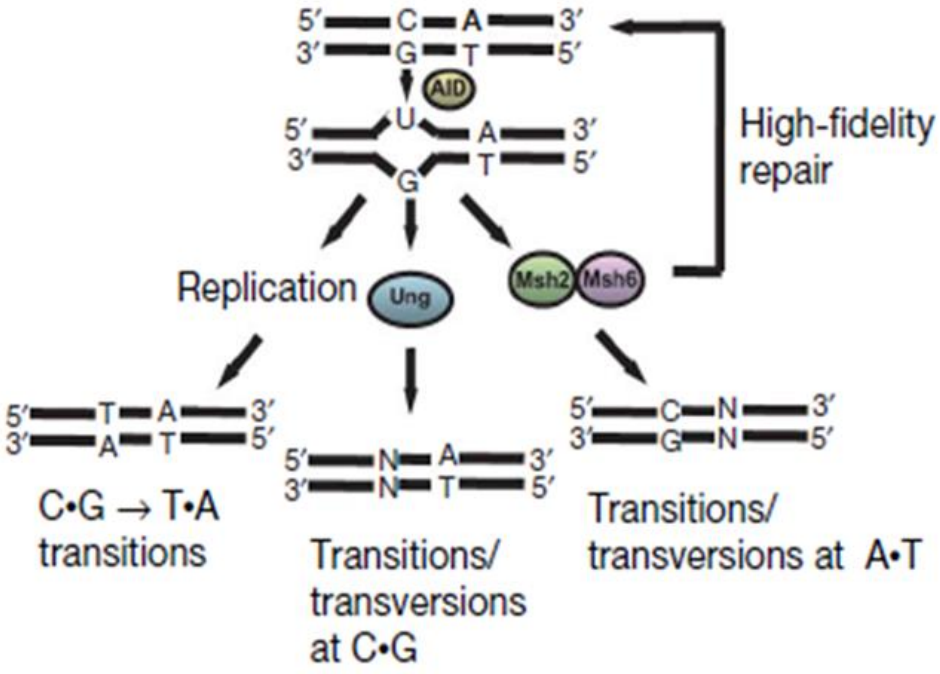

Figure 2. Model of AID-induced somatic hypermutation. Adapted from (Liu et al., 2008).

1.2.1 Regulation of AID activity

Given its targeting of genomic DNA, there are several layers of tight regulation on AID activity. At the transcriptional level, AID is induced in B cells during the GC reaction after helper T-cell mediated stimulation of B cells through CD40L and IL4 or transforming growth factor-beta (TGFβ) (Muramatsu et al., 2000). These signals induce

the transcription factors nuclear factor kappa-light-chain enhancer of activated B cells (NFκB), inhibitor of differentiation (Id)2, Id3, the E-protein E47, PAX5, E2A and STAT6 (Rebhandl et al., 2015). AID transcript levels are further regulated by alternative splicing, whereby only the full length AID variant is capable of mediating SHM and CSR (Wu et al., 2008).

Posttranslational modifications can also regulate AID activity. Numerous sites within the AID protein can be phosphorylated. In some cases, as with amino acid residues Serine3, Serine(S)38, Tyrosine(T)27 and T140, their substitution alters SHM and/or CSR *in vivo* (McBride et al., 2006; McBride et al., 2008). In addition to phosphorylation, proteasomal degradation by polyubiquitination is another way of regulating AID protein abundance and activity (Aoufouchi et al., 2008).

AID is also regulated on the level of subcellular localization and shuttles between the cytoplasm and the nucleus (Ito et al., 2004). AID is primarily localized to and is relatively stable in the cytoplasm. In addition, nuclear AID is efficiently polyubiquitinated and proteasomally degraded (Aoufouchi et al., 2008). This describes yet another level of regulation of AID activity by controlling its access to the nuclear compartment.

Several proteins have been identified to interact with AID in B cells and play important roles in its activity. Of particular importance are replication protein A (RPA) which is associated with transcription bubbles, interacts with phosphorylated AID, and helps AID recruitment to the Ig locus (Chaudhuri et al., 2004). Protein kinase A (PKA) is responsible for the phosphorylation of S38 of AID, and this allows interaction with RPA and therefore CSR (Basu et al., 2005). Closely tied with the transcription complex, AID

binds to RNA polymerase II and this binding is dependent on SPT5 colocalization which is predictive of AID-induced mutations (Pavri et al., 2010).

Overall AID expression is regulated in a number of ways including through transcriptional regulation, alternative splicing, posttranslational modifications, nuclear/cytoplasmic localization and interaction partners that specify targeting to specific DNA loci.

1.2.2 AID function: CSR and SHM

During affinity maturation in the GC, AID induces random mutations in the variable gene segment of Ig genes (SHM). By introducing random point mutations in Ig genes, AID increases the capacity of the antibody to bind and neutralize the cognate antigen by improving its affinity. Following several rounds of mutation by AID and positive selection, clones that express a higher-affinity antibody are equipped to leave the GC and differentiate into plasma or memory B cells(Kuppers and Dalla-Favera, 2001). DNA breaks occur during SHM in about 6% of mutated variable genes (Goossens et al., 1998). In addition, analyses of tumors reveal that Ig translocation breakpoints occur at sites undergoing SHM. For example, in eBL, the breakpoint at IGH is often within or near a mutated VDJ gene (Dorsett et al., 2007; Kuppers and Dalla-Favera, 2001).

AID actually acts broadly and can aberrantly target genes throughout the genome for SHM, including the proto-oncogene c-myc (Liu et al., 2008; Liu and Schatz, 2009). Although the frequency of mutations at non-Ig genes is much lower than at Ig genes (Liu et al., 2008), these mutations could initiate double-stranded breaks (DSBs) that ultimately lead to translocations with the Ig locus.

AID is also required for CSR which is a deletional recombination, resulting in the exchange of the initial constant region gene (IgM or IgD) with a downstream one, leading to an altered antibody effector function, but with the same antigen-binding specificity (Kuppers and Dalla-Favera, 2001). DSBs in Ig switch regions are obligate intermediates in CSR and are frequently involved in translocations found in sBL (Hecht and Aster, 2000).

During CSR, AID action at the specific switch regions of Ig heavy chain loci in activated B cells results in excision of a DNA fragment that is capable of circularization (Kinoshita et al., 2001). The circular DNA contains a DNA segment between Sμ (switch region for the μ isotype) and a target S region including its isotype (I) promoter, which is driven by specific cytokine stimulation before CSR (*Refer to Figure 14*). The specific isotype promoter in the circular DNA remains transcriptionally active and signals production of transient switch circle transcripts (Kinoshita et al., 2001). Therefore, isotype-specific switch circle transcripts can be detected and used as a marker of active AID and ongoing CSR.

1.2.3 Targeting of AID: transcription.

Transcription is an absolute requirement for CSR and SHM. Early studies revealed that mutational activity by AID was largely confined to the first 1-2kb from the transcriptional start site. It also was found that Ig genes undergo SHM at levels that correlated with transcription rates (Bachl et al., 2001). Pavri et al. identified Spt5, a RNA Polymerse II (PolII) elongation and stalling factor that associates with ssDNA and PolII, which is required for CSR. In B cells, Spt5 colocalizes with both AID and PolII at DNA surrounding the transcription initiation complex, which is the same region targeted during

SHM (Pavri et al., 2010). Together these findings led to the development of a model wherein AID is localized to the stalled PolII complex at promoter-proximal DNA at least in part by Spt5.

Chromatin immunoprecipitation sequencing (ChIP-Seq) experiments have discovered AID at thousands of loci on the B cell genome (Yamane et al., 2011). As mentioned earlier, SHM-like action by AID can produce aberrant promoter-proximal mutations at transcribed non-Ig genes. Numerous genes linked to B cell tumorigenesis, including c-myc, are mutated by AID but are normally protected from acquiring most mutations through the combined action of base excision and mismatch repair (Liu et al., 2008; Liu and Schatz, 2009).

1.2.4 AID and the c-myc translocation

In the c-myc/Ig translocation which is characteristic of BL, c-myc is directly joined to the switch region of an Ig locus, and hence, a role for AID catalyzing aberrant CSR and mediating this translocation was hypothesized. Indeed, subsequent studies revealed that c-myc/IgH translocations in IL6 transgenic mice (mouse model with the equivalent BL translocation and B cell plasmacytosis) are completely dependent on AID (Ramiro et al., 2004). These findings were corroborated by studies that showed AID-mediated translocations depend on UNG, which is required to make the DSBs, and are inhibited by tumor suppressors ATM, Nbs1, p19 and p53 (Ramiro et al., 2006). It has also been shown that AID expression levels determine the extent of c-myc oncogenic translocations, and the incidence of B cell transformation in transgenic AID +/- mice (Takizawa et al., 2008). Robbiani et al. also showed that deregulated expression of AID caused widespread genome instability, which required concomitant absence of the tumor suppressor p53 in

order to induce B cell lymphoma (Robbiani et al., 2009). It is known that p53 plays a protective role in B cell lymphomas, as consistently its gene is mutated in BL (Gaidano et al., 1991), and defects in p53 seem to provide the strongest enhancement of translocation (Ramiro et al., 2006; Shaffer et al., 2012).

1.3 c-myc

1.3.1 c-myc/IgH translocation in BL

The signature characteristic of BL is the inappropriately high activity of c-myc, a 64-kD protein belonging to the family of basic helix-loop-helix (bHLH) transcription factors (Hecht and Aster, 2000). c-myc protein levels are upregulated in BL through the chromosomal translocation (involving chromosomes 8 and 14) which results in the juxtaposition of the DNA coding sequences for c-myc with sequences from Ig gene enhancers. Because Ig gene enhancer elements are specifically active in mature B cells, their control of c-myc in BL cells drives inappropriately high and constitutive expression of c-myc (Hayday et al., 1984). In addition, negative regulatory sequences residing within c-myc are often removed as a direct consequence of chromosomal translocation or are mutated through other mechanisms, which further contributes to c-myc activity (Bhatia et al., 1993).

1.3.2 c-myc dysregulation in eBL

In BL tumors with the t(8;14), the positions of the breakpoints relative to the c-myc gene on chromosome 8 and the IgH gene on chromosome 14 correlate with the geographic origin of the patient (Pelicci et al., 1986). In eBL, the breakpoints on chromosome 8 occur up to 100kb 5’ to c-myc exon 1, whereas the breakpoints on chromosome 14 usually occur in the IgH joining regions. The IgH joining segments immediately flanking

the breakpoints usually have deletions and/or additions of base pairs that are characteristic of normal Ig V(D)J segment rearrangement (Haluska et al., 1986). This suggests that the breakpoints on chromosome 14 in eBL are created during V(D)J recombination. However, it is also very likely and speculated that the breaks near the IgH joining segments in eBL could be mediated through SHM by AID in the GC (Dorsett et al., 2007). Dorsett et al. argue that translocations occurring in eBL involving the V heavy chain (or light chain) region, occur in mature B cells expressing AID, but not RAG1/2 (enzymes required for V(D)J recombination in pre-B cells). They also contended that since translocations in the case of eBL indicate hypermutation in the Ig variable region, AID is the best candidate and hence SHM and/or CSR should be the mechanisms of interest. Robbiani et al. found that AID is required for the breaks in c-myc in mouse models of BL, suggesting that AID targets c-myc for SHM-like breaks found in eBL translocations (Robbiani et al., 2008). It has also already been shown that AID acts on c-myc, but high-fidelity repair at this locus predominates to such an extent that evidence of AID action is essentially erased, in normal circumstances (Liu et al., 2008; Liu and Schatz, 2009).

The c-myc gene consists of three exons: exons 2 and 3 encompass the coding sequence for c-myc protein, and exon 1 encodes an untranslated sequence that acts as a negative regulatory sequence (Bentley and Groudine, 1986). In eBL, chromosomal breakpoints involving c-myc preserve its normal genomic organization and transcriptional start sites, but the c-myc regulatory regions within exon 1 and intron 1 are frequently mutated, which results in the removal of negative regulation (Cesarman et al., 1987) (*see Figure*

3). This data advocate that abrogation of negative regulatory elements cooperates with positive regulatory Ig enhancer elements to drive c-myc expression in BL.

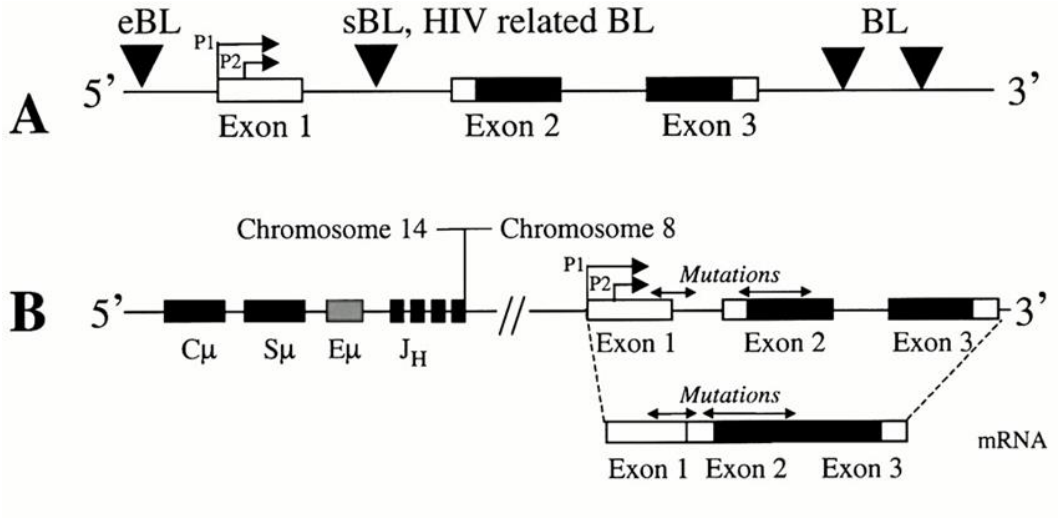

Figure 3. Position of c-myc/Ig breakpoints and mutations in (e)BL. Adapted from (Hecht and Aster, 2000).

1.3.3 Cell biologic consequences of c-myc dysregulation

c-myc is a sequence specific DNA binding transcription factor responsible for directly or indirectly regulating approximately 15% of all genes (Dang et al., 2006). The genes regulated by c-myc include those responsible for cell differentiation, proliferation, metabolism and apoptosis, all of which are potentially important in cellular transformation (Hecht and Aster, 2000) (*see Figure 4*). These pleiotropic effects are mediated through the binding of c-myc heterodimers to the promoter elements of a distinct set of downstream genes, thereby inducing or repressing their expression.

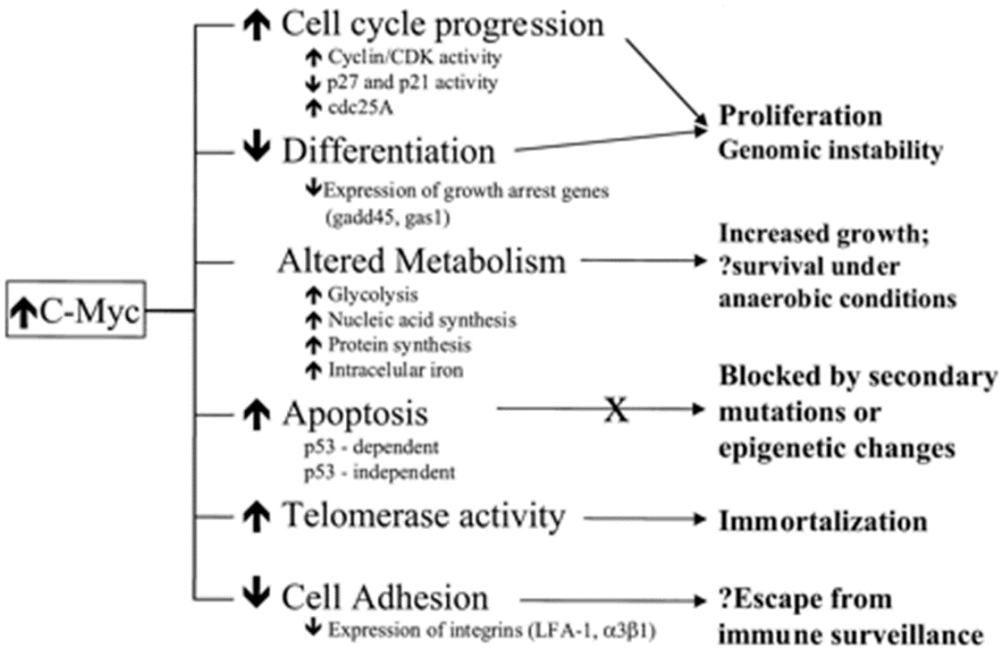

Figure 4. Summary of cell biologic effects of c-myc overexpression. (Hecht and Aster, 2000)

c-myc is expressed in all dividing cells where it enhances cell cycle progression, and is downregulated in cells undergoing cell cycle arrest or terminal differentiation (Marcu et al., 1992). In c-myc knockout fibroblasts, there is a profound reduction in cyclin D1/CDK4 and cyclin D1/CDK6. Other potential targets include the cell cycle inhibitors p27 and p21 which are downregulated by c-myc overexpression (Marcu et al., 1992). As a mechanism to prevent unscheduled cell division, the potent proliferative activity of c-myc is counterbalanced by pathways that lead to apoptosis (Harrington et al., 1994). The p-53 dependent c-myc-induced cell death pathway is triggered at least in part by ARF, a c-myc inducible gene encoding a protein that upregulates p53 expression (Eischen et al., 1999). C-myc overexpression in primary mouse embryo fibroblast cell lines is characterized by frequent spontaneous inactivation of the ARF-p53 pathway, which is consistent with its role in programmed cell death of cells with inappropriately

high c-myc expression (Zindy et al., 1998). Spontaneous inactivation of the ARF-p53 pathway is indeed frequently found in tumors arising in Eμ-Myc transgenic mice (Eischen et al., 1999). A p53-independent pathway to c-myc-induced apoptosis also exists that involves inactivation of pro-survival protein BCL2 by Bcl-2-like protein 11 (BIM) (Bissonnette et al., 1992). Murine models demonstrate BCL2 synergy with c-myc in induction of aggressive lymphomas.

1.4 EBV

EBV is a ubiquitous gamma-herpes virus that infects and persists in 95% of the adult population world-wide(Magrath, 2012). Primary infection generally occurs at an early age and is principally asymptomatic. Infectious mononucleosis may develop if infection occurs during adolescence or later. African children are infected early in life and most have sero-converted by 3 years of age, whereas in affluent countries primary infection is usually delayed until adolescence. EBV establishes a life-long persistent infection characterized by small numbers of latently infected memory B cells in the circulation and chronic lytic reactivation and viral shedding into saliva for transmission (Babcock et al., 1998; Thorley-Lawson and Allday, 2008). In culture, EBV is a very potent B cell transforming virus, activating and driving the infected B cells to be an immortalized and latently infected cell line (lymphoblastic cell line: 'LCL').

EBV is transmitted in saliva and infects B cells of the lymphoepithelium. Thorley-Lawson et al. have established the 'GC model' of EBV persistence. According to this model, EBV exploits the normal steps of B cell differentiation to establish and maintain persistent infection in resting memory B cells (Babcock et al., 1998; Thorley-Lawson,

2001). Approximately 80 proteins are encoded by the viral genome, and EBV uses four unique latency transcription programs at each stage of its B cell differentiation route, individually expressing a different set of viral antigens. (Babcock and Thorley-Lawson, 2000; Thorley-Lawson and Allday, 2008). The virus infects naïve B cells and drives them to become activated lymphoblasts using the 'growth transcription program'. This cell will then migrate into the follicle, initiate a GC reaction and establish the 'default transcription program'. The default program provides survival signals that allow the cell to exit the GC as a resting memory B cell, which then begins the 'latency transcription program'. Latently infected memory B cells during this program enter the periphery and shut down the expression of all the viral proteins, thereby avoiding detection and elimination by T cells. These cells express the tethering protein EBV nuclear antigen 1 (EBNA1) when they divide as part of homeostasis (Hochberg et al., 2004)

1.4.1 EBV and BL

The discovery of EBV in cultures of the tumor (Epstein et al., 1964) revealed that perhaps EBV is implicated in BL pathogenesis. There is also strong epidemiological evidence that EBV is involved in the pathogenesis of eBL as almost 100% of eBL tumors are EBV-positive (Magrath, 2012). Furthermore, children infected early in life who produced the highest antibody titres to EBV were found to be at the highest risk for developing the tumor (de-The et al., 1978). Notably, only cycling memory B cells express the EBV latent gene EBNA1 (Hochberg et al., 2004) which matches the gene expression pattern of BL tumor cells, which also only express EBNA1 while all other latent genes are switched off (Rowe et al., 1987).

Lytic replication and the production of infectious virus occurs when memory B cells undergo terminal differentiation into plasma cells. Life-long monitoring of the viral carrier state is dominated by CD8+ cytotoxic T lymphocytes (CTL) responses to both latent and lytic viral proteins (Khanna and Burrows, 2000). Loss of EBV-specific CTL responses is associated with an increased risk of EBV-associated lymphoproliferative disorders, pointing at a crucial role for CTL control of EBV infection (Khanna and Burrows, 2000).

During the growth transcription program, EBNA2 turns on a range of cellular activation associated genes including the proto-oncogene c-myc, which drives proliferation of the EBV-infected cells (Thorley-Lawson, 2001). Normally, deregulation of c-myc expression, as is found in eBL, would lead to apoptotic death of the cell. Through one mechanism, c-myc activates a p53-independent pathway to apoptosis that involves BIM. However, exposure to the EBV latent proteins expressed prior to entry in the GC during the growth transcription program (Paschos et al., 2012; Thorley-Lawson and Gross, 2004), and viral genes expressed in the GC (Vereide et al., 2014; Westhoff Smith and Sugden, 2013), can provide resistance to this apoptosis. Specifically, certain EBV latent proteins (EBNA3A and EBNA3C) are involved in epigenetically repressing the pro-apoptotic protein BIM (Anderton et al., 2008). This means that unlike other GC B cells, EBV-infected B cells have the ability to protect cells with the c-myc translocation from apoptosis. (Thorley-Lawson and Allday, 2008). *Figure 5* summarizes the current model of Burkitt's lymphoma pathogenesis.

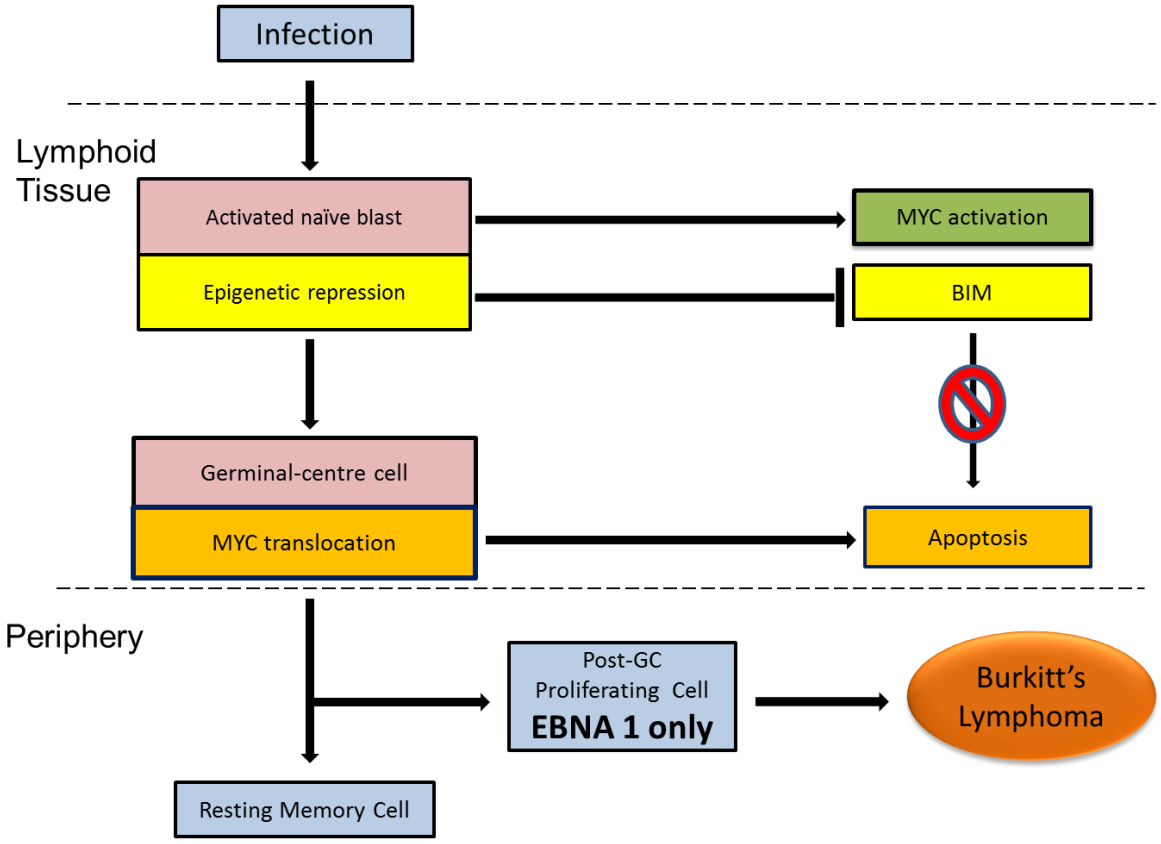

Figure 5. Current model of eBL pathogenesis. Adapted from (Thorley-Lawson and Allday, 2008).

In our lab's proposed model of EBV's role in BL:

a. When a naïve B cell is newly infected with EBV in the tonsil, it (EBNA2) will activate MYC to drive proliferation of these blasts.

b. At this time, EBV expresses certain proteins (EBNA3A and EBNA3C) which will induce the epigenetic repression of BIM, which as described earlier, normally mediates the apoptosis pathway to counterbalance MYC activation

c. The cell enters the GC with a repressed BIM and this is where the c-myc/Ig translocation occurs via AID

d. A GC B cell carrying the c-myc/Ig translocation which should have gone through apoptosis, evades this process due to the earlier repression of BIM

e. EBV infected B cells attempt to follow their normal GC B cell differentiation route to become memory B cells, but since these cells have the c-myc translocation, they continue to proliferate and express EBNA1. (So the notion is that BL is a GC cell that has left the follicle and is on its way to memory, but can't because it continues to proliferate driven by c-myc).

f. These continuously proliferating post-GC B cells are the BL tumor seeding cells.

Therefore, in our laboratory's model, EBV is not directly causing BL, but rather protects cells with a c-myc/Ig translocation from c-myc induced apoptosis.

1.4.2 EBV and malaria

P.falciparum is known to have immunosuppressive effects (Urban and Roberts, 2003). It also has been shown that acute malaria impairs the T-cell control of EBV leading to augmented numbers of circulating EBV-carrying B cells (Whittle et al., 1984). Quantification of EBV DNA in patients with acute malaria infection indicates increased viral burdens are a common feature during malaria infection (Chene et al., 2009). It has not only been demonstrated that specifically children living in malaria-endemic areas have high levels of EBV DNA in serum (Rasti et al., 2005), but also that children living in two areas with different malaria transmission intensities show a correlation between viral load and the endemicity of malaria (Moormann et al., 2005). It has additionally been shown that anti-malaria treatment leads to reduction of circulating plasma EB viral load, with the highest levels found in children with eBL (Donati et al., 2006a).

More recently, a study showed an age-related loss of T-cell responses to lytic and latent EBV antigens in children living in holoendemic malaria areas (Moormann et al., 2007).

Concurrently, it was demonstrated that during acute malaria infection, there is a concomitant increase in viral load and presence of antibodies against lytic promotors of EBV (indicative of amplified viral replication) (Rasti et al., 2005).

Torgbor et al. most recently revealed that the increased EBV load caused by malaria surges the throughput of latently infected B cells through the GC (Torgbor et al., 2014). By this logic, in the course of eBL development, the increased EBV load entering the GC caused by malaria, increases the number of cells able to tolerate the c-myc translocation produced during the GC reaction.

1.5 Malaria

Each year ~600 million people worldwide are infected with malaria parasites. The protozoan parasites of the genus *Plasmodium* (of which there are 5 species) cause malaria infection. 100% of all residents in an endemic area are periodically re-infected by *Plasmodium* parasites (Hafalla et al., 2011). Holoendemic areas are characterized by a stable transmission where infection occurs all year long and mortality is highest in the first two years of life, and infection prevalence is greater than or equal to 70% (Magrath, 2012).

1.5.1 *P.falciparum* malaria

P.falciparum causes the most severe clinical malaria and is the cause of the greatest number of malarial deaths, 1-3 million a year, primarily in young African children. *P.falciparum* is transmitted by a female Anopheles mosquito and replicates within the circulating erythrocytes of an infected individual. An encounter with malaria begins after

an infected mosquito takes a blood meal, the infective stages of the parasite are released into the circulation and migrate to the liver to infect and divide in hepatocytes. Infected hepatocytes burst and thousands of merozoites are released into the bloodstream and invade erythrocytes. The parasite develops and divides inside the erythrocyte during a 48 hour asexual lifecycle called erythrocytic schizogony, and upon rupture will release parasites that can start a new infection cycle and invade more erythrocytes. Otherwise, merozoites will differentiate into male and female gametes which can be ingested by a mosquito during a blood meal (Chene et al., 2009).

During intra-erythrocytic growth, several *P.falciparum* parasite-derived proteins are expressed, exported and then presented at the surface of the human red blood cell, the most dominant of which is *P.falciparum* erythrocyte membrane protein 1 (PfEMP1) (Chene et al., 2009).

1.5.2 PfEMP1

PfEMP1 is an adhesin that allows mature infected erythrocytes to adhere in the micro-vasculature, sequester, and thereby avoid clearance by the spleen. PfEMP1 is also a major antigenic ligand that is recognized and cleared by the host immune response. However, PfEMP1 undergoes a process known as antigenic variation which allows evasion of the antibody response and persistent infection (Chen et al., 1998). Concurrently PfEMP1 has the ability to change the receptor recognition and the tissue tropism of the infected cell causing different manifestations of the disease. PfEMP1 enables the infected erythrocyte to engage a number of receptors including intracellular adhesion molecule I (ICAM-1), CD36, thrombospondin, vascular cell-adhesion molecule 1 (VCAM-1), CD31,

endothelial cell selectin (E-selectin), chondroitin sulphate A (CSA), hyaluronic acid and to nonimmune Igs (Chen et al., 1998; Chen et al., 2000; Pasternak and Dzikowski, 2009) (*see Figure 6*).

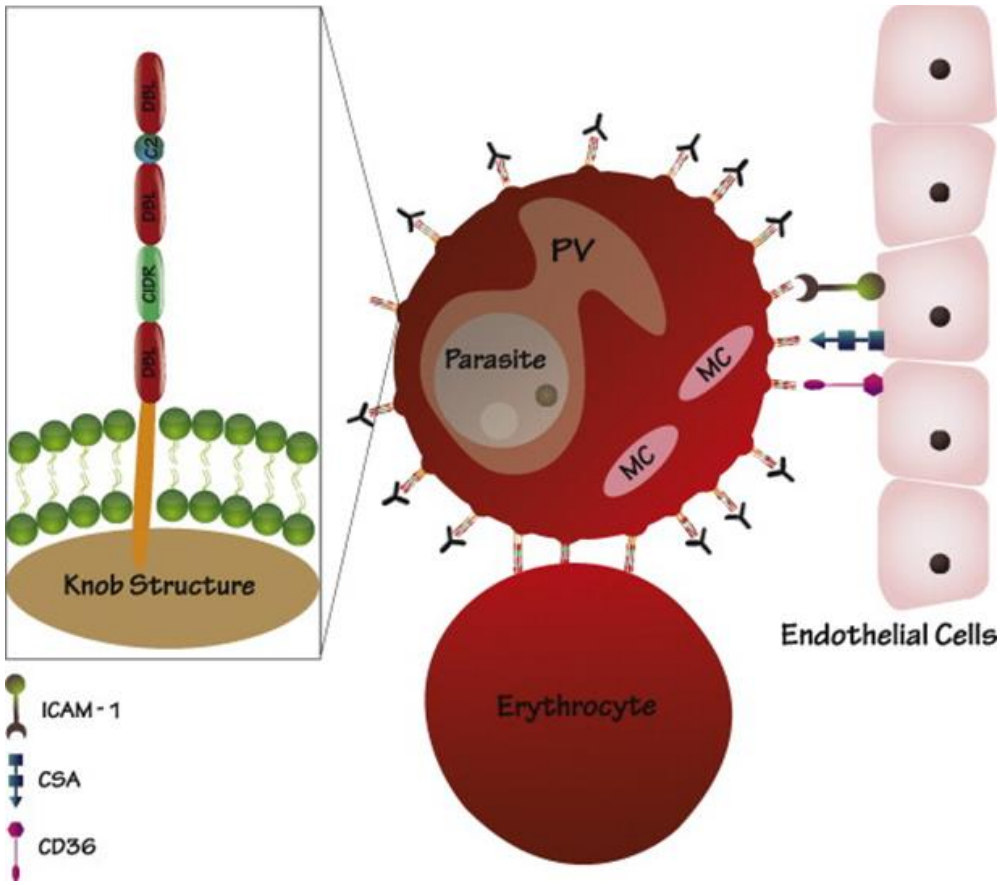

Figure 6. PfEMP1 mediates adhesion of the infected RBC. (Pasternak and Dzikowski, 2009)

PfEMP1 is a large protein, ranging in size between 200-350 kDa, encoded by a polymorphic gene family called *var* (Smith et al., 1995; Su et al., 1995). The family contains approximately 60 individual *var* genes which go through mutually exclusive expression, allowing each parasite to only express a single variant gene at a time and then

switching expression at a low rate to another *var* gene which will also be expressed in a mutually exclusive manner, thereby allowing immune evasion (Scherf et al., 1998). The single expressed *var* gene determines the antigenic, cytoadherent and virulence properties of the infected cell. Mutually exclusive expression and switching of the *var* gene appears to be tightly regulated at the transcription level in an epigenetically controlled process (Dzikowski et al., 2007). *var* gene regulation involves promoter–promoter interaction, chromatin remodeling, and sub-nuclear localization. (Chookajorn et al., 2007; Dzikowski et al., 2006; Scherf et al., 1998).

The *var* genes are composed of two exons, a conserved intron and a 5' upstream flanking sequence. Almost all PfEMP1s share some conservation in their structure, an N terminal segment (NTS); variable numbers of Duffy Binding Like domains (DBL); one or two cysteine-rich interdomain regions (CIDR); a trans-membrane (TM) domain; a C2 domain; and a conserved intra-cellular acidic terminal segment (ATS) (Chen et al., 2000). The long exon 1 of *var* genes, which codes for 2-5 DBL domains and a CIDR is exposed on the erythrocyte surface and displays considerable sequence diversity between different *var* genes. In contrast, exon 2 is an intracellular domain, which is relatively well conserved across variable *var* genes, that anchors the protein into the cytoskeleton of the host erythrocyte membrane (Pasternak and Dzikowski, 2009).

1.5.2.1 *P.falciparum* DC-J line

In order to investigate how expression of the var gene family is regulated, Dzikowski et al. produced transgenic lines of *P.falciparum* parasites in which expression of individual *var* loci could be studied. A transgenic parasite line called DC-J was selected to express a *var* gene in which the PfEMP1 coding region was replaced with blasticidin, a

chromosomally integrated drug-selectable marker, silencing all other *var* genes in the genome and effectively knocking out PfEMP1 expression (Dzikowski et al., 2006; Dzikowski et al., 2007). The DC-J line therefore with blasticidin pressure is a PfEMP1-null strain of *P.falciparum* providing an operative tool for studying PfEMP1 requirement and function.

1.5.3 PfEMP1 and polyclonal B cell activation

Polyclonal B cell activation is a prominent feature of *P.falciparum* malaria infection. It has been demonstrated that the CIDR1α is the PfEMP1 domain that binds normal nonimmune IgM (Chen et al., 2000). It has since then been shown that *P.falciparum*-infected erythrocytes adhere to and activate peripheral blood B cells from nonimmune donors (Donati et al., 2004). The infected erythrocytes interact with B cells via the CIDR1α domain of PfEMP1 which binds to CD36, PECAM-1/CD31, and to the Fab- and Fc- fragments of immunoglobulins from IgG and IgM which thereby induces proliferation and secretion of IgM (Donati et al., 2004). Donati et al. also compared the impact of CIDR1-α on the naïve and memory B cell compartments and presented that CIDR1-α preferentially activates the memory B cells. Therefore PfEMP1 serves as a polyclonal B cell activator and also plays a role in memory maintenance (Donati et al., 2006b).

Subsequently, it was shown that PfEMP1-CIDR1α sensitizes B cells to TLR9 signaling via the MyD88 adaptor molecule (Simone et al., 2011). In addition, this group validated that PfEMP1-CIDR1-α induces a persistent activation of B cells, but not directly through the BCR. Rather it acted by inducing the phosphorylation of downstream kinases such as MAPKs: ERK1/2, p38 and IKBα (Simone et al., 2011). Gene expression profiles of B

cells induced by activation by CIDR1-α and anti-Ig were also compared, revealing they were significantly different. This suggests that B cell activation, mediated by CIDR1-α is probably not only the result of the binding of CIDR1-α to surface Ig, but also due to the interaction of CIDR1-α to multiple receptors (e.g. CD31 AND CD36, which are both also expressed in human B cells) (Donati et al., 2006b).

1.5.4 Malaria transmission and the immune system

In holoendemic malaria regions of equatorial Africa, there is a stable transmission of *P.falciparum* which is characterized by recurrent exposure and repeated malaria infections throughout the year (Hafalla et al., 2011). The prevalence of the parasite in children less than 5 years of age can be as high as 90%, with a high risk of morbidity and mortality caused by *P.falciparum* infections (Bloland et al., 1999). In these same geographical regions clinical symptoms related to *P.falciparum* infections become increasingly rare with age but acquisition of protective immunity to the parasite develops slowly in children in a stepwise manner after several years of exposure (Snow et al., 2005).

Malaria severely affects the immune system, particularly B cells, as demonstrated by the presence of splenomegaly, hypergammaglobulinemia, polyclonal B cell activation, and elevated autoantibody titers (Greenwood and Vick, 1975). Only a fraction of the antibodies are specific for *Plasmodium* antigens, which is reflective of polyclonal B cell activation. Regulatory and cytotoxic T cells, γ-T cells, natural killer (NK) cells and monocytes also contribute in the immune response. In addition, cytokines play both a

protective and pathological role during *P.falciparum* infection (Perlmann and Troye-Blomberg, 2002).

It has also been shown that *P.falciparum* inhibits maturation of dendritic cells (DCs), which results in a reduction of the T-cell proliferative responses to malarial antigens. PfEMP1 is responsible for the binding of infected RBCs, via CD36 to DCs (Urban et al., 1999). Subsequently, a mouse model of *P.falciparum* confirmed that blood-stage parasites affect the maturation and alters the cytokine secretion pattern of DCs and inhibit CD8+ T cell responses (Ocana-Morgner et al., 2003).

It is likely the combined circumstance of exposure to malaria parasites, activation of the immune system, and concurrent infections by viruses (e.g. EBV) that Burkitt's lymphoma is capable of emerging at a high frequency.

1.5.5 TLRs, TLR9

Toll-like receptors (TLRs) are pattern recognition receptors that recognize a wide range of microbial motifs at the cell surface or within endosomes and trigger innate immunity. Most TLRs use the downstream adaptor molecule myeloid differentiation factor 88 (MyD88). Upon activation, MyD88 initiates signaling cascades that activate NF-κb and activator protein 1 (AP-1) which leads to inflammatory responses (Akira and Takeda, 2004). TLRs are highly expressed on antigen-presenting cells such as macrophages and DCs and promote their maturation making them involved in T- and B-cell responses. It has been reported that in human naïve B cells, most TLRs are expressed at low levels, but the expression of TLR9 is rapidly induced following BCR activation; whereas in memory B cells, TLRs are expressed at constitutively high levels (Bernasconi et al., 2003). Human memory B cells proliferate and differentiate to Ig-secreting plasma cells in

response to CpG DNA, a TLR9 agonist, while naïve B cells will only do so if concurrently triggered through the BCR (Bernasconi et al., 2003). It is important to note that BCR-antigen complexes internalize and induce TLR9, which leads to a synergistic signaling through NF-κB and MAPKs phosphorylation (Chaturvedi et al., 2008). TLRs are known to be involved in the innate immune responses to a variety of pathogens, including *Plasmodium* (Akira and Takeda, 2004). Early studies revealed that *P.falciparum* expresses a TLR9 ligand during erythrocytic schizogony (Pichyangkul et al., 2004). This TLR9 ligand was later discovered to be the malaria pigment hemozoin (Coban et al., 2005).

1.5.6 Hemozoin

Hemozoin is the crystalline pigment granule produced within the blood stage of infection as a result of hemoglobin digestion by *Plasmodium* parasite. It has been shown that hemozoin purified from *P.falciparum* activates the innate immune system mediated by TLR9 in a MyD88-dependent pathway (Coban et al., 2005). In addition, in this same study it was reported that the *P.falciparum*-induced activation of dendritic cells was inhibited by chloroquine (CQ), a common antimalarial drug. Torgbor et al. later determined that hemozoin is readily taken up by human B cells and in combination with surface-Ig crosslinking is capable of stimulating AID expression and is therefore an AID agonist (Torgbor et al., 2014).

1.5.7 Malaria and BL

As mentioned earlier, there is a strong geographic and climatic correlation between eBL and malaria infection (Burkitt, 1962). BL is mostly found in the ‘lymphoma belt’ of sub-

Saharan Africa (Wright, 1967) which also coincides with the geography of hyper- and holo-endemic malaria in Africa (Wright, 1971) (*see Figure 1*). Epidemiological analysis also reveals that in Africa where eBL cases are the highest, about 96% of malaria is caused by *P.falciparum*. There is relative protection from BL by residence in urban or highland areas where malaria transmission is lower (Morrow, 1985). The first intervention study attempting to study the role of malaria in BL was carried out through a chloroquine treatment program in Tanzania from 1977 to 1982. Following the start of the intervention, the incidence of BL began to drop rapidly (from ~ 4 in 100,000 to 0.5 in 100,000) (Geser et al., 1989). It is also important to note that there is a close correlation between age incidence of eBL and the age of acquiring maximum levels of anti-malarial Ig (Geser et al., 1989). In addition, it has been reported that children with eBL showed similar changes in lymphocyte composition just like children with *P.falciparum* malaria, i.e. a reduction in the proportion of CD3+ cells (Futagbi et al., 2007).

A widely held idea on the role of malaria in eBL is the immense impact on the immune system by malaria and resulting increased EBV load (Moormann et al., 2005; Rochford et al., 2005). Malaria is immunosuppressive for T cell responses including those targeting EBV (Donati et al., 2004; Ho et al., 1986). It is also a polyclonal activator of B cells and causes lytic reactivation of EBV in B cells in culture (Donati et al., 2004). Patients with malaria had higher levels of EBV infection compared to healthy patients (Moormann et al., 2005). However, it should be mentioned that immunosuppressed patients with high EBV loads succumb to immunoblastic lymphomas and not BL; in other words, malaria must be playing another role in the pathogenesis of eBL besides increasing EBV loads because that alone is not sufficient to cause BL (Hopwood and Crawford, 2000; Thorley-

Lawson and Allday, 2008). HIV-BL is relevant in understanding malaria-induced immunosuppression in BL. In AIDS patients immunosuppression and the resultant increase in EBV loads again leads to susceptibility to immunoblastic lymphoma and not BL. The additional cofactor in HIV infection that could lead to HIV-BL is speculated to be the chronic B cell activation associated with repeat infections, which is exactly what happens during malaria (Thorley-Lawson and Allday, 2008). As mentioned earlier, in holoendemic malaria areas, the prevalence of the parasite in children less than 5 years of age can be as high as 90%. In addition, parasitemia levels are the highest before 1 year of life which coincides with when EBV infection occurs.

Torgbor et al. have since shown *P.falciparum,* through its chronic B cell stimulation causes deregulated AID expression, while increasing the throughput of EBV-infected B cells transiting the GC (Torgbor et al., 2014). This work describes the circumstance when during *P.falciparum* infection the simultaneous increased frequency of EBV-infected B cells in the GC can provide cells with tolerance for c-myc translocations (by preventing apoptosis via BIM, as described earlier) for which there is an increased risk due to the induced higher AID expression. Another study demonstrated that intensity of malaria transmission correlated with AID expression levels in the presence of EBV in PBMCs (Wilmore et al., 2015).

Recently, Robbiani et al. utilized the *P.chabaudi* mouse model of malaria on a p53-null background, to show that repeated infections with this species of malaria parasite resulted in the accumulation of widespread DNA damage and translocations in the GC cells (Robbiani et al., 2015).

A fruitful line of investigation to follow up on recent work was therefore to determine the impact of the specific *P.falciparum*-induced deregulated AID expression on AID function (*see Results and Discussion sections*) (also see *Appendix, Figure A4*).

1.6 Thesis goal and synopsis

The goal of this work was to more clearly elucidate the role of *P.falciparum* malaria in eBL pathogenesis by studying AID function. To achieve this objective, *ex vivo* and *in vitro* experiments were carried out primarily on human tonsil B cells. The *in vitro* studies focused on AID and its activity, which was identified by the presence of transiently-expressed switch circle transcripts produced during stimulation by *P.falciparum* parasite extract in particular B cell subsets.

1.6.1 Project Rationale

Endemic BL is the most common pediatric cancer in equatorial Africa. The link between *P.falciparum* malaria and eBL has been an enigma for more than 50 years, and has remained relatively unexplained until recently. This area of research is crucial; until the exact mechanism of malaria infection in BL pathogenesis is uncovered we cannot develop a complete understanding of eBL. Demonstrating and molecularly explaining that malaria is an active agent and predisposing factor behind eBL in equatorial Africa will buttress the necessity for the control of malaria, which in turn will not only intercede with the affliction of malaria, but will prevent the number of childhood deaths caused by eBL. The potential paramount translational impact is to eradicate eBL by controlling malaria in equatorial Africa.

1.6.2 Hypothesis and thesis summary

We hypothesize that *P.falciparum* plays an important role and provides a predisposing context for eBL, by inducing an increased rate of AID activity. We have proposed that BL arises when a c-myc/Ig translocation occurs via AID activity in a cell made tolerant by EBV. Specifically, we hypothesize that the signals from the BCR and TLR9 required to activate AID in GC cells are both provided by *P.falciparum*. Our lab has recently shown that *P.falciparum* extracts can stimulate AID expression in tonsil B cells *in vitro* and individuals chronically infected with *P.falciparum* have elevated numbers of GC B cells and higher AID expression (Torgbor et al., 2014). They additionally showed that this was due, at least in part, to the action of hemozoin, a malarial byproduct and known inducer of TLR9.

Through the studies described in this thesis (*see Results and Discussion sections*), we correlated augmented AID expression induced by *P.falciparum* with increased activity, and therefore an increased risk for c-myc/Ig translocations. We also began to probe into a *P.falciparum*-specific antigen, PfEMP1 and demonstrated its requirement for optimal AID induction, which could function through the BCR. Finally, we also revealed specific B cell subpopulations that are targeted by *P.falciparum* for prompting increased AID activity. The data presented here for the first time ascertains that *P.falciparum* malaria specifically induces increased AID activity in the disease setting of BL. High AID activity in B cells stimulated with *P.falciparum* is evidence for the parasite increasing the probability for a c-myc/Ig translocation to occur in GC B cells, which could seed eBL.

2. Materials and Methods

2.1 Tonsils

Palatine tonsils were obtained from patients 14 years or younger undergoing routine tonsillectomy at Tufts Medical Center, Boston, MA ('Boston tonsils': parasite-free control samples) or Komfo Anokye Teaching Hospital, Kumasi, Ghana ('Ghana tonsils': with evidence of malaria parasite). Four Boston tonsils and three Ghana tonsils were used for sequencing and mutation analysis in this thesis work. Twenty seven Boston tonsils were used for *in vitro* stimulation assays.

Malaria tonsils (obtained between October 2008 and April 2009) were processed and tested for the presence of parasite DNA at the Kumasi Center for Collaborative Research in Tropical Medicine (KCCR), Kumasi, Ghana, stored in liquid nitrogen and shipped to Tufts University School of Medicine on dry ice.

The identical procedure and reagents were used for harvesting tonsils in Boston and Kumasi.

2.2 Isolation of tonsillar mononuclear cells and peripheral blood mononuclear cells

2.2.1 Tonsillar mononuclear cells (MNCs) isolation

Tonsil tissue was cut into small pieces in ice-cold PBSA (1X PBS + 0.5% bovine serum albumin) and then minced using a razor blade. Supernatants were pipetted through a cell strainer (0.7µM) into 50mL conical tubes. Supernatants were pelleted by centrifugation at 1,600 rpm at room temperature for 10 minutes. Pellets were resuspended and brought to 50mL with PBSA. 25mL was layered onto 20m Ficoll-paque plus (GE Healthcare Biosciences) and then spun at 2,000 rpm for 30 minutes at room temperature, without

using the brake. MNCs were collected from the resultant buffy coat using a Pasteur pipette and transferred to a new tube. After centrifugation at 1,500 rpm for 10 minutes and cell counting, cells were washed and frozen in fetal bovine serum (FBS) (Sigma) plus 10% dimethyl sulfoxide (DMSO) at 1 x 10^8 cells/mL. Cells were then aliquoted in cryovials and kept on ice for 5 minutes, followed by storage at -80°C or liquid nitrogen. Tonsil MNCs used for stimulation assays were isolated and counted as described as above followed by the method described in the stimulation assay section (2.4.3) of materials and methods.

2.2.2 Peripheral blood mononuclear cells (PBMCs) isolation

Blood samples from six (6) control donors were collected into vacutainer blood collection tubes (BD Biosciences) by venipuncture and diluted with 1x PBS at a ratio of 1:1. 20mL of diluted blood was carefully layered onto an equal volume of Ficoll-paque plus (GE Healthcare Biosciences) and spun at 2,000 rpm for 30 minutes at room temperature without using a brake. MNCs were collected from the buffy coat and transferred into a new tube. After centrifugation at 1,500 rpm for 10 minutes and cell counting, cells were washed and then frozen in fetal bovine serum (FBS) (Sigma) plus 10% dimethyl sulfoxide (DMSO) at 5 x 10^7 cells/mL. Cells were then aliquoted in cryovials and kept on ice for 5 minutes, followed by storage at -80°C or liquid nitrogen.

2.2.3 Purification of PBMC and tonsil B cell sub-populations

Tonsil MNCs or PBMCs were thawed in FBS/RPMI and spun down at 1,500 rpm for 5 minutes. Cells were resuspended in PBSA (1X PBS + 0.5% bovine serum albumin). Cells were resuspended at 5 x 10^6 cells/ 100uL PBSA for staining. A list of extracellular

staining antibody dilutions for purifying specific B cell subsets has been provided in the *Appendix, Table A1*.

2.2.4 Extracellular Staining for flow cytometry (MoFlo)

The cells are stained for the Fluorescence-Activated Cell Sorting (FACS) flow cytometry procedure (Tufts Core Facility) for either 1: isolating and sorting naïve and GC B cells for downstream PCR and mutation analysis or 2: sorting live B cells post-stimulation assay. For extracellular staining, the appropriate concentration of fluorochrome-conjugated antibody was added to cells in polypropylene tubes, vigorously mixed and incubated for 15 minutes at room temperature in the dark. (*See Appendix, Table A1,* for complete list of extracellular staining antibodies and dilutions). Cells were washed once with PBSA, vortexed, and spun down at 1,500 rpm for 5 minutes. Cells were resuspended in 300µL PBSA and stored at 4°C until FACS.

2.3 Purification of genomic DNA, PCR and sequencing

Pools of 2,000 B cells (Naïve or GC) were directly sorted into a 96-well PCR plate (Denville) using a MoFlo FACS (Cytomation). Naïve and GC B cells were isolated from Boston & Ghana tonsils, as well as from PBMCs for downstream mutation analysis. Extracellular staining (as described above) was used to separate naïve cells, which are CD10-, CD27- and IgD+, from tonsil MNCs and PBMCs. GC cells, which are CD19 + (pan B cell marker), CD10 + (GC B cell marker) were separated from tonsil MNCS.

2.3.1 Proteinase-K digestion of isolated tonsil or PBMC B cells

Pools of 2,000 cells were sorted directly in wells of a 96 well plate (Denville) already containing an enzyme mix containing Proteinase K enzyme (Roche) for cellular digestion: (0.25mg/mL Proteinase K enzyme, 10mM Tris HCL, 1.5mM $MgCl_2$). Cells

were digested in a PCR thermal cycler with the following cycling temperature program: 50°C for 120 minutes, 95°C for 20 minutes, 4°C hold. Genomic DNA of cells were stored in -20°C until further use.

2.3.2 PCR of c-myc exon 1 & 2, β-globin, and IgVH

PCR reactions were performed with Platinum Pfx polymerase (Invitrogen) (annealing temperature and cycling conditions varied depending on gene amplified; *see Appendix, Table A2*) using template DNA derived from 2,000 (GC or Naïve) B cells sorted either from tonsil MNCs or PBMCs. For the amplification of the Ig-VH regions, primers and conditions as listed in (Kuppers et al., 2013) were employed. A list of primer sets for the amplification of all other genes has been provided in the *Appendix Table A2*. PCR products were visualized and purified from a 1.5% agarose gel.

2.3.3 Cloning of PCR products and Sequencing mutation analysis

2.3.3.1 Cloning

PCR products were extracted and purified from a 1.5% agarose gel using a gel extraction kit (Qiagen). TOPO blunt-end cloning was carried out according to the manufacturer's instructions (Invitrogen). Bacterial colonies (~100 per gene analyzed) were picked and DNA was purified using a DNA miniprep kit (Qiagen). DNA preps were sent out for sequencing which was performed by the in-house Tufts Core Sequencing Facility or Genewiz (MA, USA).

2.3.3.2 Sequencing and mutation analysis

Sequencing analysis was carried out using Vector NTI software (Invitrogen) to screen for mutations against wildtype sequences (see *Appendix, Table A2* for Genbank accession numbers of all genes analyzed) and to determine a mutation rate (number of cells mutated

out of total number of cells analyzed) and frequency (number of base pairs mutated per total number of base pairs analyzed) for non-Ig and Ig genes in Boston and Ghana B cells. For Ig mutation analysis, sequences were matched and analyzed using the IgBlast tool (NCBI- NIH).

2.4 Plasmodium falciparum extract stimulation assay

2.4.1 Maintenance of P.*falciparum* wildtype (3D7) and PfEMP1-null (DC-J) cultures, and preparation of parasite extracts

A procedure for *in vitro* cultivation and maintenance of *P. falciparum* culture has been established (Jensen et al., 1979). An agreement has been made with the American Red Cross to receive blood products for our research (American Red Cross, Boston). O+ red blood cells was used to initiate and maintain the erythrocyte culture which was infected with the *P. falciparum* 3D7 or DC-J strain (kindly provided by Dr. Kirk Deitsch, Weill Cornell Medical College). 3D7 and DC-J lines were cultivated at 5% hematocrit in a complete parasite culture media: RPMI 1640 (Corning), 0.5% Albumax II (Invitrogen), 50mg/L Hypoxanthine, 25mM HEPES (Corning), 50mg/L Gentamicin (MP Biomedicals). Parasites were incubated at 37°C, in incubator chambers (Billups-Rothenberg) with an atmosphere of 5% Oxygen, 5% Carbon Dioxide, and 90% nitrogen. DC-J parasites were cultured in media containing 2µg/mL Blasiticidin S HCl (Invitrogen) to select for integration at the targeted *var* locus. The infected cultures were monitored for parasitemia by preparing blood smears and viewing under the microscope every 48 hours. The parasites were harvested from several large-scale cultures over a 2-5 month span.

Erythrocytes which were infected with parasite at a high parasitemia (> 4%) were lysed using a Saponin (Fisher) lysis solution (10% Saponin in 1X PBS). 20mL cultures were spun down at 2000rpm for 5 minutes. Supernatant was aspirated and pellet was resuspended in 2mL 1x PBS with 20 µL Saponin lysis solution added. The solution was rocked gently for 2 minutes to allow lysis of red blood cells. Lysed erythrocytes were spun down at 14,000 rpm for three minutes, followed by 2 rounds of washing with 1x PBS and centrifugation at 6,000rpm for 3 minutes. Finally, the pellet which contains the free parasite was resuspended in 100µL PBS (several suspensions were frozen together) and frozen at 80C until sonication and measurement of protein concentration. These crude parasite extracts were ultimately used for *in vitro* stimulation assays.

2.4.2 Determination of PfEMP1 expression in P.*falciparum* strains

RNA was extracted from synchronized ring stage parasites ~16 hours post invasion. RNA extraction was performed with Trizol Reagent (Invitrogen). RNA to be used for cDNA synthesis was purified on a PureLink column (Invitrogen) according to the manufacturer's protocol. Purified RNA was treated with DNAse I (Invitrogen) to degrade contaminating genomic DNA. cDNA synthesis was carried out from 800ng total RNA in a reaction volume of 40µl, with Iscript reverse transcriptase (BioRad) according to the manufacturer's instructions. For qRT PCR reactions to detect transcription from all *var* genes present in the 3D7 genome, we employed the primer set described in (Salanti et al., 2003).

2.4.3 Stimulation Assay

2.4.3.1 Isolation of B cell subsets

For a subset of experiments, specific B cells sub-populations were purified using custom-designed EasySep immunomagnetic isolation kits (StemCell Technologies) prior to the *in vitro* stimulation assay according to the manufacturer's instructions. This cell isolation procedure was used to separate populations which were CD10+/CD27+ (GC/Memory), CD10-/CD27- (Naïve) CD10 alone (GC), or CD27 alone (Memory).

2.4.3.2 Stimulation assay

Fresh tonsil MNCs were isolated as described above and resuspended at $1x10^6$ cells/mL in pre-warmed PBSA. Carboxyfluorescien diacetate, succinyl ester (CFSE) was added to to the cells at a concentration of 5µM. Several rounds of washes with at least double the volume with ice-cold complete culture media [RPMI 1640 (Corning) supplemented with 10% fetal bovine serum (Sigma), 100 IU pennicillin streptomycin (Corning), 2mM sodium pyruvate (Corning), 1µg/mL Ciprofloxacin hydrochloride (MP Biomedicals)] with centrifugation at 1,500rpm for 5 minutes was carried out. Cells were finally resuspended in fresh pre-warmed complete culture media. A final concentration of 0.25µg/mL CD40-ligand (ebiosciences), 5ng/mL IL-4 (ebiosciences), 3µM CpG (Hycult Biotechnology), 2.5µg/mL Anti-Ig (Jackson Immunoresearch), and varying concentrations (as shown) of parasite extracts were used in the stimulation. Cells were harvested on day 5 (day 4, 5 and 6 for 1^{st} set of stimulation assays), stained with CD19-APC and then B cells were sorted with the MoFlo as described above. Prior CFSE staining delineates the level of proliferation taking place in the cells and was used as a marker of cell division during sorting.

2.5 Purification of RNA, RT-PCR, and quantitative real time PCR (qRT-PCR)

2.5.1. RNA extraction, cDNA synthesis

After cell sorting, ~$2x10^5$ cells were spun down at 2,000 rpm for 5 minutes and pellet was resuspended in 500µL Trizol (Invitrogen). 100µL chloroform was added and allowed to sit at room temperature for 5 minutes before spinning at 11,500 rpm for 15 minutes at 4°C. The aqueous phase containing RNA was transferred to new centrifuge tubes and 2µL GlycoBlue (Life Technologies) was added, tubes were vortexed and allowed to sit at room temperature for 10 minutes followed by centrifugation at 11,500 rpm for 10 minutes at 4°C. Supernatant was poured off and 500µL 75% EtOH was added, followed by centrifugation at 9,200rpm for 5 minutes at room temperature. Supernatant was once again carefully poured off without losing pellet. Tubes with pellets were left to air dry for ~10 minutes before resuspending in 50µL dH_20 and measuring RNA concentration using the Nanodrop (Thermo Scientific). For the cDNA synthesis reaction, the Iscript cDNA synthesis kit was used (Biorad). A master mix was prepared which included 4µL of 5X iScript reaction mix, 1µL of reverse transcriptase, 250ng of purified RNA, plus dH_20 to make a 20µL reaction. All reactions were performed on an Applied Biosystems PCR machine (thermal cycler). The protocol was as follows: one cycle of 5 minutes at 25°C, 30 minutes at 42°C, 5 minutes at 85°C.

2.5.2 qRT PCR using Taqman assays

For real time PCR, custom Taqman (Life Technologies) probes were designed for IgG1 switch circles, while a pre-developed assay for AID and β-actin was used (see *Appendix, Table A3,* for list of primers/probes). For all real time PCR reactions, a master mix was

prepared containing 10µL IQ supermix (BioRad), 1µL of a 20X primer-probe mix (Life Technologies) and 5µL dH20. 4µL of cDNA was added to 16µL master mix with a final reaction volume of 20µL. All real time PCRs were performed in a Bio-Rad iCycler. The protocol was as follows: step 1, one cycle of 3 minutes at 95°C; step 2, 55 cycles of 15 seconds at 95°C and 1 minute at 60°C. Analysis requires determining the relative expression of AID or IgG1 switch circle against β-actin using the delta-delta C_t method. (MyiQ, followed by Microsoft Excel was used to analyze real time PCR data).

2.6 Statistical Analysis

The Chi square test was performed to compare mutation frequencies of genes analyzed from Boston or Ghana tonsil B cells. Data from *P.falciparum* in vitro B cell stimulation assays are expressed as error bars of mean + standard error of mean (calculated using Microsoft Excel). Data sets were compared by the student two tailed paired *t* test (using Graph Pad Prism). Significance was considered achieved when the p value was < 0.05.

3. Results

3.1 Assessing AID-induced mutation frequency in Boston and Ghana human B cells

In order to test the hypothesis that malaria is associated with aberrant AID activity, specifically its ability to mutate non-Ig genes via SHM, purified B cells from tonsils obtained from malaria infected (Ghana) and uninfected control (Boston) patients who were matched for age and sex were examined. Human B cell populations corresponding to Naïve cells (IgD+, CD10-, CD27-) and GC cells (CD10+CD19+) were isolated by fluorescence-activated cell sorting from these two tonsil donor types (*Figure 7a*). In addition, naïve B cells were isolated from the peripheral blood of control donors using the same signature markers (CD27-, IgD+). To profile the B cell subsets being utilized for mutation analysis, AID mRNA expression of Boston tonsil naïve and GC cells were compared (n=3) (*Figure 7B*). As expected, the tonsils have a significantly higher (overall 5 fold; p value = 0.023) AID mRNA level in the GC when compared to naïve which have a minimal background level of AID (*Figure 7B*).

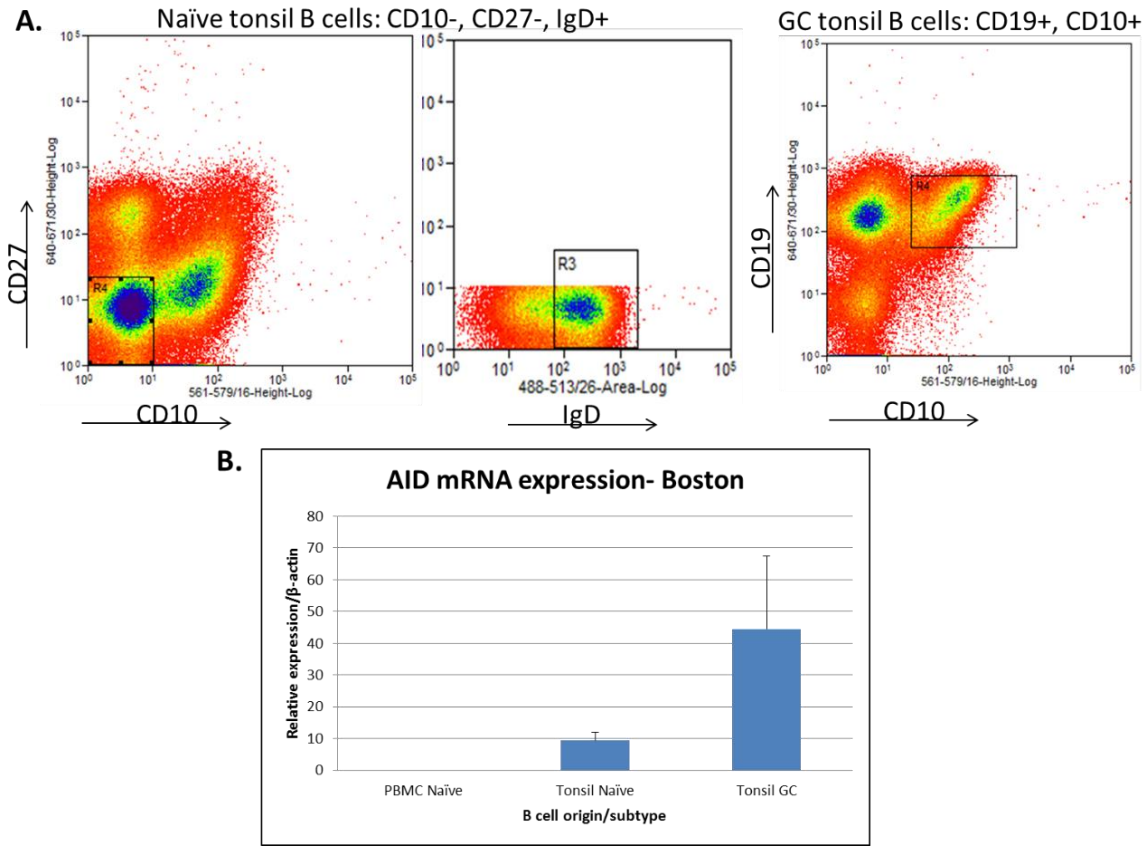

Figure 7. Tonsil Naïve and GC B cells express AID at different levels. MoFlo was used for sorting separate pools of tonsil B cell fractions from processed tonsil MNCs. Naïve B cells: CD10-PE and CD27-APC antibodies were used for staining cells and the CD10-/CD27- cells were selected [(A) first panel R4], from which IgD+ cells were stained for using IgD-FITC antibody and collected [(A) second panel R3]. GC B cells: CD10-PE and CD19-APC antibodies were used to stain for CD10+/CD19+ cells and collected [third panel R4]. AID mRNA expression levels were measured by qRT-PCR and compared in Boston PBMC (n=6) Naïve and tonsil (n=3) Naïve and GC B cells (B).

To evaluate the presence of AID mutational activity, c-myc exon 1 and 2 were analyzed, regions previously shown to represent a major cluster of mutations in BL, (*see introduction, Figure 3*) in both Boston and Ghana tonsils. Appropriate controls were also assessed from the same samples: Beta globin served as a negative control for AID activity while rearranged IgVH genes were also analyzed for somatic mutations, providing a positive control for AID activity via SHM. PCR was used to generate amplicons for c-myc exon 1 and 2, β-globin and IgVH, followed by cloning and sequencing from bacterial colonies. The sequencing results summarized in table 2A and 2B indicate that in Boston, c-myc not only demonstrates a similar mutation rate (percentage of cells mutated), but also mutation frequency (number of mutations per base pairs analyzed) in naïve and GC B cells ($37x10^{-5}$/bp and $38\ x10^{-5}$/ bp respectively). The same holds true for Ghana tonsils in which the mutation frequency shows an insignificant difference with Boston tonsils ($50\ x10^{-5}$/bp and $23\ x10^{-5}$/bp respectively; p value = > 0.05) in both naïve and GC B cells (*see Table 2B).* Overall, there is no parallel between AID expression and mutation frequencies in non-Ig genes. 1: There is essentially no difference between Boston and Ghana GC B cell mutation frequency for c-myc, despite the already-established variance in AID mRNA levels from these two backgrounds and 2: Although it is known that naïve B cells barely express while the GC highly expresses AID, there seems to be no significant increase in mutation frequency for c-myc in the GC when compared to the naïve state. Together, these results do not confirm our hypothesis that AID mRNA expression levels will correlate with aberrant mutation of non-Ig genes. However we do see the expected association between AID levels and classical SHM. The heavy chain sequences of Ig were also studied, which demonstrated a mutation frequency

of approximately 4 for every 100 base pairs in Boston, and 5 for every 100 base pairs in Ghana, which is within the physiological range of AID-induced mutations in the GC (Kuppers and Dalla-Favera, 2001). Also the GC mutation frequency is approximately 7 fold above the mutation frequency for naïve Ig (0.6 per 100 bp in Boston and 0.5 per 100 bp in Ghana), as also reported in literature. β-globin consistently showed low numbers of mutations in any of the cells from which it was amplified giving a mutation frequency of 11×10^{-5}/bp which can be considered the PCR-mediated DNA polymerase misincorporation rate. Naïve B cells were sorted from the peripheral blood of control donors (Boston, n=6) as an additional negative control for AID activity. Overall, the mutation frequency in all genes analyzed, including Ig are insignificantly lower than or similar to what was found in the same naïve B cell subset from tonsils (*Table 2*), as expected.

A.

MUTATED CELLS (%)				
Origin/ cell type	cMYC exon 1	cMYC exon 2	IgVH	β-globin
Boston Germinal Center	28/132 (21)	23/128 (18)	31/32 (97)	3/72 (4)
Boston Tonsil Naive	17/ 87 (20)	27/98 (28)	20/32 (62)	3/79 (4)
Boston PBMC Naïve	18/145 (12)	24/101 (24)	33/89 (37)	1/29 (3)
Ghana Tonsil Germinal Center	10/78 (13)	7/72 (9)	21/22 (95)	6/80(8)
Ghana Tonsil Naive	13/47 (28)	8/46 (17)	16/29 (55)	6/90(7)

B.

MUTATIONS (MutFreq x10^{-5}/bp)				
Origin/ cell type	cMYC exon 1- 554bp	cMYC exon 2 -701bp	IgVH -~250bp	β-globin -392bp
Boston Tonsil Germinal Center	28 in 73,128bp (38)	25 in 89,728 (28)	311 in 8,356bp (3722)	3 in 28,222 (11)
Boston Tonsil Naive	17 in 45,501bp (37)	31 in 68,698 (45)	49 in 8,226bp (596)	3 in 30,968 (10)
Boston PBMC Naive	21 in 80,330bp (26)	26 in 70,801 (37)	70 in 23,557bp (297)	1 in 11,368 (9)
Ghana Tonsil Germinal Center	10 in 43,212 (23)	10 in 50,472 (20)	302 in 5,928bp (5094)	6 in 31.360 (19)
Ghana Tonsil Naive	13 in 26,038bp (50)	9 in 32,246 (28)	39 in 7,595bp (513)	6 in 35,280 (17)

Table 2. Mutation analysis of genes in Boston and Ghana tonsils. **2A.** Mutated cells (%) are the number of cells harboring mutations over the total number of cells sequenced. **2B**. Mutations (x10^{-5}/bp) are the total number of mutations found per base pair analyzed. Mutation frequency is calculated by dividing the number of mutational events by total number of base pairs analyzed.

3.2 P.falciparum induces AID in human B cells in vitro potentially using PfEMP1

3.2.1 *P.falciparum* 3D7 strain induces AID in B cells *in vitro*

In order to directly support our hypothesis that malaria can heighten AID activity, we have pursued *in vitro* evidence that *P.falciparum* can stimulate AID expression and function. *P.falciparum* extract (3D7 strain) was produced from large-scale infected erythrocyte cultures. Tonsil MNCs from malaria-free donors (Boston) were isolated and cultured. These cells were stimulated for 4-6 days using *P.falciparum* extract (or CpG as a positive control) CD40-L and IL-4. At each time point, the cells were harvested and assessed for AID mRNA induction. *Figure 8a* shows the gated populations from the stimulated cultures of the day 5 time point corresponding to CD19-APC+ (y-axis), and all levels of CFSE expression (x-axis). It is clear that upon addition of agonists CD40-L and IL4, we begin to detect proliferating cells, i.e. loss of CFSE, which increases even further with CpG DNA and *P.falciparum* extract, revealing that stimulation of the B cells is occurring. *Figure 8b* shows a reproduced result of AID mRNA expression levels after various stimulating conditions, on day 4, 5 and 6. β-actin was used as a control mRNA for calculation of AID mRNA using the delta-delta CT method. By day 5, there is a 5 fold increase of AID mRNA in *P.falciparum* extract (+CD40-L and IL-4) - stimulated B cells as compared to CD40-L/IL-4-stimulated cells (*Figure 8b*). These results using newly prepared *P.falciparum* 3D7 parasite extract are consistent with previous studies performed by our laboratory (Torgbor et al., 2014).

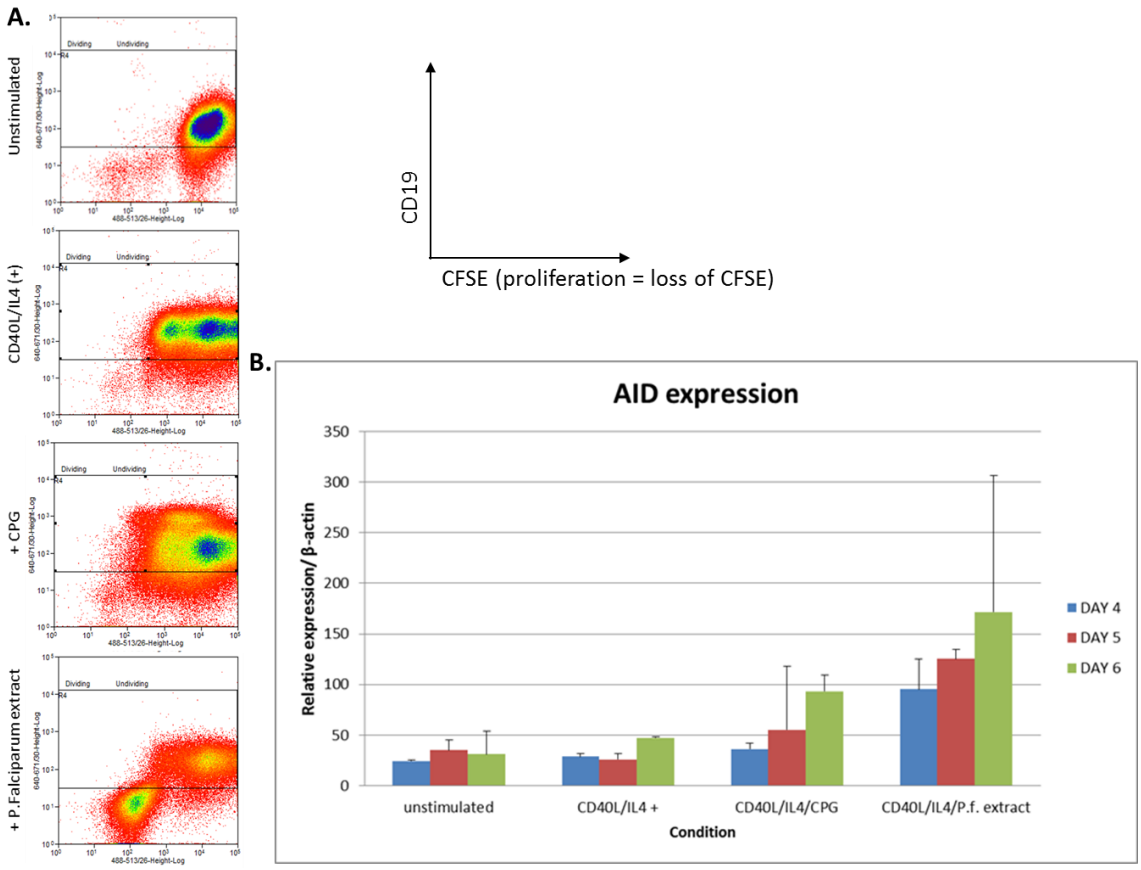

Figure 8. *P.falciparum* extract stimulation of AID mRNA in normal tonsil B cells. Whole tonsil MNCs were unstimulated or stimulated with either CD40-L/IL-4 alone or + CPG, or + *P.falciparum* extract for 4, 5 and 6 days. MoFlo was used for sorting CD19-APC +/ CFSE-FITC +/- for each condition shown (A). A. show FACS plots (and inset: description of axes in each plot) on day 5. qRT-PCR was used to determine relative expression of AID mRNA (B) to β-actin. AID expression for each time point and treatment are shown.

3.2.2 Studying PfEMP1

Through the *in vitro* stimulation assay, it has been shown that AID levels increase in response to *P.falciparum* extract (3D7 strain- wildtype). However, the study of key components of the parasite, in addition to hemozoin (Torgbor et al., 2014), that function in inducing AID still remains. In order to investigate the specific antigen of *P.falciparum*-PfEMP1, I have generated extract from a *P.falciparum* strain lacking the PfEMP1 protein (culture kindly provided by Dr. Kirk Deitsch, Weill Cornell Medical College) called the DC-J parasite line. Using the DC-J extract provides insight into the significance of PfEMP1 in AID induction. To recap, PfEMP1 is a protein specifically expressed by *P.falciparum* on the surface of infected erythrocytes, which is known to bind Ig and activate B cells, and also we postulate that it is providing the BCR signaling for AID induction (Donati et al., 2006b; Donati et al., 2004). Quantitative real time PCR was carried out to detect transcription from *var* genes (the *var* gene family comprises 60 genes that encode PfEMP1) present in the 3D7 genome *(Figure 9)*. The wildtype 3D7 strain was predominantly expressing *var* PFD1015c while expression of the rest of the *var* family was virtually undetectable (*Figure 9*). The mutant DC-J strain which was cultured under blasticidin pressure (*see introduction, section 1.5.2.1*) exclusively expressed blasticidin, as expected, while there was no expression of *var* genes *(Figure 9)*.

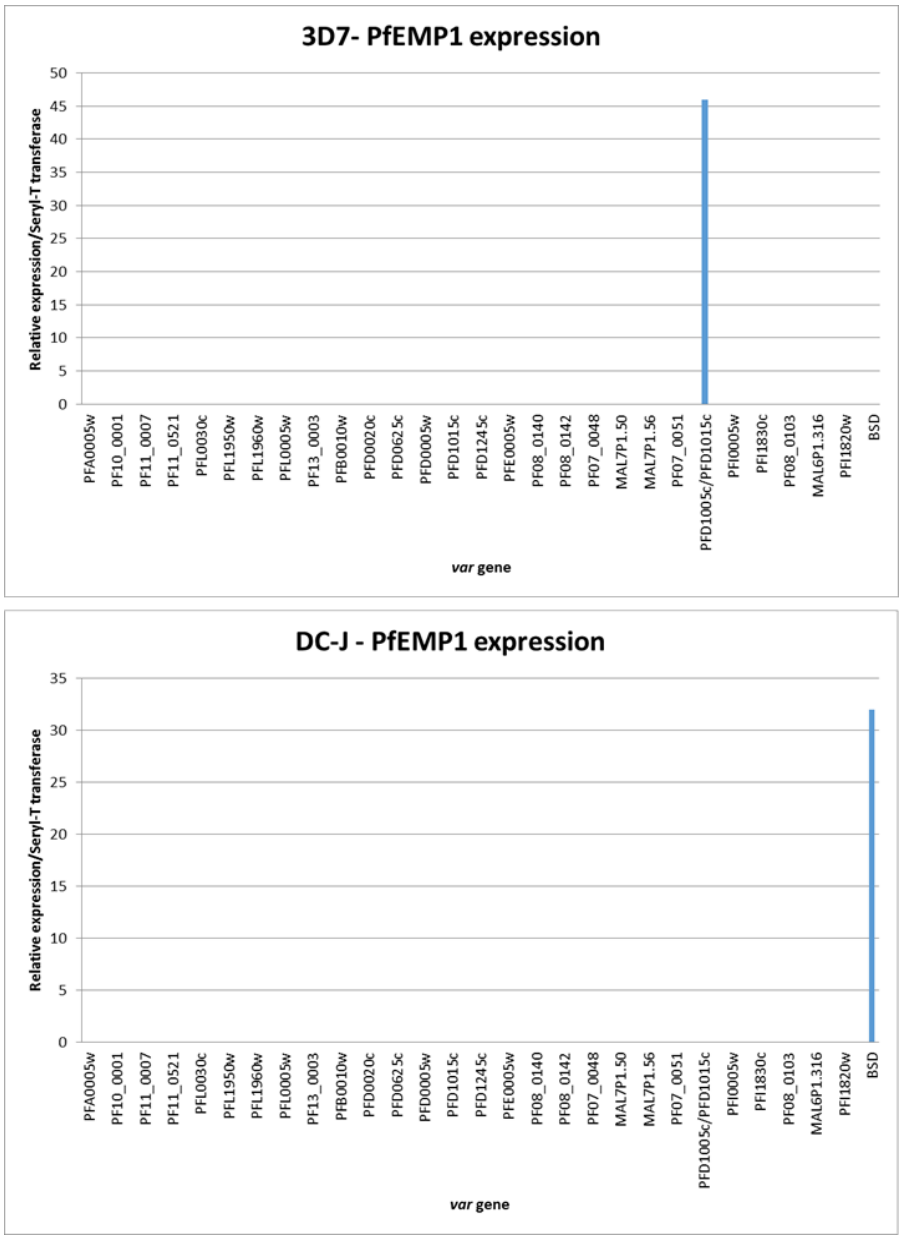

Figure 9. 3D7 and DC-J strains express or do not express PfEMP1. The vertically rotated panels include the names of all *var* genes that encode PfEMP1; BSD is blasticidin. 3D7 (top panel) is the wildtype *P.falciparum* strain and the mutant strain with silenced PfEMP1 is DC-J (bottom panel). qRT-PCR was used to determine the relative expression of specific var gene expression to β-actin in both the 3D7 and DC-J strains maintained in the lab.

3.2.3 PfEMP1 is required for P.*falciparum* to maximally induce AID *in vitro*

The maximal concentration (as described in the literature and previously used by our lab's studies: 10µg/mL) of the original 3D7 and DC-J parasite extracts in combination with CD40L/IL4 were used to stimulate tonsil MNCs from healthy control donors for 5 days (*Figure 10*). This experiment was performed 4 times, with the average demonstrating the reproducible trend of AID induction under these stimulating conditions (*Figure 10*). This experiment demonstrates that while *P.falciparum* extract (+CD40L/IL4) clearly induces AID, the PfEMP1-null extract (+CD40L/IL4) has significantly less impact on AID mRNA levels at the same concentration, similar to the levels of stimulation with CpG (statistically insignificant difference between CpG- and DC-J- stimulation of AID). Most importantly, overall, the difference in AID induction by 3D7 vs. DC-J extract is statistically significant (p value = 0.003). P values for the impact of 3D7 extract on AID mRNA expression when compared to the other conditions were as follows: CD40L/IL – 0.04, CpG- >0.05 (due to anomalous high AID signal produced in assay 4).

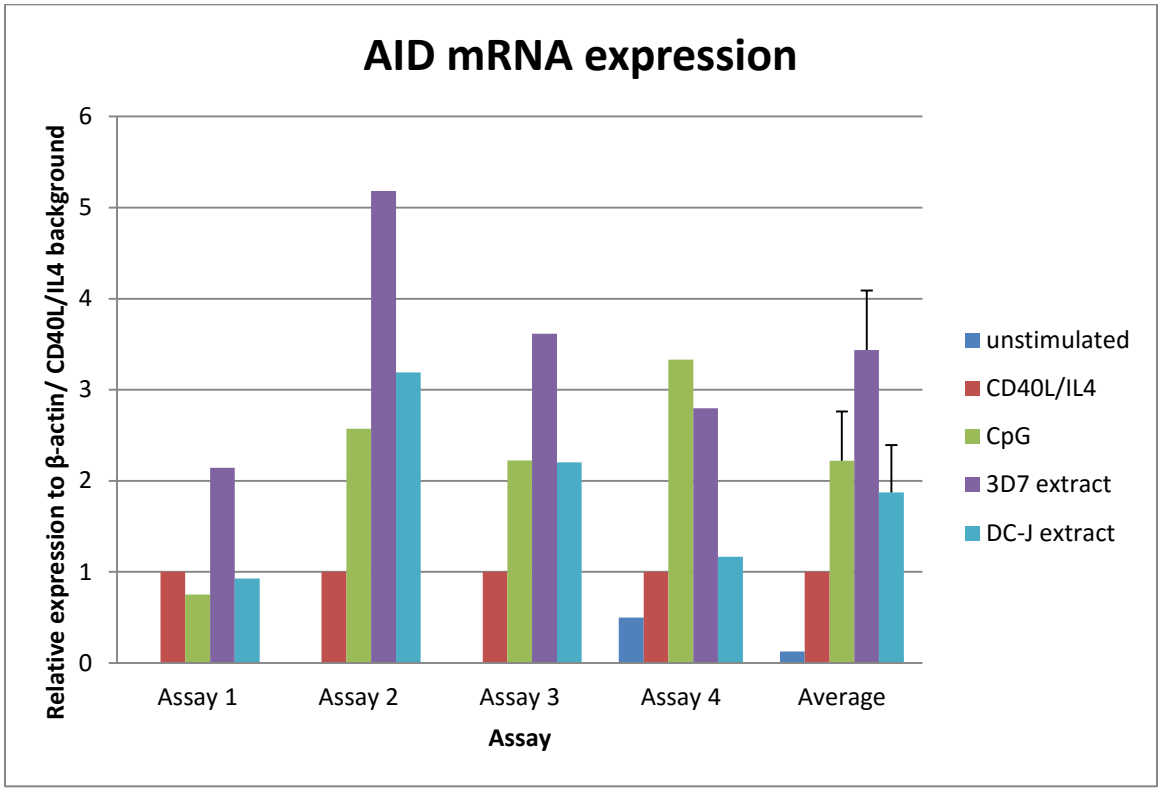

Figure 10. *P.falciparum* 3D7 and DC-J parasite extract stimulation of AID mRNA in normal tonsil B cells. Whole tonsil MNCs were unstimulated or stimulated with either CD40-L/IL-4 alone, +CPG, + *P.falciparum* 3D7 or DC-J extract for 5 days. qRT-PCR was used to determine relative expression of AID mRNA to β-actin. Values for each condition were normalized to the CD40L/IL4 control to allow comparison between experiments. AID expression for each condition and experiment are shown, with the average shown in the right-most cluster.

3.2.3.1 Parasite extract concentration titration

A new batch of *P.falciparum* 3D7 and DC-J extracts were prepared to conduct further experiments and additional variable stimulating conditions. The new batch of parasite extracts were prepared as done previously. The latest extracts were titrated for concentrations ranging from 0 [CD40L/IL4 alone with no parasite extract added] to 40µg/mL in inducing AID (*Figure 11*). This experiment was performed so that we could not only experiment with higher concentrations than originally used (10µg/mL), but also to confidently establish the fact that DC-J is less effective at inducing AID than 3D7 at the same optimal concentration. *P.falciparum* 3D7 and DC-J simultaneously reached its maximal AID induction signal at 40µg/mL (*Figure 11*). It is important to note that 3D7 caused a dramatic increase in AID induction at concentrations above 10µg/mL, whereas DC-J reached its maximal ability to induce AID at 10µg/mL and never increased beyond the AID signal produced at that concentration (*Figure 11*). In addition, DC-J was able to induce AID at 80µg/mL at similar levels as with 10, 20, or 40 µg/mL, whereas cells stimulated with 3D7 at 80 µg/mL did not survive and therefore unusable for AID expression analysis at concentrations higher than 40µg/mL. Therefore, the concentration that provided the maximal AID induction for both parasite extracts concurrently: 40µg/mL, was chosen for stimulation experiments, including the summary of consistent AID induction by these parasite strains described below in *Figure 12*.

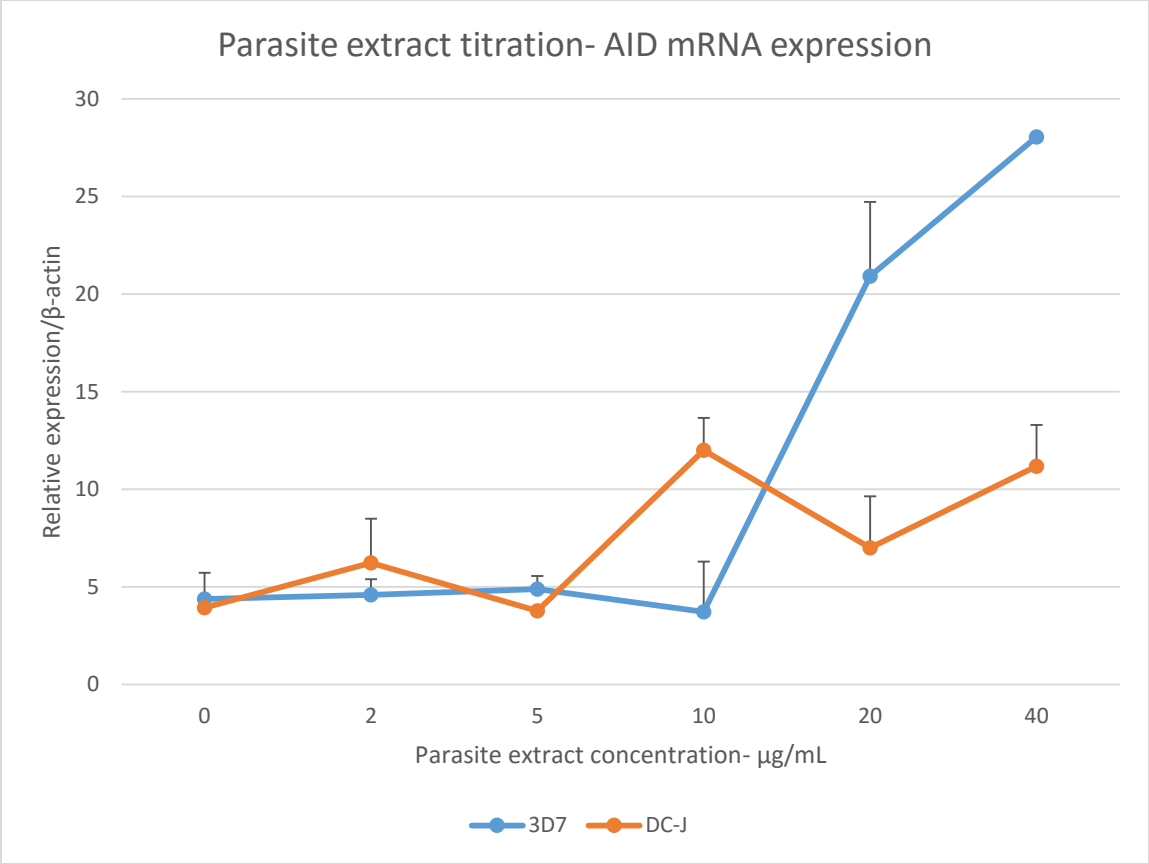

Figure 11. Parasite extract (P.*falciparum:* 3D7 and DC-J) concentration titration in stimulating AID mRNA in normal tonsil B cells. Whole tonsil mononuclear cells were stimulated with CD40-L/IL-4 + 3D7 or DC- extracts for 5 days at a range of concentrations (0-40µg/mL). 0µg/mL represents cells stimulated with CD40L/IL4 alone with no parasite extract. qRT-PCR was used to determine relative expression of AID to β-actin.

3.2.3.2 AID is optimally induced with PfEMP1

The optimal concentrations (40µg/mL) of the newest 3D7 and DC-J parasite extracts (*see Figure 11*) were determined. This concentration was used for both 3D7 or DC-J in combination with CD40L/IL4 for stimulating tonsil MNCs from control donors for 5 days (*Figure 12*). This experiment again demonstrates that while 3D7 extract (+CD40L/IL4) clearly induces AID, the DC-J extract (+CD40L/IL4) has much less impact on AID mRNA levels at the same concentration (p value = 0.02).

DC-J is only able to induce AID at similar levels to CpG-stimulated cultures overall. Results shown in *figure 12* demonstrate CpG stimulated cultures induce AID at a higher level than DC-J extract; however this is due to one anomalous result for CpG stimulation out of n=3, giving the misrepresentative impression of CpG having higher AID inducing capability than actually consistently shown in experiments (*see Figure 10*). Since the DC-J strain lacks PfEMP1 but still makes hemozoin, the results fit our prediction that the mutant strain would be as effective as CpG but less so than wild type parasite extract in inducing AID. Overall these results support the notion that PfEMP1 is crucial for the activation of the BCR and therefore maximal AID induction.

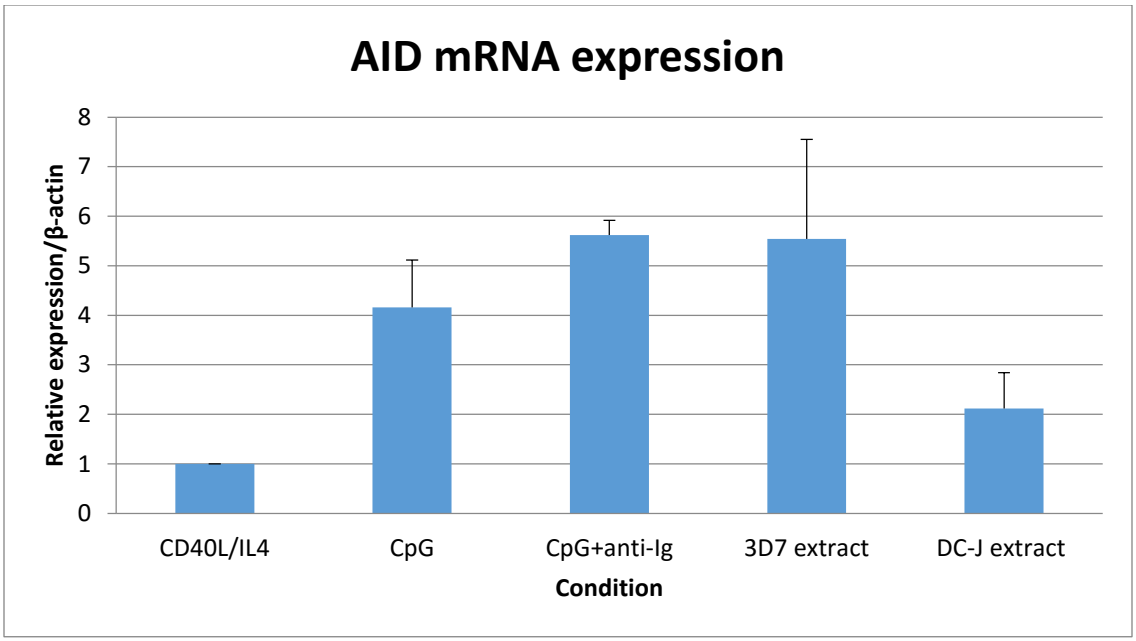

Figure 12. Overall comparison of 3D7 and DC-J extract stimulation of AID mRNA in normal tonsil B cells. Whole tonsil mononuclear cells were stimulated with either CD40-L/IL-4 alone, +CPG with or without anti-Ig, + 3D7 extract, or + DC-J extract for 5 days. qRT-PCR was used to determine relative expression of AID mRNA to β-actin. Values for each condition were normalized to the CD40L/IL4 control to allow appropriate comparison between experiments. n=3. P values compared to CD40L/IL4- alone: CpG: > 0.05, CpG + anti-Ig: 0.01, 3D7: 0.04, DC-J: > 0.05.

3.3. PfEMP1 likely uses surface-Ig crosslinking to induce AID

3.3.1 Anti-Ig complements DC-J and CpG

The results involving the impact of DC-J extract on AID induction agreeably fits our model that PfEMP1 is required for surface Ig crosslinking. In order to corroborate this further, an assay was performed in which we complemented the mutant strain with anti-Ig, to provide it with the capability of BCR activation via surface Ig crosslinking and compared with the wild type extract in terms of AID induction (*Figure 13*). We found similar trends as previously shown: CpG is complemented by anti-Ig, inducing AID to similar levels as with the wild type parasite extract. The DC-J extract again was unable to induce AID any higher than when stimulated with CpG *(Figure 13)*. We found that introducing surface Ig crosslinking to the mutant strain rescued AID expression to levels even higher than with wildtype parasite extract (not statistically significant). This means that surface Ig crosslinking can complement the DC-J extract in inducing AID. However, the conditions/ concentration needed to be optimized, since the complementation of DC-J with anti-Ig is having a dramatically high impact on AID induction compared to the signal with the wildtype extract. This could be due to hemozoin content and/or PfEMP1 which is present in the 3D7 extract, not acting directly through the BCR like anti-Ig (*see Discussion*).

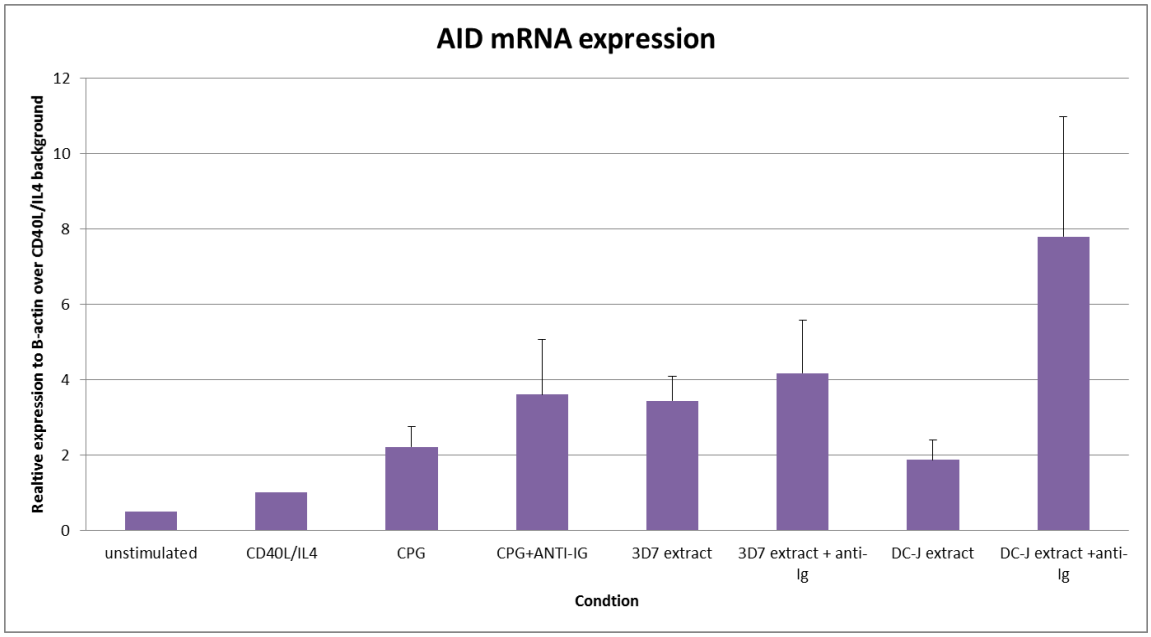

Figure 13. *P.falciparum* 3D7 and DC-J parasite extract complementation by anti-Ig and stimulation of AID mRNA in normal tonsil B cells. Whole tonsil MNCs were stimulated with either CD40-L/IL-4 alone, +CpG, + *P.falciparum* 3D7 or DC-J extract with or without anti-Ig for 5 days. qRT-PCR was used to determine relative expression of AID mRNA to β-actin. Values for each condition were normalized to the CD40L/IL4 control to allow comparison between experiments. AID expression for each condition are shown.

3.3.1.1 New optimal concentration of DC-J is complemented by anti-Ig to induce AID to levels produced by stimulation with 3D7

Using the new batch of parasite extracts at a newly defined optimal concentration (40µg/mL), the stimulation assay testing surface Ig crosslinking as explained above was carried out (*Figure 14*). Results were similar as with the prior batch of extract: CpG is complemented by anti-Ig (p value = 0.003), inducing AID to similar levels as with the wild type parasite extract and DC-J induced AID to similar levels as with CpG (*Figure 13 and Figure 14*) We found that introducing surface Ig crosslinking to the optimal concentration of the new DC-J extract rescued AID expression to levels similar to with 3D7 extract (*Figure 14*). This indicates that: 1. Surface-Ig crosslinking can complement the DC-J extract in inducing AID and 2. The mechanism of PfEMP1 is likely through the BCR (*see Discussion*).

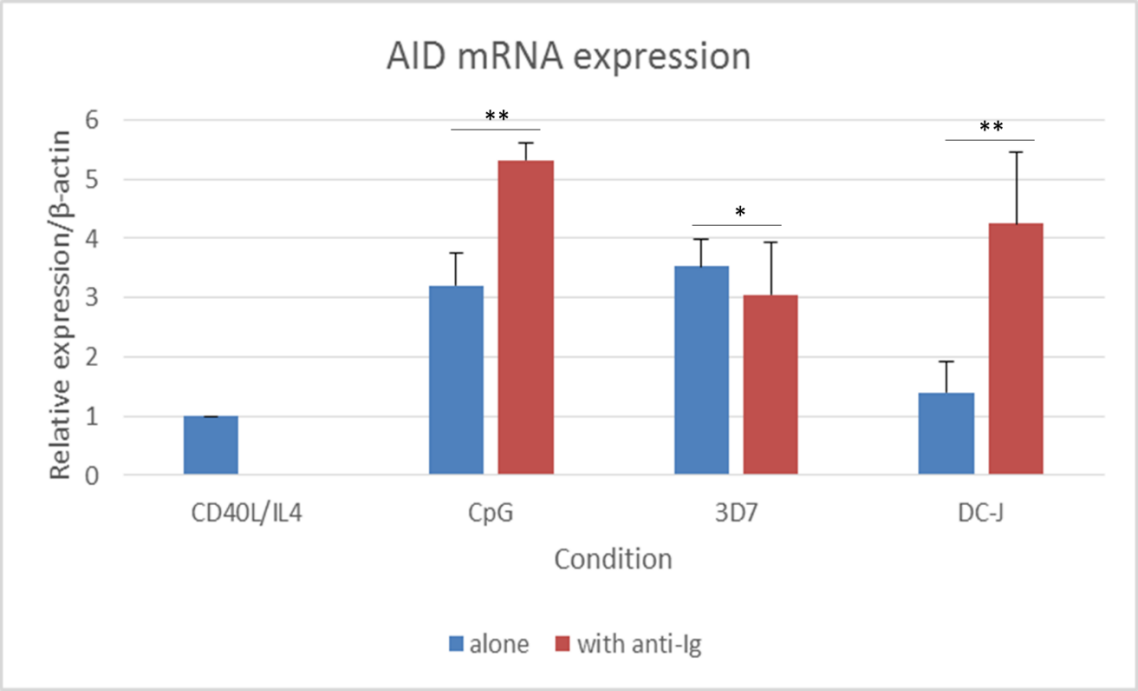

Figure 14. *P.falciparum* strains: 3D7 and DC-J complementation by anti-Ig. 3D7 (wildtype) and DC-J (mutant, PfEMP1-null) extracts were used at 40μg/mL to stimulate normal tonsil MNCs along with CD40L/IL4 for 5 days. (This concentration was determined to result in maximal AID induction for both strains). qRT-PCR was used to determine relative expression of AID mRNA to β-actin under each of the stimulating conditions. n=3. * = statistically insignificant, i.e. p value = > 0.05, ** = statistically significant; i.e. p value = < 0.05.

3.4 P.falciparum-induced AID is active/ capable of class switch recombination

3.4.1. Is *P.falciparum*- induced AID active?

An important question that is being addressed here is whether AID that is induced by *P.falciparum* is actually active. IgG1 switch circle transcripts are a marker of ongoing CSR (Kinoshita et al., 2001). qRT-PCR was carried out to detect IgG1 switch circles in cells stimulated with the wild type and mutant *P.falciparum* extracts utilizing both an original and a newly designed primer/probe set (*Figure 15*). This has been tested in several experiments and was confirmed to be amplifying the correct gene-fusion product through sequencing (not shown). Earlier incorrectly published methods that led to the necessity for designing this specific switch circle assay is described in the *Appendix*.

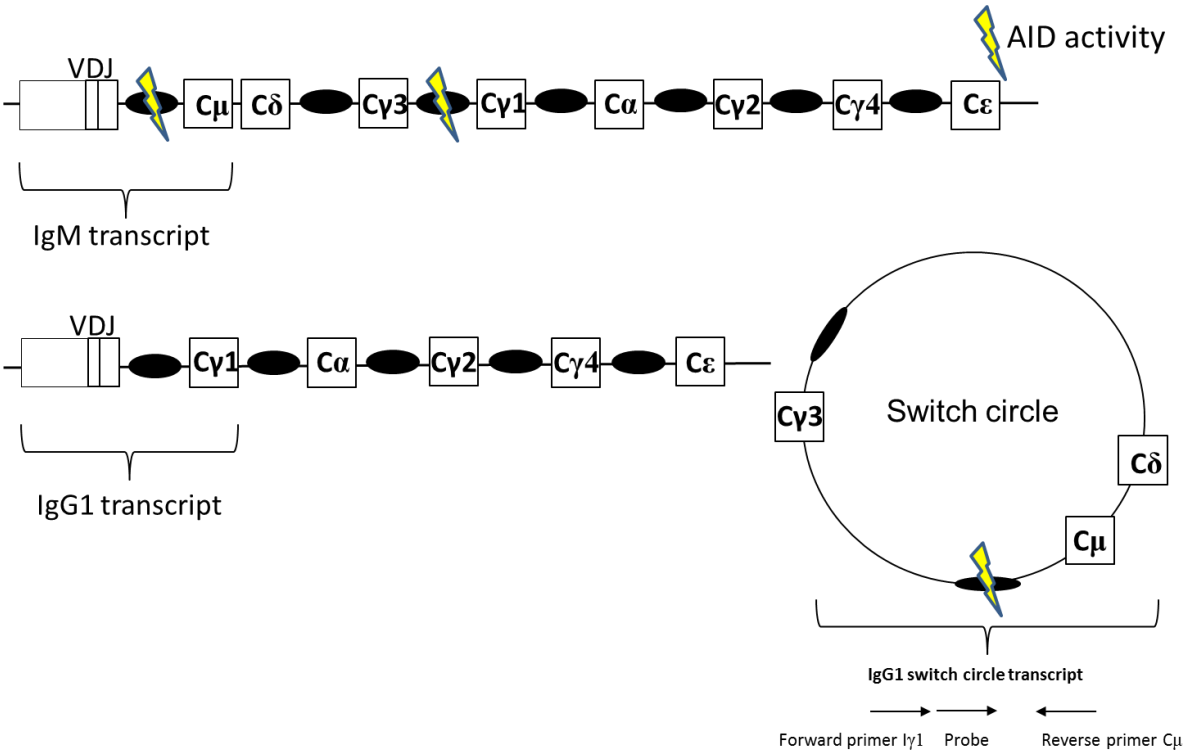

Figure 15. IgG1 switch circle assay design. AID creates double stranded breakpoints (shown by yellow lightning symbols) at class-specific switch (S) regions (shown by black ovals) of the Ig heavy chain gene. A cytokine signal (CD40L/IL4) creates breakpoints in the switch regions 5' to the μ heavy chain constant region and 5' to the γ1 heavy chain constant region. After excision of the intervening segment, recombination occurs to allow active transcription of γ1 heavy chain mRNA, and consequently production of an IgG1 transcript. The excised gene segment circularizes and produces an IgG1-specific switch circle transcript. Forward primer, probe, and reverse primers (shown) were designed to specifically detect the transient byproduct of AID-induced class-switching to the IgG1 isotype.

Whole tonsil MNCs were stimulated using 3D7 and DC-J extracts in combination with CD40L/IL4 for 5 days, and analyzed for levels of AID and IgG1 switch circle transcript expression (*Figure 16A*). AID, as seen before, was induced by CD40L/IL4 alone as well as in combination with 3D7 or DC-J, with or without anti-Ig, and followed the consistent pattern in induction levels under each of these conditions. IgG1 switch circles were produced at a significantly higher level (p value = 0.01) in 3D7-stimulated cells when compared to CD40L/IL4-stimulation alone. However, it is important to note that IgG1 switch circles could only be highly detected in cultures stimulated with parasite, but not with CD40L/IL4 alone (*Figure 16A*). This result was puzzling, as it is well established in the literature that CD40L and IL4 provide the cytokine signals that induce switching to IgG1. It is important to note that we are testing population with whole tonsil MNCs, which includes GC and memory cells, besides naïve B cells. The prediction was that the GC and memory B cells would interfere with the signal for IgG1 switch circles under certain conditions. It is also noticeable that anti-Ig consistently seems to reduce the AID (see *Figure 14* and *16A*) and IgG1 switch circle signals produced by stimulation in combination with 3D7 extract, although insignifantly (*see Discussion*).

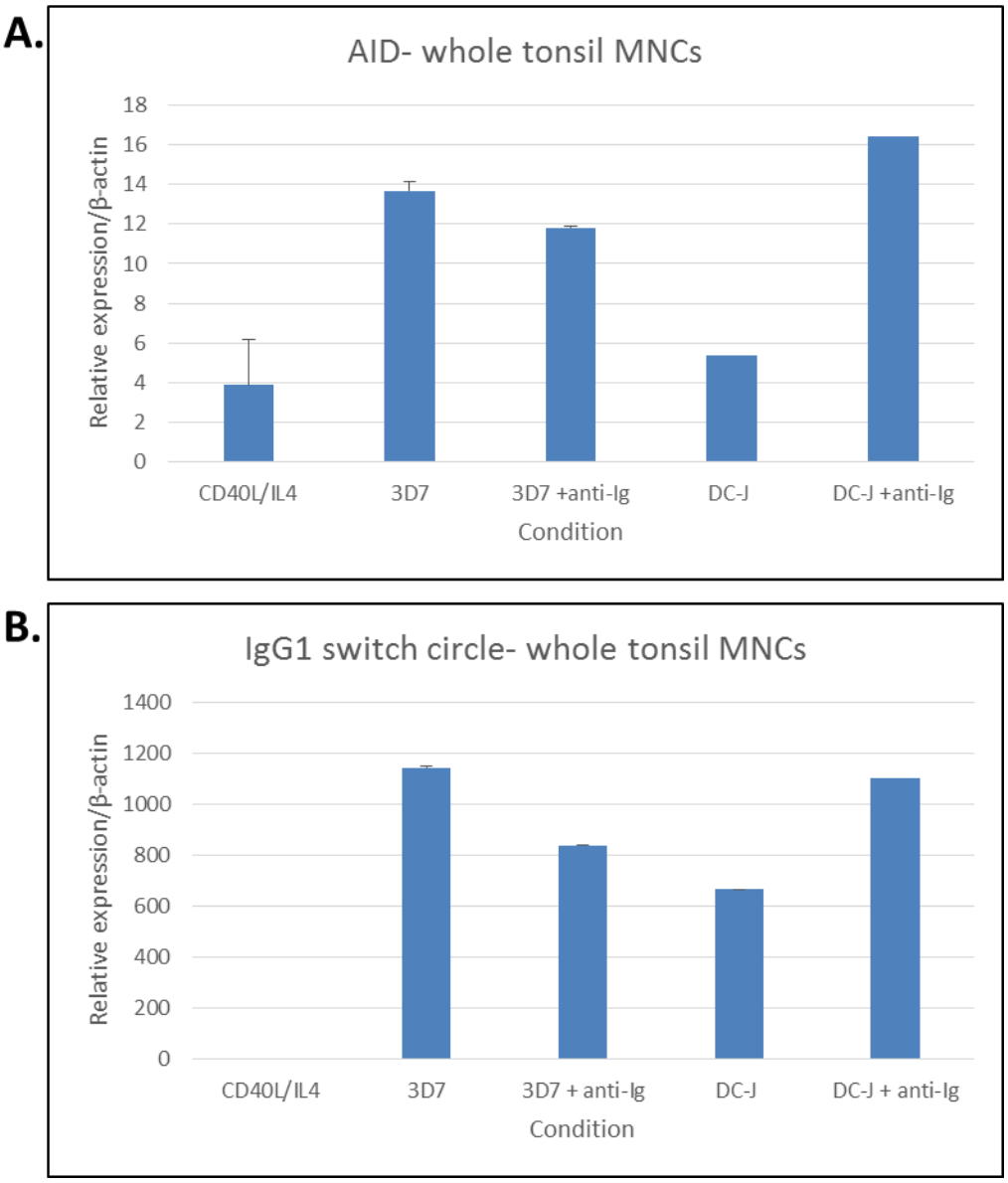

Figure 16. Parasite stimulation of AID and IgG1 switch circle mRNA in whole tonsil MNCs. Whole tonsil MNCs were stimulated with either CD40-L/IL-4 alone or + 3D7 or DCJ extract with or without anti-Ig for 5 days. qRT-PCR was used to determine relative expression of AID (A) and IgG1 switch circle (B) mRNA to β-actin.

3.4.2 *P.falciparum* extracts targeting specific B cell subpopulations

Therefore, I devised a technique using immuno-magnetic cell isolation for collecting only naïve B cells (CD10 and CD27- depleted cells) prior to stimulation. These cells should not express any IgG1 switch circle transcripts, unless produced as a result of class switching during stimulation. The population we are left with post-depletion of CD10 and CD27 cells represents naïve B cells. The purity of the CD10/CD27- depletion procedure was confirmed using MoFlo (*Figure 17A*). The naïve B cells were stimulated with CD40L/IL4 alone, or in combination with 3D7 or DC-J extracts, with or without anti-Ig as performed with whole tonsil MNCs. What we found was detection of AID and IgG1 switch circle transcripts in cultures stimulated with CD40L/IL4 alone, which is exactly what we would expect in naïve B cells stimulated with this cytokine signature (*Figure 17B,C*). However, the surprising result was a complete lack of signal for the parasite-stimulated (both with 3D7 and DC-J) naïve B cells (*Figure 17B,C*), even though there was a confirmed signal for both AID and IgG1 switch circles in the whole tonsil MNC population stimulated with both parasites (*Figure 17A,B*).

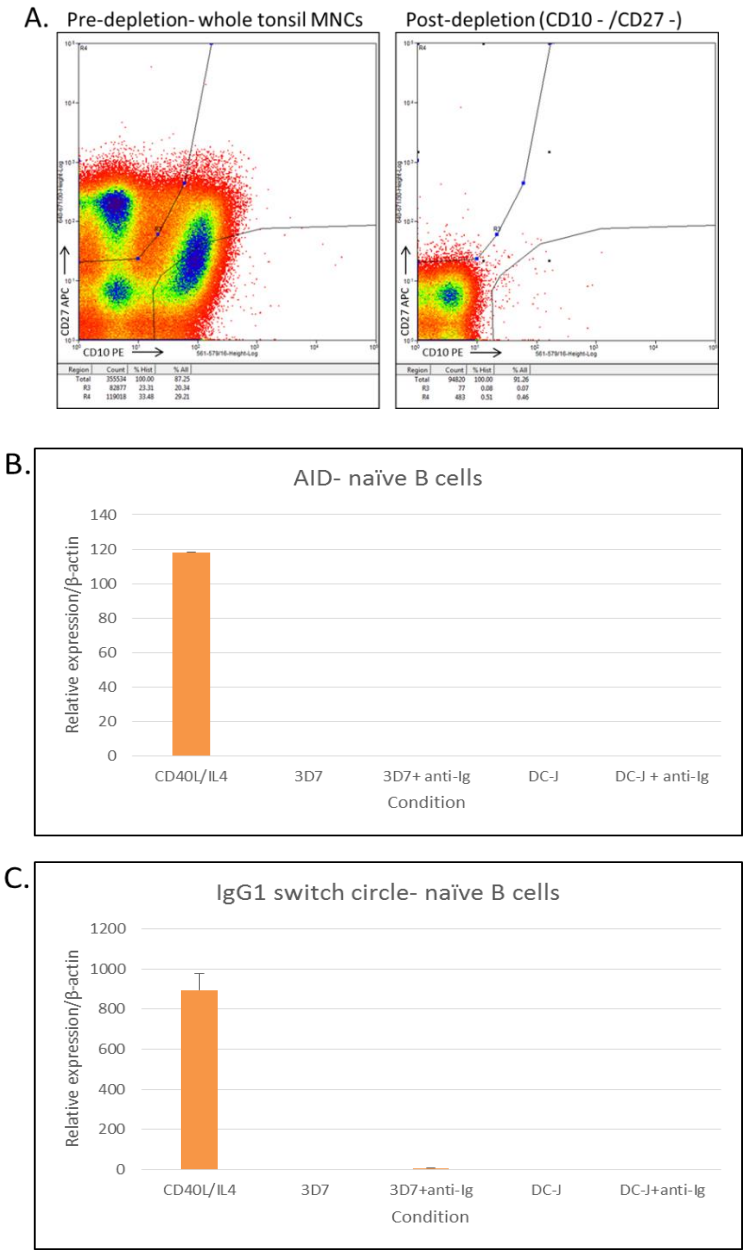

Figure 17. Parasite stimulation of AID and IgG1 switch circle mRNA in naïve B cells. A) StemSep magnetic cell isolation was used on the same tonsil MNCS used in *Figure 16* for depleting CD10 and CD27 cells, resulting in a naïve B cell population. Cell populations before and after the depletion procedure, stained with CD10-PE and CD27-APC and analyzed using MoFlo is shown. n=2. B, C) Naïve B cells were stimulated with either CD40-L/IL-4 alone or + 3D7 or DCJ extract with or without anti-Ig for 5 days. qRT-PCR was used to determine relative expression of AID (B) and IgG1 switch circle (C) mRNA to β-actin.

3.4.3 *P.falciparum* extracts impact non-naïve B cells for AID induction

Next, a tonsil was used not only for the stimulation of the whole tonsil MNC and naïve B cell populations, but also the CD10+ and CD27+ cells (whole tonsil MNCs underwent a magnetic depletion of CD10+ and CD27+ cells to give us this population). The CD10+/ CD27+ cells specifically represent the GC and memory B cell populations from the tonsil. The purity (>95%) of the CD10+/CD27+ selection procedure was confirmed using staining specific for the positive-selection magnetic particles on the MoFlo (*see Figure 18*). The GC/memory cells, just like the naïve B cells were stimulated with CD40L/IL4 alone, or in combination with 3D7 or DC-J extracts (*Figure 19*). The naïve B cells repeated the same result as observed before in that AID and IgG1 switch circle mRNA was induced in cultures stimulated with CD40L/IL4 alone, as expected, but not in cultures stimulated with 3D7 and DC-J extracts (*Figure 19A*). Interestingly, the parasite-stimulated GC/memory B cells (CD10+/CD27+) provided an AID and IgG1 switch circle signal, as seen in whole tonsil MNCs *(Figure 19B).* In addition, AID and IgG1 switch circle mRNA expression was lower for the mutant DC-J strain when compared to the wildtype 3D7 extract, as consistently seen previously. This confirms that in fact, naïve B cells are not stimulated by 3D7 or DC-J parasites, but rather it is the GC and/or memory B cells that are capable of being stimulated to produce active AID.

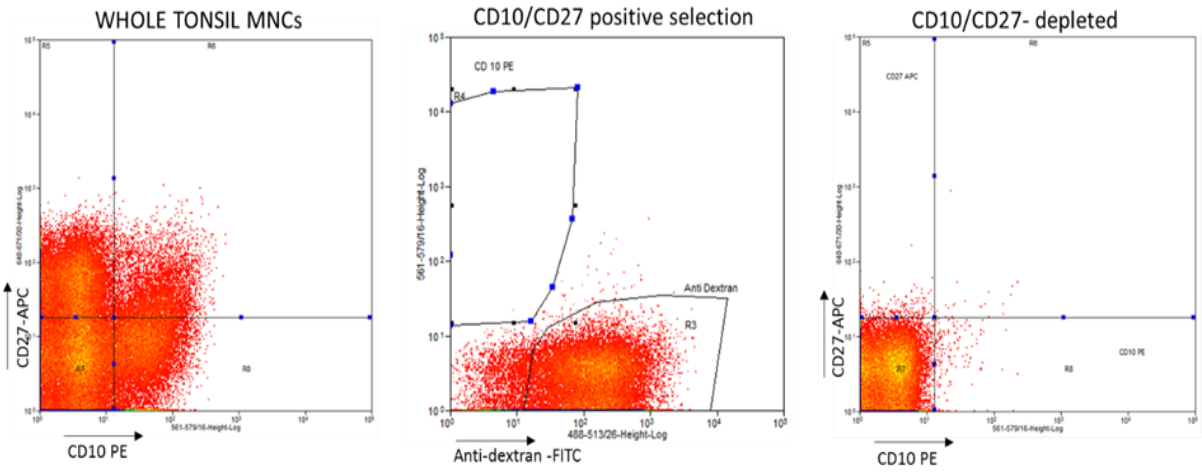

Figure 18. Extracellular staining MoFlo purity check of CD10/CD27 positive selection. CD10+ and CD27+ cells were isolated together from whole tonsil MNCs using positive selection via dextran- coated magnetic particles. Subsequently, the positively selected population was stained with anti-dextran-FITC (see middle panel). Staining the remaining population (CD10/CD27- depleted) with CD10-PE and CD27-APC distinguished true isolation of CD10+ or CD27+ cells from the whole tonsil MNC population (see left panel: whole tonsil MNCs before CD10/CD27 positive selection, stained with CD10-PE and CD27-APC for reference). Black arrows indicate respective staining that was applied to each population for analysis.

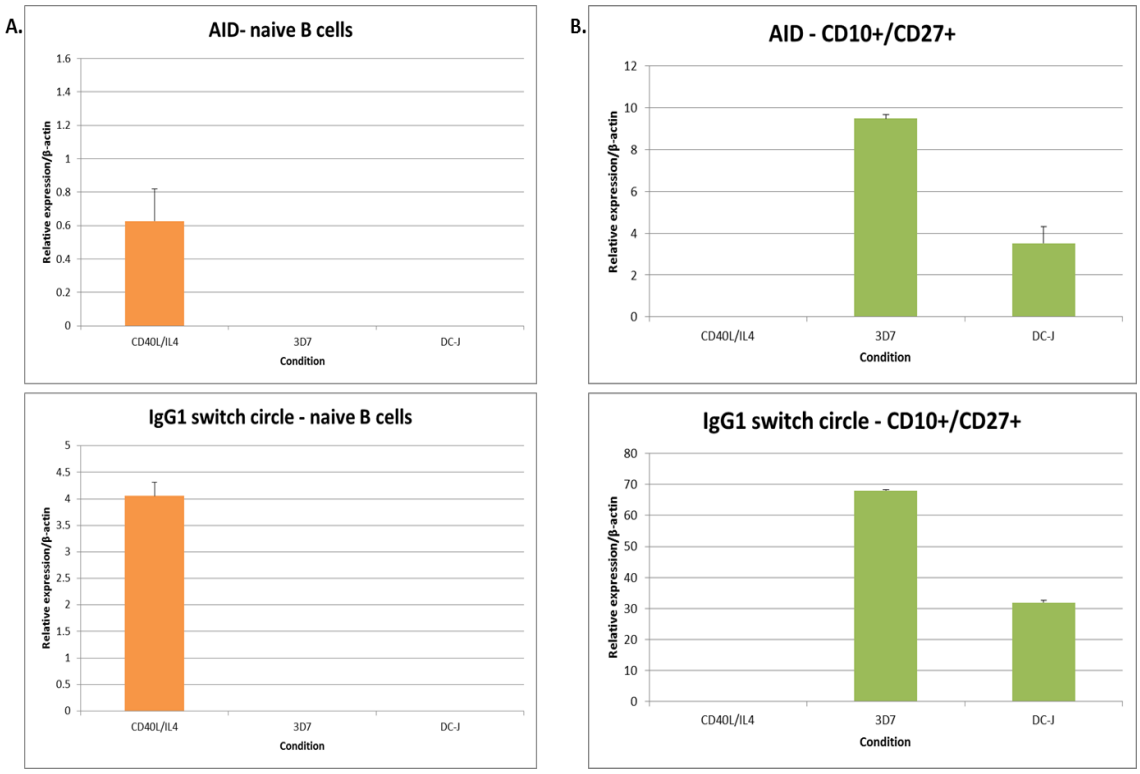

Figure 19. Parasite stimulation of AID and IgG1 switch circle mRNA in naïve B and GC/memory B cells. A) Naïve B cells (whole tonsil MNCs depleted of CD10 and CD27) or B) GC & memory B cells (CD10+ and CD27+ cells selected from whole tonsil MNCs) were stimulated with either CD40L/IL4 alone or + 3D7 and + DC-J extracts for 5 days. qRT-PCR was used to determine relative expression of AID (top graphs) and IgG1 switch circle (bottom graphs) mRNA to β-actin.

3.4.4 Parasite extracts cause CSR in GC and memory B cells

Next, GC (CD10+) or memory (CD27+) B cells were assessed separately for AID induction and IgG1 switch circle production. The purity of the CD10+ and CD27+ cell positive selection procedures were again confirmed on the MoFlo (*see Figure 20*) What we found was both GC and memory B cells alone are able to undergo class switching in response to 3D7 extracts (*Figure 21B*). However, an AID signal is not detectable for parasite-stimulated separate populations (CD10+ alone or CD27+ alone). This is even though AID is clearly induced when GC and memory B cells are together, whether it be when isolated together (C10+/CD27+ population) or separately and then reconstituted together (CD10+ cells reconstituted with CD27+ cells) at the same time point (*Figure 21A*). These results highlight the unstable and transient nature of AID expression in culture, particularly in separated B cell subsets. Nonetheless, the consistent production of IgG1 switch circles (n=3) in 3D7-stimulated cultures suggests that indeed *P.falciparum* acts on the GC and memory B cell compartments in inducing AID activity.

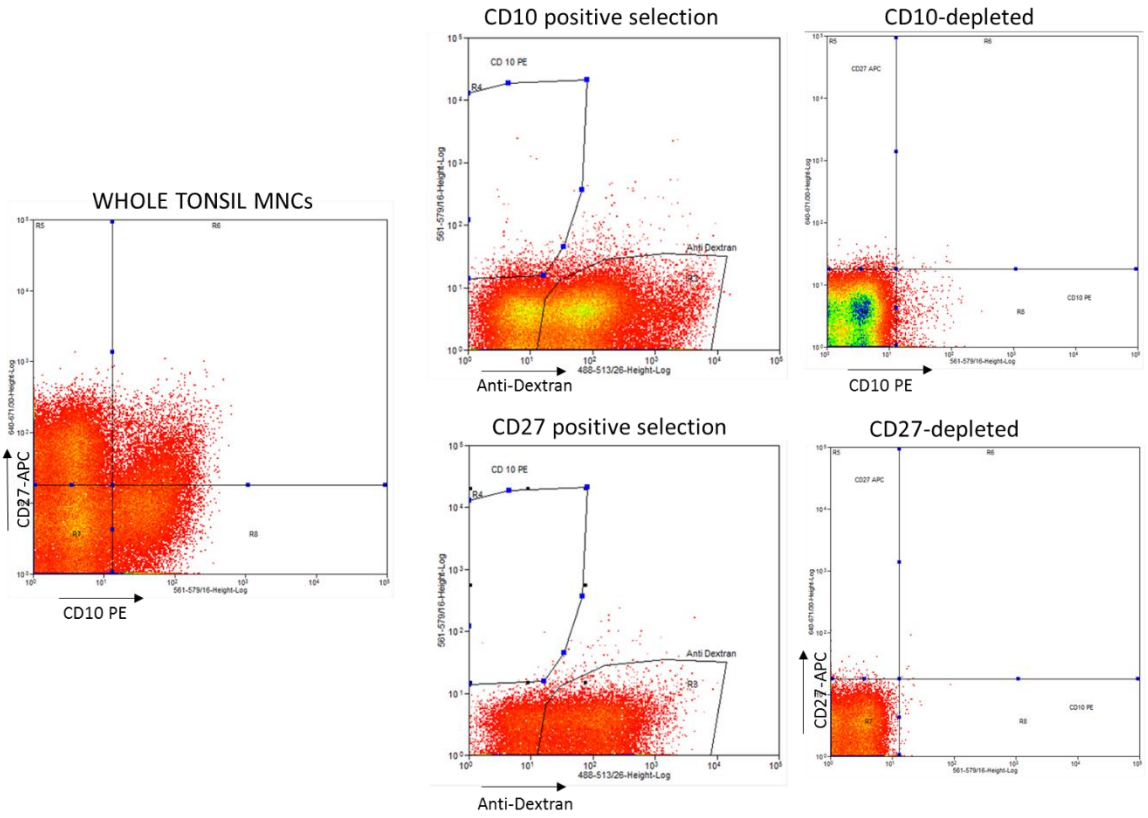

Figure 20. Extracellular staining MoFlo purity check of separate CD10 and CD27 positive selection. CD10+ and CD27+ cells were isolated separately from whole tonsil MNCs using positive selection via dextran-coated magnetic particles. Subsequently, positively selected populations were stained with anti-dextran-FITC (see middle panels). Staining the leftover populations (CD10-depleted or CD27-depleted) with CD10-PE or CD27-APC distinguished true isolation of CD10+ or CD27+ cells from the whole tonsil MNC population (see left panel: whole tonsil MNCs before CD10 or CD27 isolation, stained with CD10-PE and CD27-APC for reference). Black arrows indicate respective staining that was applied to each population for analysis.

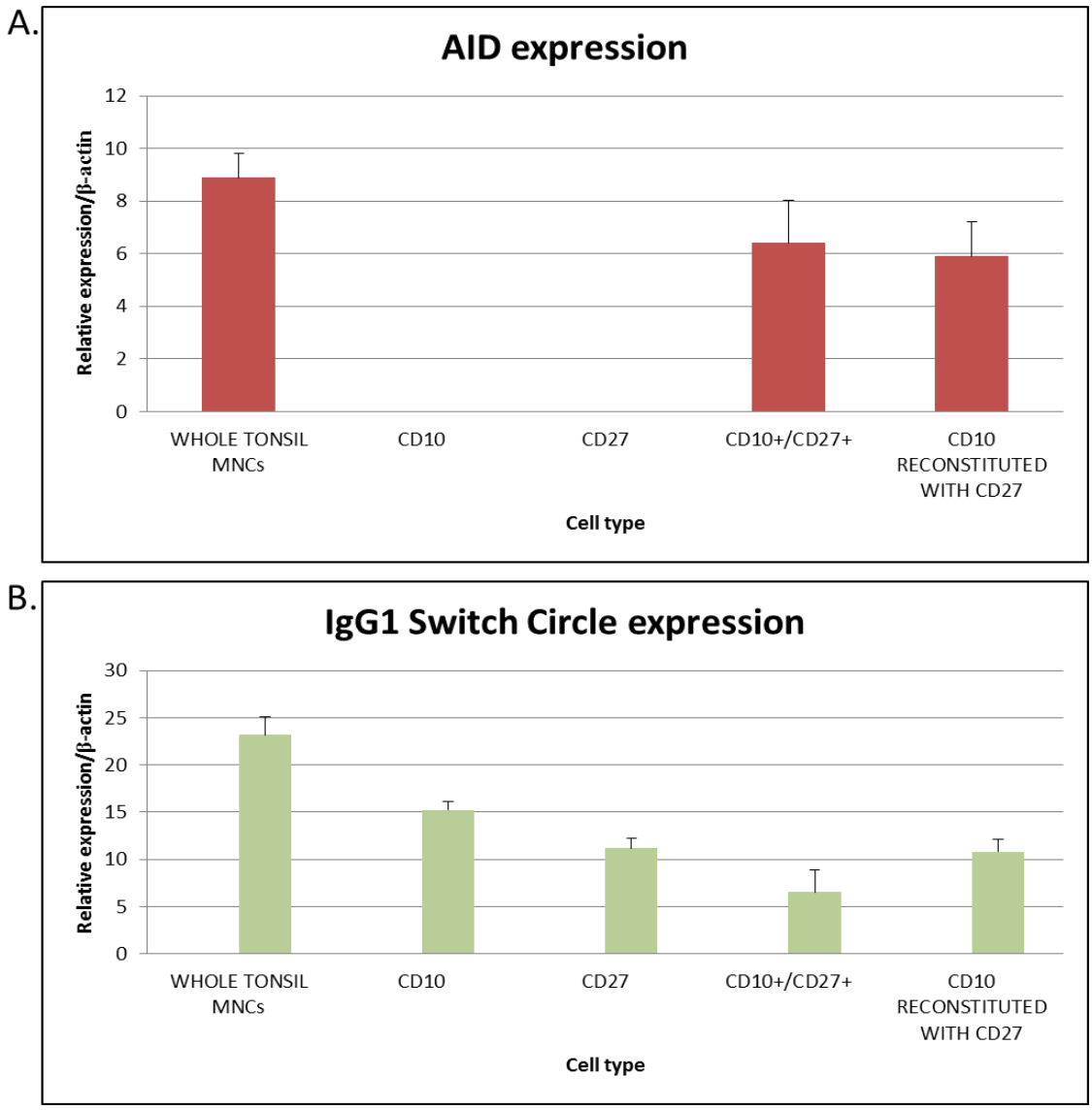

Figure 21. P.*falciparum* extract stimulation of AID and IgG1 switch circle mRNA in whole tonsil MNCs, GC, or memory B cells. qRT-PCR was used to determine relative expression of AID (top graph) and IgG1 switch circle (bottom graph) mRNA to β-actin in: whole tonsil MNCs, GC (CD10+), memory (CD27+), GC/memory (CD10+/CD27+), and isolated GCs reconstituted with memory B cells (CD10+ reconstituted with CD27+) stimulated with 3D7 extracts (+CD40L/IL4) for 5 days.

3.5. Summary of key findings

Taken together, my data provides supporting elucidation on the significant role *P.falciparum* plays in the steps leading to eBL pathogenesis:

1. *P.falciparum* is capable of inducing AID expression and activity.

2. *P.falciparum* requires antigen PfEMP1 in order to optimally induce AID.

3. *P.falciparum* targets the GC and memory B cell compartment for inducing class switching.

The *in vitro* stimulation assays have shown that the P.*falciparum* extract not only induces AID mRNA but also causes the production of IgG1 switch circles, which is an established marker of ongoing CSR. Therefore, for the first time it is clear *P.falciparum* is capable of stimulating AID both in terms of expression and functionality.

In order to address the question of what components of the *P.falciparum* parasite are functioning in AID induction, extracts of the DC-J strain were utilized, which lacks the *P.falciparum*-specific protein- PfEMP1. We have found that the DC-J extract only triggers AID induction at levels similar to what is produced by the control agonist CpG, and significantly lower than with 3D7 extracts (the wildtype strain of *P.falciparum*).

Finally, isolation of specific B cell subpopulations for stimulation assays revealed that *P.falciparum* does not in fact stimulate naïve B cells to induce AID, but rather targets the GC and memory B cell compartments, as demonstrated by the production of IgG1 switch circles in both of these B cell subtypes.

Discussion of my findings and future implications for the study of *P.falciparum* and its role in eBL will be discussed in the next chapter.

4. Discussion and Future Directions

4.1 AID-induced mutation frequency in Ghana vs. Boston do not correlate to in vivo levels of AID mRNA expression in GC B cells.

Studies from our lab demonstrated *P.falciparum* targets GC B cells by deregulating the expression of AID (Torgbor et al., 2014). More specifically, Torgbor et al. showed that in Ghana tonsil GC B cells, there is an overall 5-fold increase in AID mRNA expression when compared to control tonsils (*see Figure 23*) (Torgbor et al., 2014). By this logic, our expectation was to see a concomitant increase in AID-induced mutations in tonsil GC B cells from Ghana when compared to Boston. Naïve and GC B cells were analyzed from three Boston and two Ghana tonsils. The AID mRNA expression level of the Boston tonsils specifically used for this mutation analysis (n=3), matched up closely to what was observed in tonsils from this background by Torgbor et al. There was no RNA leftover for the Ghana tonsil cells used for this mutation study to do a simultaneous measurement of Ghana GC AID levels. However, Charles Torgbor had previously profiled AID expression in one of the two Ghana tonsils used for this mutation analysis. Considering his original data, there is similarly about a 5-fold increase in AID expression when compared to the overall Boston measurement. (*Figure 24*). Therefore, we used two different backgrounds (Ghana - malaria and Boston - malaria-free) for GC B cells, knowing that Ghana on the whole expresses AID at a significantly higher level in this cell type.

c-myc exons 1 and 2 were analyzed in Ghana and Boston B cells. These loci within c-myc have been shown to acquire mutations in BL (see introduction *Figure 3*). Since c-

myc is involved in the characteristic lesion of BL, it was appropriate to study this locus for AID mutational activity in the two backgrounds.

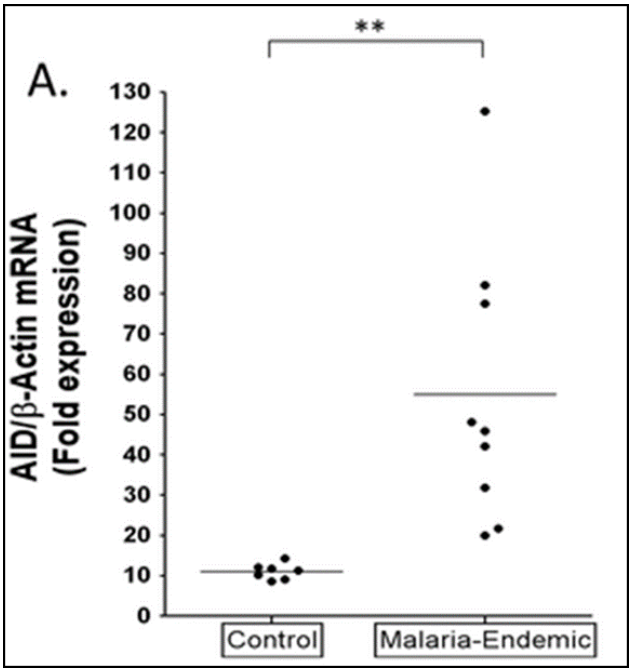

Figure 22. **AID mRNA expression in GC B cells from malaria-endemic region (Ghana) and non-malaria region (Boston)**. Adapted from (Torgbor et al., 2014).

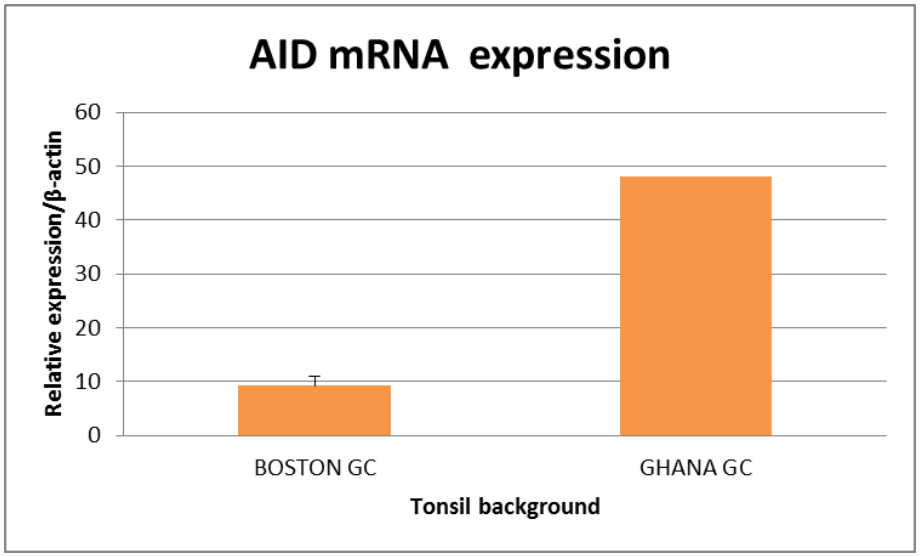

Figure 23. Overall AID mRNA expression in Boston and Ghana tonsil GC B cells. AID mRNA expression levels were measured by qRT-PCR and compared in Boston tonsil GC B cells (n=3) vs. Ghana tonsil GC B cells (n=1).

Contrary to what we expected, we found that there was no significant difference in mutation rate or frequencies in c-myc from Ghana vs. Boston (insignificant p-value) (*Table 2*) which does not support our prediction that AID targets c-myc for mutation at a higher level in individuals with malaria.

Therefore, our mutation analysis results indicate that higher AID mRNA expression in Ghana tonsil GCs do not detectably correlate with anomalous AID activity *in vivo*. We are confident that this is not a technical issue, since upon analyzing rearranged IgVH genes for somatic mutations, we found a mutation frequency within the reported physiological range for both naïve and GC B cell subsets (*Table 2*) (Kuppers and Dalla-Favera, 2001). This indicates that we can observe normal levels of somatic hypermutation by AID in these cells. Concurrently, β-globin served as a negative control and exhibited little to no mutations, as one would expect (*Table 2*). In the future it would be preferable to utilize non-B cells as a negative control, i.e. cells in which AID is not expressed, to function as a true negative control for AID mutational activity.

The attained results could be accounted for by several explanations:

1. We have been studying the whole population of GC B cells from tonsils. But we currently have not confirmed if AID is expressed in more cells, or just very highly in a small population of cells. Perhaps, if we use intracellular staining of AID to detect cells expressing high AID and specifically analyze mutations in these, we could observe distinct differences. Until now, we have been looking at all GC B cells, irrespective of individual AID expression.

2. It is known that p53 is mutated in ~30% of eBL tumors (Lindstrom and Wiman, 2002). In addition, recently Robbiani et al. demonstrated that BL translocations will only occur in a mouse model of malaria with high AID expression if p53 has been deleted (Robbiani et al., 2015). So in order to observe mutations, these particular cells would have needed to evade apoptosis. It is very probable that in the tonsil cells analyzed, the 'damaged' cells with deleterious mutations will go by undetected as those cells likely would have undergone apoptosis.

3. These results could also be indicative of a lack of increased AID-induced mutation accumulation despite higher levels of AID. A potential reason for not detecting higher levels of AID-induced mutations in cells shown to have an overall higher level of AID expression, could be due to the fact that high-fidelity repair mechanisms, as previously described (Liu et al., 2008), are active for c-myc in the analyzed individuals, essentially masking the actual AID activity at this locus. This also ties in with the p53-mediated protective mechanisms that are in place, as described earlier, which would drive damaged cells caused by aberrant AID activity through the apoptosis pathway.

It is also important to mention that the time lapse between AID transcript levels increasing and expression of protein and the actual appearance of mutations in c-myc due to its aberrant activity has not been clearly defined. It is possible that these same cells collected at alternative time points would display more evidence of AID action. In addition, as discussed above, techniques for pinpointing specific cells with varying levels of AID expression may be necessary. Currently, the isolation and assessment of all GC

cells regardless of individual AID expression, could potentially be predominantly representative of cells with usual AID levels.

Altogether, there are two lines of thought that could explain the results that we gathered from the mutation analysis of c-myc in Ghana vs. Boston. Either high-fidelity repair or protective mechanisms/ the apoptosis pathway, could be shielding the individual from amassing mutated cells as they are potentially dangerous, especially when a proto-oncogene such as c-myc is a target. Or, in the future, alternative analysis techniques can be utilized to more closely examine the specific cells of interest (i.e. the GC cells with higher vs. normal AID expression), which may reveal differences.

4.2. P.falciparum induces active AID at least in part via PfEMP1

People living in the holoendemic malaria region are exposed to many additional infectious agents, creating a possibility that the *in vivo* tonsil samples used for mutation analysis are not demonstrating a direct effect of malaria. Introducing *P.falciparum* to primary B cells *in vitro* determines whether increased AID induction and activity is directly caused by malaria.

Results so far gathered using self-developed 3D7 extract for *in vitro* stimulation are consistent with previous results (Torgbor et al., 2014). By day 5, there is a 5 fold increase of AID mRNA in *P.falciparum* extract (+CD40-L and IL-4) - stimulated B cells as compared to CD40-L/IL-4-stimulated cells and this is statistically significant (p value = 0.003). (*Figure 8b*).

Although it has been shown that *P.falciparum* binds B cells and causes AID induction (Donati et al., 2004; Torgbor et al., 2014), this is the first time an attempt has been made to evaluate AID action in the GC environment (where the c-myc/Ig translocation occurs), by means of malaria. This brings us closer to the real physiology in the attempt to decipher how malaria might contribute to eBL via its effect on the GC. Our data show that *P.falciparum* is capable of prompting AID activity (class switching), which suggests that the parasite provides appropriate signals for full activation of AID. Through the *in vitro* stimulation assay, and detection of IgG1 switch circle transcripts (*see Figure 15 and Appendix, switch circle assay design*), we were able to confirm that the parasite is capable of inducing functional AID (*Figure 16*) significantly more than CD40L/IL4 alone (p value = 0.01). Therefore, not only was AID expression induced by malaria, as

consistently seen before, but also a product of its activity was detected, confirming the malaria-prompted AID to be active.

Subsequent to the design and execution of these switch circle experiments, and during literature review for writing this thesis, we came across a largely inaccessible, but relevant study which demonstrated that incubation of human B cells from the peripheral blood induces AID and class switch recombination (Potup et al., 2009). In this study, conventional PCR was utilized in order to detect IgG switch circle transcripts, which gave a signal in 2 out of the 4 experiments stimulated with parasite extract (+CD40L/IL4). However, IgG switch circle transcripts were also detected in 2 out of the 4 experiments stimulated just with CD40L/IL4 alone (Potup et al., 2009), deeming this result inconclusive in terms of demonstrating class switching to IgG from IgM as a result of malaria.

Therefore, this latest data (*Figure 16*) for the first time ascertains that *P.falciparum* malaria infection induces increased AID activity in the disease setting of BL. In addition, these results provide a consistent quantitative determination of increased AID activity (higher levels of IgG1 switch circles produced) specifically as a result of *P.falciparum*, when compared to the impact of control agonists (CD40L/IL4) alone. It may be a fruitful direction to analyze levels of alternative switch circles in addition to IgG1 (e.g. IgG2, IgG4, IgE) as it is plausible that the *P.falciparum* is capable of causing a shift of switching to other isotypes when inducing AID, as other cytokines and stimulants are capable of doing.

We have additionally continued to address the question of what components of the parasite are acting in inducing AID by utilizing the extract of the *P.falciparum* line, DC-J which lacks the *P.falciparum*-specific protein PfEMP1. As mentioned earlier, studies from our lab revealed that hemozoin, a malarial metabolic byproduct and known activator of TLR9 (Parroche et al., 2007), is capable of appreciably augmenting AID expression in the presence of CD40L/IL4 (Torgbor et al., 2014). We have found that DC-J is unable to trigger AID induction to the same levels as with the wildtype *P.falciparum* extract, 3D7 (p value = 0.03, 0.02) (*Figure 10 and 12*). In fact, DC-J is only able to induce AID at similar levels to CpG-stimulated cultures (insignificant p value). Since the DC-J strain lacks PfEMP1 but still makes hemozoin, this fits our prediction that the mutant strain would be as effective as CpG but less so than wild type parasite extract in inducing AID. This result also indicates that PfEMP1 is a requisite for maximal AID induction.

We also have demonstrated that surface Ig-crosslinking complements the DC-J extract in inducing AID. We have already consistently shown that without PfEMP1, *P.falciparum* can only induce AID to equivalent levels to that of CpG and not as well as with the wildtype extract (*Figure 10 and 12*). Subsequently, we performed assays in which we complemented the DC-J strain with anti-Ig, to provide it with the capability of BCR activation via surface Ig crosslinking. Again, we found similar trends as before, with CpG being complemented by anti-Ig, and inducing AID to (higher or) similar levels as with stimulation using the 3D7 extract (*Figure 13 and 14*). The mutant extract which lacks PfEMP1 again was unable to induce AID any higher than with CpG (*Figure 13 and 14*). Interestingly, using the first batch of parasite extract that was prepared in the lab, we

found that with the addition of anti-Ig, it not only brought the mutant DC-J strain's induction of AID up to the wildtype 3D7 extract levels, but even higher (*Figure 13*). This suggests that anti-Ig is certainly serving the purpose of PfEMP1, and potentially the anti-Ig worked better than PfEMP1 in activating the BCR. One way of explaining this result is that the concentration of the parasite extract had not been optimized prior to this assay and perhaps the DC-J extract was not being utilized at an optimal concentration. Carrying out a titration of the 3D7 and DC-J parasite extracts seemed to decrease this dramatic rise in AID signal with anti-Ig stimulation (*see Figure 11 and Figure 14*). Surface Ig-crosslinking using anti-Ig needs to be further scrutinized however, and can be done so by carrying out dose-response curves with anti-Ig.

As mentioned above, optimization for the parasite extract concentration needed to be determined, and the assay repeated. Following preparation of a new set of parasite extracts, and titration of a range of concentrations (*Figure 11*), we determined an optimal concentration that works for maximal AID induction through the wildtype 3D7 and mutant DC-J extracts. Repeating the *in vitro* assays testing surface-Ig crosslinking using anti-Ig alongside the new extracts, we were able to resolve the dramatic increase in AID induction through DC-J extract + anti-Ig to match levels similar to the wildtype 3D7 extract (*Figure 14*). An important point to take into consideration is that when protein concentration is determined for parasite extracts, it does not account for hemozoin content. However, since we know hemozoin plays a significant role in AID induction, it is critical to measure the levels of hemozoin content in each parasite extract batch that is prepared. Differences in hemozoin quantity across parasite extract batches, for both 3D7 and DC-J could explain the variability we have observed in terms of optimal

concentrations and levels of AID induction. Knowing the amount of hemozoin would also shed more light on the dosing impact on AID induction, and also more strongly confirm its stimulating ability in the *in vitro* assays. There are methods that have been produced for measuring hemozoin concentration and content and can be used in this context in the future (Levesque et al., 1999).

The overall message from these experiments is that PfEMP1 is likely to be essential for AID induction through the BCR, as shown by the effects of anti-Ig in combination with CpG or with the DC-J parasite extract. We already know that PfEMP1 is capable of binding to and activating Ig (Chen et al., 2000; Donati et al., 2006b). Taking these results together with previous studies regarding TLR9 activation and AID induction through hemozoin (Parroche et al., 2007; Torgbor et al., 2014), we can infer that *P.falciparum* can provide both the BCR and TLR9 signals. Interestingly, only *P.falciparum* can provide the combination of the requisite signals for AID induction (BCR and TLR9) through its specific ligands, as PfEMP1 is only expressed by the *falciparum* strain along with the production of hemozoin. This also would explain the exclusive link of *P.falciparum* malaria with eBL.

A fruitful future direction with this research is to test exogenous PfEMP1 during *in vitro* stimulation assays, to determine its impact on AID expression and function. If PfEMP1 as we hypothesize and our current data strongly suggests, does act through the BCR, we should observe a rescue of normal AID induction patterns using soluble PfEMP1 protein alongside the DC-J extract. In addition, experiments utilizing hemozoin as we did in the

past (Torgbor et al., 2014), in combination with exogenous PfEMP1 should shed more light on and confirm whether these two malarial components serve as the TLR9 and BCR modes of AID induction by malaria. In addition, tools for analyzing gene expression profiles in B cells unstimulated or stimulated with malarial parasite such as RNA-sequencing would be particularly useful for future work. RNA sequencing could be used to highlight and categorize genes that are specifically impacted by malaria infection. This would open up more avenues for alternative or additional pathways that are impacted by malaria (e.g. cell cycle regulation, apoptosis, regulation of AID), which could be tied in with the direct BCR and TLR9 routes that have recently been investigated by this thesis.

4.3. P.falciparum induces active AID in the GC and memory B-cell compartments

It is well established that CD40L and IL4 are traditional 'T-cell help' and cytokine signatures that are capable of activating naïve B cells. Therefore, it came as no surprise that the combination of CD40L and IL4 during *in vitro* stimulation of whole tonsil MNCs was consistently capable of inducing AID expression (e.g. *Figure 8)*. However, this stimulating combination was unable to induce the production of IgG1 switch circles in the same whole tonsil MNC population (*Figure 16B*). (IgG1 switch circles were detectable in CD40L/IL4-stimulated cells by the real time assay, however there were lower levels than that produced in unstimulated cells, which equates to no induced IgG1 switch circles/ lack of ongoing CSR). The unstimulated cells demonstrate a high level of IgG1 switch circles (not graphically shown; relative expression of AID in unstimulated cells was subtracted from values determined for all other stimulating conditions).

However, what we do see is that the parasite extracts (both 3D7 and DC-J) are capable of inducing AID and IgG1 switch circles in whole tonsil MNCs (*Figure 16A,B*). These results recapped that whole tonsil MNCs includes B cell subsets, such as GCs and memory, which could have a background level of ongoing CSR/ IgG1 switch circles that is overshadowing the stimulating impact of CD40L/IL4 on these cells. Additionally, we deduced the parasite extract may act on a different compartments of B cells compared to CD40L/IL4, and therefore this drove us to evaluate stimulation of different B cell subsets for AID induction and activity. Also of note, is that anti-Ig when combined with the 3D7 extract in stimulating whole tonsil MNCs seems to reduce the AID and IgG1 switch circle signals when compared to 3D7-stimulated alone (Figure 16), although insignificantly. Perhaps, after saturation of the optimal concentration of 3D7 extract, anti-Ig begins to have an inhibitory effect. This issue can be resolved by carrying out a competition assay of 3D7 and a dose response titration of anti-Ig.

Figure 17 shows an interesting finding demonstrating that, as we expected, CD40L/IL4 induces functional AID (determined by AID and IgG1 switch circle mRNA) in naïve B cells. However, what was unanticipated is that the parasite extracts (+CD40L/IL4) were unable to induce a signal for either AID expression or CSR to IgG1 in naïve B cells. Contrary to what we expected, *P.falciparum* does not stimulate AID in naïve B cells in the same manner as it does in whole tonsil MNCs (*Figure 17*). This was also confirmed when we further assessed B cell subsets: naïve B cells, as well as GC and memory B cells (CD10+/CD27+), discovering that the parasite induces active AID in the CD10+/CD27+ cells, but not in the naïve cells at the same time point (*Figure 19*). These results do not rule out the possibility that the parasite is activating naïve B cells, as this has not entirely

been confirmed. In the future, it is necessary to establish a time course assay for AID induction in response to parasite stimulation in naïve B cells. It could certainly be that the kinetics of AID expression and activity is changed in B cell subsets such as naïve B cells when analyzed separately in culture. Subsequently, we analyzed individual CD10+ (GC) or CD27+ (memory) populations in order to define the B cells targeted by *P.falciparu*m, specifically. Interestingly, *P.falciparum* extract was capable of stimulating CSR to IgG1 in both the GC and memory B cell subsets (*Figure 21*).

Evidently, CD10+ and CD27+ cells separately and alone, stimulated with parasite, are unable to provide a signal for AID expression (even though they provide evidence of ongoing CSR/ production of transient IgG1 switch circles) (*Figure 21A*). Again, this requires further investigation through a time course assay and/or analysis of AID kinetics in separate B cells subsets upon parasite stimulation, as it is plausible that when tonsil B cell subsets are separated (naïve, GC, memory), they do not act in the way that they would do so physiologically in an environment where they are never in isolation.

To recap, the relative expression of AID in this experiment was calculated by subtracting the value for the unstimulated condition for each B cell subset from each of the values for the corresponding parasite-stimulated B cell subsets. Consequently, AID levels for each of these B cell subpopulations, unstimulated, is not shown. As expected though, we did see a base level of AID expression in the unstimulated GC (CD10+) population; however, this was higher than the level you see upon stimulation with parasite, and therefore theoretically there was no detectable augmentation of AID expression at this time point in

separate GC and memory B cell populations with parasite stimulation. However, when CD10+ and CD27+ cells are isolated and then reconstituted together, or isolated together, we see increased AID expression, which correlates with the IgG1 switch circles, the production of which is also augmented with parasite stimulation, when compared to the unstimulated state (*Figure 21*). Upon these observations, it is feasible to think that the *in vitro* assays need to more closely mimic the *in vivo* setting where B cell subpopulations coexist, and are never activated separately. These results also point out the instability of AID expression *in vitro*, especially in separated B cell subpopulations. In any case, it is clear that under all cell-separating protocols (whole tonsil MNCs, CD10+, CD27+, separately or together (*see Figure 18 and 20*), *P.falciparum* is capable of inducing CSR to IgG1 (*Figure 21B*), backing the premise that it prompts functional AID.

Overall, these provocative results have ascertained the targeting of *P.falciparum* for AID induction in specific B cell subsets. For the first time, it has become apparent that *P.falciparum* has the ability to stimulate AID activity in the specific cell type of origin for BL, the GC (*Figure 21B*). The GC is already known to exclusively express AID at high levels and are in rapid proliferation mode which would be an ideal setting for the parasite. It is possible to conceive that *P.falciparum* augments AID to such a level in the GC that it begins to lose specificity and target non-Ig genes (an implicit event during the course of BL development). The new data also reveals the memory B cell is a target for *P.falciparum* in stimulating AID activity. It has been demonstrated that children having acute *P.falciparum* infection have an increased proportion of the circulating memory B cell subset compared to the same children 4 weeks post recovery (Asito et al., 2008). It

has also been shown that the CIDR1α domain of PfEMP1 preferentially activates the memory B cell compartment (Donati et al., 2006b). Taking this knowledge into consideration, it perhaps does not come as a surprise to see *P.falciparum* extracts impacting memory B cells by inducing CSR (*Figure 21B*). One mode of thought is that the parasite does indeed target memory B cells for reactivation and drives them to undergo secondary GC reactions. In fact, secondary GC reactions have been shown in IgM+ memory cells (Seifert et al., 2015). This adds to a plausible model of how *P.falciparum* malaria increases the risk for eBL: the parasite stimulates rapidly proliferating GC B cells, as well as reactivates the memory B cells and drives them to undergo secondary GC reactions, during which deregulated expression of AID and earlier infection with EBV will provide the induction of DNA damage/ production of chromosomal translocations and protection from apoptosis required for eBL (*see Figure 24*). In addition, succeeding these results, it points out that the AID-induced mutation analysis in Ghana vs. Boston tonsil cells would be more informative if we compare the memory B cell subset in the future. So far, we have been able to demonstrate deregulated expression and increased function of AID in *P.falciparum*-stimulated B cells. Additional future work that should be performed is analysis of DNA damage and/or translocations in human B cells in response to *P.falciparum* infection. This can be achieved through cytogenetic techniques which have been initiated and described in the Appendix (*see Appendix, Figure A2*). These experiments for the first time would analyze the effects on DNA in human B cells caused directly by *P.falciparum,* as so far this has only been analyzed in mouse models with the *P.chabaudi* parasite (Robbiani et al., 2015).

To end with, high AID activity inducing class switching to IgG1 in B cells stimulated with *P.falciparum*, is evidence for the parasite increasing the probability for a c-myc/Ig translocation to occur in GC B cells, which could seed eBL (*see Figure 24*). PfEMP1 potentially plays the important role of BCR activation, alongside already known hemozoin-induced TLR9 activation. It remains to be seen however how PfEMP1 (exogenous protein), with its specific variable domains, serves in AID induction. In addition, in the future, it is crucial that the changes in the gene expression profile of B cells as a response to *P.falciparum* infection are deciphered. This will point towards additional pathways and malaria-specific alterations that could play significant roles in eBL pathogenesis.

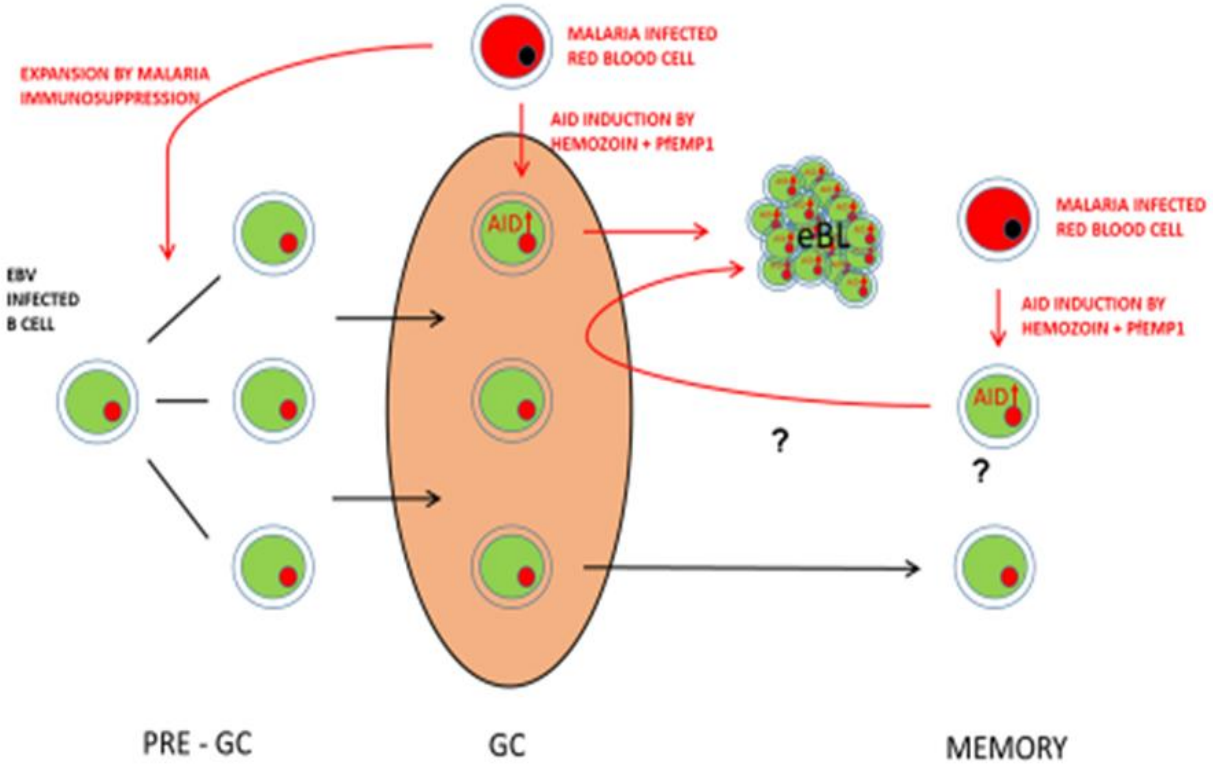

Figure 24. Model: How *P.falciparum* increases the risk for eBL. Malaria is immunosuppressive and this results in a highly elevated throughput of EBV-infected cells in the GC (Torgbor et al., 2014). *P.falciparum* causes increased expression of AID in GC cells (Torgbor et al., 2014), and this deregulated expression can lead to DNA damage, translocations and lymphoma, as shown in mouse models. (Robbiani et al., 2015). This thesis has not only revealed that *P.falciparum* is capable of deregulating AID expression in both GC and memory B cells (which could reenter the GC?), but also that stimulation with this specific parasite induces truly functional AID that carries out class switching to IgG1 in whole tonsil MNCs. In this context, for the first time *P.falciparum* has directly been shown to have functional effects on AID in the GC where eBL originates. Taken altogether, this model explains that *P.falciparum* specifically will synergistically increase the risk that eBL will arise.

5. Appendix

Antibody	Clone	Species	Company	Catalogue no.	Dilution/ 100µL cells
CD10-PE	H110a	Mouse	BD Biosciences	555375	2µL (1/50)
CD19-APC	H1B19	Mouse	BD Biosciences	555415	2µL (1/50)
CD27-APC	MT271	Mouse	BD Biosciences	558664	2.5µL (1/50)
IgD-FITC		Goat	Southern Biotechnologies	2032-02	20µL of 1/100 (1/500)
Anti-Dextran-FITC		Mouse	Stem Cell Technologies	60026F1	2.5µL (1/50)

Table A1. List of antibodies used for extracellular staining

Gene	Genbank Accession no.	Primers	PCR conditions
c-myc	X00364.2	Forward 5' TGAGTCTCCTCCCCACCTTC 3' Reverse 5' CCAAATCTCTCCAGATCTGC 3'	**94°C 5 min** **94°C 15 sec** **60°C 30 sec x 25** **68°C 3 min 30 sec** **4°C hold**
β-globin	NC0001.10	Forward 5' CTGAGGAGAAGTCTGCCGTTAC 3' Reverse 5' GTGCAGCTCACTCAGTGTGGC 3'	**94°C 5 min** **94°C 15 sec** **60°C 15 sec x 25** **68°C 30 sec** **4°C hold**

Table A2. List of primers and PCR conditions for PCR/ mutation analysis

Gene	Life Technologies Assay no./ Forward & Reverse primers	Probe
AID	Hs00221068-m1 AICDA	
β-actin	4333762T	
IgG1 Switch Circle	Forward 5’ GGGCAGGGTCAGCAGTGC 3’ Reverse 5’ CGGATGCACTCCC 3’	5’ CCTCTCAGCCAGGACCAA 3’

Table A3. List of primer/ probe sets for qRT-PCR of AID, IgG1 switch circles and β-actin.

Disovering incorrect switch circle assay design- 2015

In order to correlate sequencing data with AID expression, AID mRNA levels in PBMC naïve B cells was determined (*Figure 7b*). PBMC naïve B cells gave no signal, while tonsil naive B cells gave a minute signal which can be considered background, confirming that there is virtually no AID expressed in naïve B cells, as expected. I also sought out to determine IgG1 switch circle transcript expression (using switch circle-detecting primers and probe described in (Benko et al., 2014)) in PBMC naïve B cells. Surprisingly, this gave me a very high signal consistently (*Appendix Figure A1*). This was puzzling for two reasons: 1. It has been established that naïve B cells do not undergo CSR and therefore should not be producing switch circle transcripts and 2. Switch circle transcripts can't be produced without AID, which is known (and has been shown in *Figure 7b*) to not be expressed in these cells. Similar high signals for 'switch circles' were also produced in unstimulated whole tonsil MNCs of the *in vitro* assays, which was also unexpected (not shown). This triggered me to check the real time PCR reagents, as well as the product itself to confirm the correct region is being amplified. Upon further investigation, and contact with the author of the paper from which the primer/probe set was chosen (Benko et al., 2014), I determined the group had utilized incorrect primers for amplifying the IgG1 switch circle transcript, and in fact was amplifying the IgM transcript (*Appendix Figure A1*). The author has since contacted the editor of this paper and has worked on retracting the portions which involve the switch circle. This therefore dismissed my previous data involving the switch circle using these primers, as it was amplifying the wrong transcript.

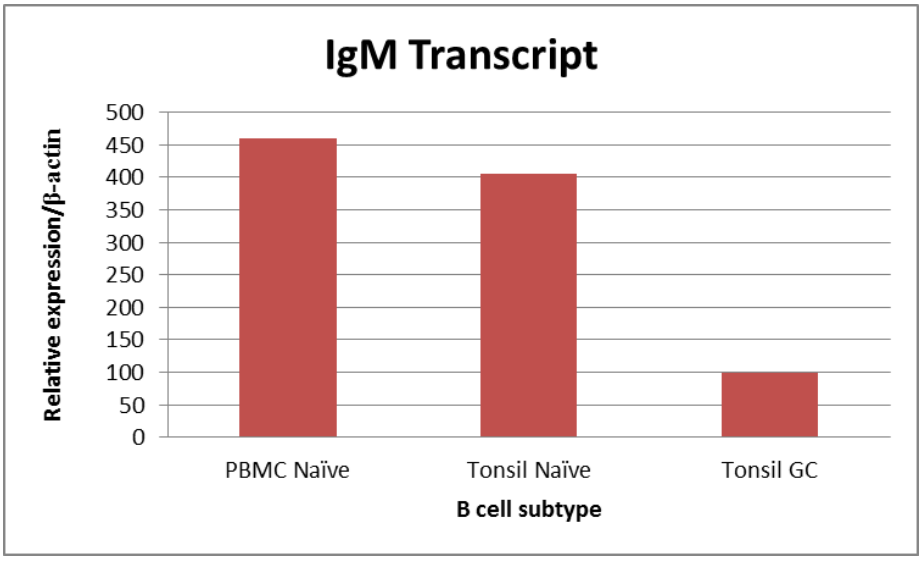

Figure A1. IgM transcript expression in Boston tonsil and PBMC cells. What was thought to be amplifying IgG1 switch circle transcript was discovered to actually be detecting IgM transcript. Expression levels were determined by qRT-PCR and compared in naïve B cells from PBMC (n=6), naïve and GC cells from tonsil (n=3) all of Bostonian origin. These expression level patterns for IgM are as expected in these B cell subtypes.

Subsequently, I designed a new primer and probe set for amplifying the correct gene fusion product which includes Iγ and Cμ, both of which can only be in close proximity of each other as a result of IgG1 class switching, and during transient IgG1 switch circle expression (*see Results, Figure 15*). This new switch circle assay has been confirmed to be amplifying the correct gene product through sequencing, and has been utilized for detecting IgG1 switch circle transcripts for *in vitro* stimulation assays.

Chromosomal damage and/or rearrangements in P.falciparum-stimulated B cells in vitro

Fluorescence in situ hybridization (FISH) is a common approach in detecting and estimating the frequency of c-MYC translocations in normal tissues. Giemsa banding analysis provides a visible karyotype that allows identification and grouping of chromosomes. In the first experiments, we looked for generic DNA damage and rearrangements in the eBL line RAJI. This cell line served as a control for the detection of the (8,14) translocation and experimental optimization. Giemsa-stained chromosomes spread from metaphase-arrested cells were analyzed. These studies were carried out in collaboration with Dr. Janet Cowan (Cytogenetics, Tufts Medical Center). The uniform karyotype of RAJI demonstrates the reciprocal (8;14, q24;q32) translocation indicated by red arrows, as well as several other unbalanced rearrangements shown by blue arrows (*Figure A2*). To specifically detect c-MYC/Ig translocations it will be necessary to develop two-color fluorescence *in situ* hybridization with probes for the Ig heavy chain locus Cμ region and the c-MYC gene. Initially these probes can be used separately with telomere probes to see what fraction of total chromosome breakage is occurring in the Ig and c-MYC loci. Ultimately combinations of the probes will allow us to see if and to what extent Ig/c-MYC translocations are occurring spontaneously in the GC cells. Ultimately, these forms of chromosomal analysis can be used on *P.falciparum*-stimulated tonsil mononuclear cell cultures. The G-banding and telomere studies should provide a good insight into whether the elevated levels of AID are associated with more damage. If so, one should be encouraged to move onto translocation-specific analysis.

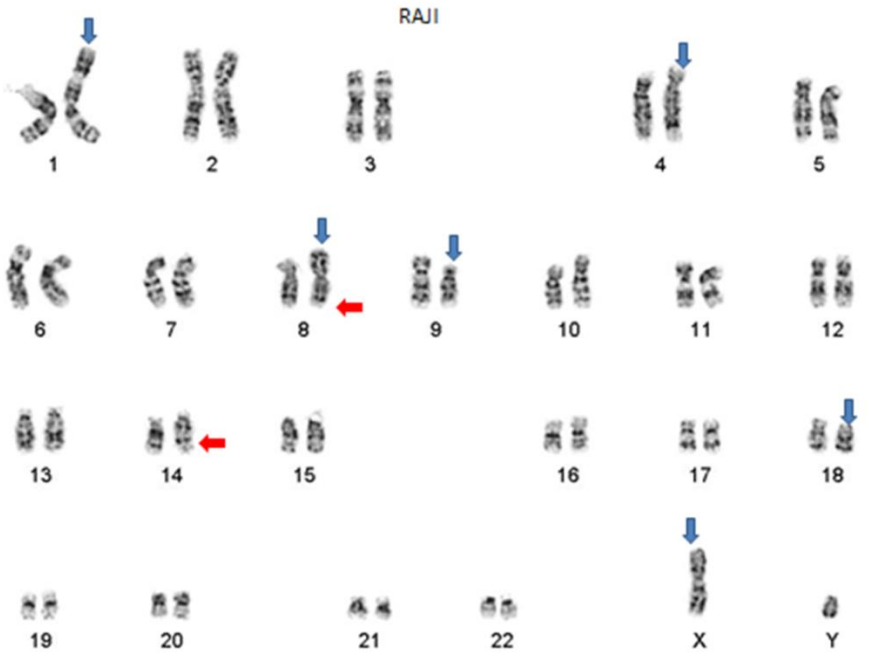

Figure A2. Karyotype of Giemsa-stained RAJI cells. All chromosomal rearrangements, reciprocal and nonreciprocal are shown. Red arrows point out translocation 8,14. Blue arrows indicate abnormal unbalanced rearrangements between chromosomes. Adapted from images of Janet Cowan, Tufts Medical Center.

6. References

Akira, S., and Takeda, K. (2004). Toll-like receptor signalling. Nature reviews Immunology *4*, 499-511.

Anderton, E., Yee, J., Smith, P., Crook, T., White, R.E., and Allday, M.J. (2008). Two Epstein-Barr virus (EBV) oncoproteins cooperate to repress expression of the proapoptotic tumour-suppressor Bim: clues to the pathogenesis of Burkitt's lymphoma. Oncogene *27*, 421-433.

Aoufouchi, S., Faili, A., Zober, C., D'Orlando, O., Weller, S., Weill, J.C., and Reynaud, C.A. (2008). Proteasomal degradation restricts the nuclear lifespan of AID. The Journal of experimental medicine *205*, 1357-1368.

Asito, A.S., Moormann, A.M., Kiprotich, C., Ng'ang'a, Z.W., Ploutz-Snyder, R., and Rochford, R. (2008). Alterations on peripheral B cell subsets following an acute uncomplicated clinical malaria infection in children. Malaria journal *7*, 238.

Babcock, G.J., Decker, L.L., Volk, M., and Thorley-Lawson, D.A. (1998). EBV persistence in memory B cells in vivo. Immunity *9*, 395-404.

Babcock, G.J., and Thorley-Lawson, D.A. (2000). Tonsillar memory B cells, latently infected with Epstein-Barr virus, express the restricted pattern of latent genes previously found only in Epstein-Barr virus-associated tumors. Proceedings of the National Academy of Sciences of the United States of America *97*, 12250-12255.

Bachl, J., Carlson, C., Gray-Schopfer, V., Dessing, M., and Olsson, C. (2001). Increased transcription levels induce higher mutation rates in a hypermutating cell line. Journal of immunology (Baltimore, Md : 1950) *166*, 5051-5057.

Basu, U., Chaudhuri, J., Alpert, C., Dutt, S., Ranganath, S., Li, G., Schrum, J.P., Manis, J.P., and Alt, F.W. (2005). The AID antibody diversification enzyme is regulated by protein kinase A phosphorylation. Nature *438*, 508-511.

Benko, A.L., Olsen, N.J., and Kovacs, W.J. (2014). Glucocorticoid inhibition of activation-induced cytidine deaminase expression in human B lymphocytes. Molecular and cellular endocrinology *382*, 881-887.

Bentley, D.L., and Groudine, M. (1986). A block to elongation is largely responsible for decreased transcription of c-myc in differentiated HL60 cells. Nature *321*, 702-706.

Bernasconi, N.L., Onai, N., and Lanzavecchia, A. (2003). A role for Toll-like receptors in acquired immunity: up-regulation of TLR9 by BCR triggering in naive B cells and constitutive expression in memory B cells. Blood *101*, 4500-4504.

Bhatia, K., Huppi, K., Spangler, G., Siwarski, D., Iyer, R., and Magrath, I. (1993). Point mutations in the c-Myc transactivation domain are common in Burkitt's lymphoma and mouse plasmacytomas. Nature genetics *5*, 56-61.

Bissonnette, R.P., Echeverri, F., Mahboubi, A., and Green, D.R. (1992). Apoptotic cell death induced by c-myc is inhibited by bcl-2. Nature *359*, 552-554.

Bloland, P.B., Boriga, D.A., Ruebush, T.K., McCormick, J.B., Roberts, J.M., Oloo, A.J., Hawley, W., Lal, A., Nahlen, B., and Campbell, C.C. (1999). Longitudinal cohort study of the epidemiology of malaria infections in an area of intense malaria transmission II. Descriptive epidemiology of malaria infection and disease among children. The American journal of tropical medicine and hygiene *60*, 641-648.

Burkitt, D. (1958). A sarcoma involving the jaws in African children. The British journal of surgery *46*, 218-223.

Burkitt, D. (1962). Determining the climatic limitations of a children's cancer common in Africa. British medical journal *2*, 1019-1023.

Burkitt, D.P. (1972). Classics in oncology. A sarcoma involving the jaws in African children. CA: a cancer journal for clinicians *22*, 345-355.

Cesarman, E., Dalla-Favera, R., Bentley, D., and Groudine, M. (1987). Mutations in the first exon are associated with altered transcription of c-myc in Burkitt lymphoma. Science (New York, NY) *238*, 1272-1275.

Chaturvedi, A., Dorward, D., and Pierce, S.K. (2008). The B cell receptor governs the subcellular location of Toll-like receptor 9 leading to hyperresponses to DNA-containing antigens. Immunity *28*, 799-809.

Chaudhuri, J., Khuong, C., and Alt, F.W. (2004). Replication protein A interacts with AID to promote deamination of somatic hypermutation targets. Nature *430*, 992-998.

Chen, Q., Barragan, A., Fernandez, V., Sundstrom, A., Schlichtherle, M., Sahlen, A., Carlson, J., Datta, S., and Wahlgren, M. (1998). Identification of Plasmodium falciparum erythrocyte membrane protein 1 (PfEMP1) as the rosetting ligand of the malaria parasite P. falciparum. The Journal of experimental medicine *187*, 15-23.

Chen, Q., Heddini, A., Barragan, A., Fernandez, V., Pearce, S.F., and Wahlgren, M. (2000). The semiconserved head structure of Plasmodium falciparum erythrocyte membrane protein 1 mediates binding to multiple independent host receptors. The Journal of experimental medicine *192*, 1-10.

Chene, A., Donati, D., Orem, J., Mbidde, E.R., Kironde, F., Wahlgren, M., and Bejarano, M.T. (2009). Endemic Burkitt's lymphoma as a polymicrobial disease: new insights on the interaction between Plasmodium falciparum and Epstein-Barr virus. Seminars in cancer biology *19*, 411-420.

Chookajorn, T., Dzikowski, R., Frank, M., Li, F., Jiwani, A.Z., Hartl, D.L., and Deitsch, K.W. (2007). Epigenetic memory at malaria virulence genes. Proceedings of the National Academy of Sciences of the United States of America *104*, 899-902.

Coban, C., Ishii, K.J., Kawai, T., Hemmi, H., Sato, S., Uematsu, S., Yamamoto, M., Takeuchi, O., Itagaki, S., Kumar, N., *et al.* (2005). Toll-like receptor 9 mediates innate immune activation by the malaria pigment hemozoin. The Journal of experimental medicine *201*, 19-25.

Conticello, S.G. (2008). The AID/APOBEC family of nucleic acid mutators. Genome biology *9*, 229.

Dang, C.V., O'Donnell, K.A., Zeller, K.I., Nguyen, T., Osthus, R.C., and Li, F. (2006). The c-Myc target gene network. Seminars in cancer biology *16*, 253-264.

de-The, G., Geser, A., Day, N.E., Tukei, P.M., Williams, E.H., Beri, D.P., Smith, P.G., Dean, A.G., Bronkamm, G.W., Feorino, P., *et al.* (1978). Epidemiological evidence for causal relationship between Epstein-Barr virus and Burkitt's lymphoma from Ugandan prospective study. Nature *274*, 756-761.

Donati, D., Espmark, E., Kironde, F., Mbidde, E.K., Kamya, M., Lundkvist, A., Wahlgren, M., Bejarano, M.T., and Falk, K.I. (2006a). Clearance of circulating Epstein-Barr virus DNA in children with acute malaria after antimalaria treatment. The Journal of infectious diseases *193*, 971-977.

Donati, D., Mok, B., Chene, A., Xu, H., Thangarajh, M., Glas, R., Chen, Q., Wahlgren, M., and Bejarano, M.T. (2006b). Increased B cell survival and preferential activation of the memory compartment by a malaria polyclonal B cell activator. Journal of immunology (Baltimore, Md : 1950) *177*, 3035-3044.

Donati, D., Zhang, L.P., Chene, A., Chen, Q., Flick, K., Nystrom, M., Wahlgren, M., and Bejarano, M.T. (2004). Identification of a polyclonal B-cell activator in Plasmodium falciparum. Infection and immunity *72*, 5412-5418.

Dorsett, Y., Robbiani, D.F., Jankovic, M., Reina-San-Martin, B., Eisenreich, T.R., and Nussenzweig, M.C. (2007). A role for AID in chromosome translocations between c-myc and the IgH variable region. The Journal of experimental medicine *204*, 2225-2232.

Dzikowski, R., Frank, M., and Deitsch, K. (2006). Mutually exclusive expression of virulence genes by malaria parasites is regulated independently of antigen production. PLoS pathogens *2*, e22.

Dzikowski, R., Li, F., Amulic, B., Eisberg, A., Frank, M., Patel, S., Wellems, T.E., and Deitsch, K.W. (2007). Mechanisms underlying mutually exclusive expression of virulence genes by malaria parasites. EMBO reports *8*, 959-965.

Eischen, C.M., Weber, J.D., Roussel, M.F., Sherr, C.J., and Cleveland, J.L. (1999). Disruption of the ARF-Mdm2-p53 tumor suppressor pathway in Myc-induced lymphomagenesis. Genes & development *13*, 2658-2669.

Epstein, M.A., Achong, B.G., and Barr, Y.M. (1964). VIRUS PARTICLES IN CULTURED LYMPHOBLASTS FROM BURKITT'S LYMPHOMA. Lancet (London, England) *1*, 702-703.

Futagbi, G., Welbeck, J.E., Tetteh, J.K., Hviid, L., and Akanmori, B.D. (2007). Selective activation of TCR-gammadelta+ cells in endemic Burkitt's lymphoma. Malaria journal *6*, 69.

Gaidano, G., Ballerini, P., Gong, J.Z., Inghirami, G., Neri, A., Newcomb, E.W., Magrath, I.T., Knowles, D.M., and Dalla-Favera, R. (1991). p53 mutations in human lymphoid malignancies: association with Burkitt lymphoma and chronic lymphocytic leukemia. Proceedings of the National Academy of Sciences of the United States of America *88*, 5413-5417.

Geser, A., Brubaker, G., and Draper, C.C. (1989). Effect of a malaria suppression program on the incidence of African Burkitt's lymphoma. American journal of epidemiology *129*, 740-752.

Goossens, T., Klein, U., and Kuppers, R. (1998). Frequent occurrence of deletions and duplications during somatic hypermutation: implications for oncogene translocations and heavy chain disease. Proceedings of the National Academy of Sciences of the United States of America *95*, 2463-2468.

Greenwood, B.M., and Vick, R.M. (1975). Evidence for a malaria mitogen in human malaria. Nature *257*, 592-594.

Hafalla, J.C., Silvie, O., and Matuschewski, K. (2011). Cell biology and immunology of malaria. Immunological reviews *240*, 297-316.

Haluska, F.G., Finver, S., Tsujimoto, Y., and Croce, C.M. (1986). The t(8; 14) chromosomal translocation occurring in B-cell malignancies results from mistakes in V-D-J joining. Nature *324*, 158-161.

Harrington, E.A., Fanidi, A., and Evan, G.I. (1994). Oncogenes and cell death. Current opinion in genetics & development *4*, 120-129.

Hayday, A.C., Gillies, S.D., Saito, H., Wood, C., Wiman, K., Hayward, W.S., and Tonegawa, S. (1984). Activation of a translocated human c-myc gene by an enhancer in the immunoglobulin heavy-chain locus. Nature *307*, 334-340.

He, B., Qiao, X., and Cerutti, A. (2004). CpG DNA induces IgG class switch DNA recombination by activating human B cells through an innate pathway that requires TLR9 and cooperates with IL-10. Journal of immunology (Baltimore, Md : 1950) *173*, 4479-4491.

Hecht, J.L., and Aster, J.C. (2000). Molecular biology of Burkitt's lymphoma. Journal of clinical oncology : official journal of the American Society of Clinical Oncology *18*, 3707-3721.

Ho, M., Webster, H.K., Looareesuwan, S., Supanaranond, W., Phillips, R.E., Chanthavanich, P., and Warrell, D.A. (1986). Antigen-specific immunosuppression in human malaria due to Plasmodium falciparum. The Journal of infectious diseases *153*, 763-771.

Hochberg, D., Middeldorp, J.M., Catalina, M., Sullivan, J.L., Luzuriaga, K., and Thorley-Lawson, D.A. (2004). Demonstration of the Burkitt's lymphoma Epstein-Barr virus phenotype in dividing latently infected memory cells in vivo. Proceedings of the National Academy of Sciences of the United States of America *101*, 239-244.

Hopwood, P., and Crawford, D.H. (2000). The role of EBV in post-transplant malignancies: a review. Journal of clinical pathology *53*, 248-254.

Ito, S., Nagaoka, H., Shinkura, R., Begum, N., Muramatsu, M., Nakata, M., and Honjo, T. (2004). Activation-induced cytidine deaminase shuttles between nucleus and cytoplasm like apolipoprotein B mRNA editing catalytic polypeptide 1. Proceedings of the National Academy of Sciences of the United States of America *101*, 1975-1980.

Jensen, J.B., Trager, W., and Doherty, J. (1979). Plasmodium falciparum: continuous cultivation in a semiautomated apparatus. Experimental parasitology *48*, 36-41.

Khanna, R., and Burrows, S.R. (2000). Role of cytotoxic T lymphocytes in Epstein-Barr virus-associated diseases. Annual review of microbiology *54*, 19-48.

Kinoshita, K., Harigai, M., Fagarasan, S., Muramatsu, M., and Honjo, T. (2001). A hallmark of active class switch recombination: transcripts directed by I promoters on looped-out circular DNAs. Proceedings of the National Academy of Sciences of the United States of America *98*, 12620-12623.

Kuppers, R., and Dalla-Favera, R. (2001). Mechanisms of chromosomal translocations in B cell lymphomas. Oncogene *20*, 5580-5594.

Kuppers, R., Schneider, M., and Hansmann, M.L. (2013). Laser-based microdissection of single cells from tissue sections and PCR analysis of rearranged immunoglobulin genes from isolated normal and malignant human B cells. Methods in molecular biology (Clifton, NJ) *971*, 49-63.

Levesque, M.A., Sullivan, A.D., and Meshnick, S.R. (1999). Splenic and hepatic hemozoin in mice after malaria parasite clearance. The Journal of parasitology *85*, 570-573.

Lindstrom, M.S., and Wiman, K.G. (2002). Role of genetic and epigenetic changes in Burkitt lymphoma. Seminars in cancer biology *12*, 381-387.

Liu, M., Duke, J.L., Richter, D.J., Vinuesa, C.G., Goodnow, C.C., Kleinstein, S.H., and Schatz, D.G. (2008). Two levels of protection for the B cell genome during somatic hypermutation. Nature *451*, 841-845.

Liu, M., and Schatz, D.G. (2009). Balancing AID and DNA repair during somatic hypermutation. Trends in immunology *30*, 173-181.

Magrath, I. (1990). The pathogenesis of Burkitt's lymphoma. Advances in cancer research *55*, 133-270.

Magrath, I. (2012). Epidemiology: clues to the pathogenesis of Burkitt lymphoma. British journal of haematology *156*, 744-756.

Marcu, K.B., Bossone, S.A., and Patel, A.J. (1992). myc function and regulation. Annual review of biochemistry *61*, 809-860.

McBride, K.M., Gazumyan, A., Woo, E.M., Barreto, V.M., Robbiani, D.F., Chait, B.T., and Nussenzweig, M.C. (2006). Regulation of hypermutation by activation-induced cytidine deaminase phosphorylation. Proceedings of the National Academy of Sciences of the United States of America *103*, 8798-8803.

McBride, K.M., Gazumyan, A., Woo, E.M., Schwickert, T.A., Chait, B.T., and Nussenzweig, M.C. (2008). Regulation of class switch recombination and somatic mutation by AID phosphorylation. The Journal of experimental medicine *205*, 2585-2594.

Moormann, A.M., Chelimo, K., Sumba, O.P., Lutzke, M.L., Ploutz-Snyder, R., Newton, D., Kazura, J., and Rochford, R. (2005). Exposure to holoendemic malaria results in elevated Epstein-Barr virus loads in children. The Journal of infectious diseases *191*, 1233-1238.

Moormann, A.M., Chelimo, K., Sumba, P.O., Tisch, D.J., Rochford, R., and Kazura, J.W. (2007). Exposure to holoendemic malaria results in suppression of Epstein-Barr virus-specific T cell immunosurveillance in Kenyan children. The Journal of infectious diseases *195*, 799-808.

Morrow, R.H., Jr. (1985). Epidemiological evidence for the role of falciparum malaria in the pathogenesis of Burkitt's lymphoma. IARC scientific publications, 177-186.

Muramatsu, M., Kinoshita, K., Fagarasan, S., Yamada, S., Shinkai, Y., and Honjo, T. (2000). Class switch recombination and hypermutation require activation-induced cytidine deaminase (AID), a potential RNA editing enzyme. Cell *102*, 553-563.

Muramatsu, M., Sankaranand, V.S., Anant, S., Sugai, M., Kinoshita, K., Davidson, N.O., and Honjo, T. (1999). Specific expression of activation-induced cytidine deaminase (AID), a novel member of the RNA-editing deaminase family in germinal center B cells. The Journal of biological chemistry *274*, 18470-18476.

Ocana-Morgner, C., Mota, M.M., and Rodriguez, A. (2003). Malaria blood stage suppression of liver stage immunity by dendritic cells. The Journal of experimental medicine *197*, 143-151.

Omukunda, E., Githeko, A., Ndong'a, M.F., Mushinzimana, E., Atieli, H., and Wamae, P. (2013). Malaria vector population dynamics in highland and lowland regions of western Kenya. Journal of vector borne diseases *50*, 85-92.

Parkin, D.M., Bray, F., Ferlay, J., and Jemal, A. (2014). Cancer in Africa 2012. Cancer epidemiology, biomarkers & prevention : a publication of the American Association for Cancer Research, cosponsored by the American Society of Preventive Oncology *23*, 953-966.

Parroche, P., Lauw, F.N., Goutagny, N., Latz, E., Monks, B.G., Visintin, A., Halmen, K.A., Lamphier, M., Olivier, M., Bartholomeu, D.C., *et al.* (2007). Malaria hemozoin is immunologically inert but radically enhances innate responses by presenting malaria DNA to Toll-like receptor 9. Proceedings of the National Academy of Sciences of the United States of America *104*, 1919-1924.

Paschos, K., Parker, G.A., Watanatanasup, E., White, R.E., and Allday, M.J. (2012). BIM promoter directly targeted by EBNA3C in polycomb-mediated repression by EBV. Nucleic acids research *40*, 7233-7246.

Pasternak, N.D., and Dzikowski, R. (2009). PfEMP1: an antigen that plays a key role in the pathogenicity and immune evasion of the malaria parasite Plasmodium falciparum. The international journal of biochemistry & cell biology *41*, 1463-1466.

Pavri, R., Gazumyan, A., Jankovic, M., Di Virgilio, M., Klein, I., Ansarah-Sobrinho, C., Resch, W., Yamane, A., Reina San-Martin, B., Barreto, V., *et al.* (2010). Activation-induced cytidine deaminase targets DNA at sites of RNA polymerase II stalling by interaction with Spt5. Cell *143*, 122-133.

Pelicci, P.G., Knowles, D.M., 2nd, Magrath, I., and Dalla-Favera, R. (1986). Chromosomal breakpoints and structural alterations of the c-myc locus differ in endemic and sporadic forms of Burkitt lymphoma. Proceedings of the National Academy of Sciences of the United States of America *83*, 2984-2988.

Perlmann, P., and Troye-Blomberg, M. (2002). Malaria and the immune system in humans. Chemical immunology *80*, 229-242.

Pichyangkul, S., Yongvanitchit, K., Kum-arb, U., Hemmi, H., Akira, S., Krieg, A.M., Heppner, D.G., Stewart, V.A., Hasegawa, H., Looareesuwan, S., *et al.* (2004). Malaria blood stage parasites activate human plasmacytoid dendritic cells and murine dendritic cells through a Toll-like receptor 9-dependent pathway. Journal of immunology (Baltimore, Md : 1950) *172*, 4926-4933.

Potup, P., Kumsiri, R., Kano, S., Kalambaheti, T., Looareesuwan, S., Troye-Blomberg, M., and Maneerat, Y. (2009). Blood stage Plasmodium falciparum antigens induce immunoglobulin class switching in human enriched B cell culture. The Southeast Asian journal of tropical medicine and public health *40*, 651-664.

Ramiro, A.R., Jankovic, M., Callen, E., Difilippantonio, S., Chen, H.T., McBride, K.M., Eisenreich, T.R., Chen, J., Dickins, R.A., Lowe, S.W., *et al.* (2006). Role of genomic instability and p53 in AID-induced c-myc-Igh translocations. Nature *440*, 105-109.

Ramiro, A.R., Jankovic, M., Eisenreich, T., Difilippantonio, S., Chen-Kiang, S., Muramatsu, M., Honjo, T., Nussenzweig, A., and Nussenzweig, M.C. (2004). AID is required for c-myc/IgH chromosome translocations in vivo. Cell *118*, 431-438.

Rasti, N., Falk, K.I., Donati, D., Gyan, B.A., Goka, B.Q., Troye-Blomberg, M., Akanmori, B.D., Kurtzhals, J.A., Dodoo, D., Consolini, R., *et al.* (2005). Circulating epstein-barr virus in children living in malaria-endemic areas. Scandinavian journal of immunology *61*, 461-465.

Rebhandl, S., Huemer, M., Greil, R., and Geisberger, R. (2015). AID/APOBEC deaminases and cancer. Oncoscience *2*, 320-333.

Robbiani, D.F., Bothmer, A., Callen, E., Reina-San-Martin, B., Dorsett, Y., Difilippantonio, S., Bolland, D.J., Chen, H.T., Corcoran, A.E., Nussenzweig, A., *et al.* (2008). AID is required for the chromosomal breaks in c-myc that lead to c-myc/IgH translocations. Cell *135*, 1028-1038.

Robbiani, D.F., Bunting, S., Feldhahn, N., Bothmer, A., Camps, J., Deroubaix, S., McBride, K.M., Klein, I.A., Stone, G., Eisenreich, T.R., *et al.* (2009). AID produces DNA double-strand breaks in non-Ig genes and mature B cell lymphomas with reciprocal chromosome translocations. Molecular cell *36*, 631-641.

Robbiani, D.F., Deroubaix, S., Feldhahn, N., Oliveira, T.Y., Callen, E., Wang, Q., Jankovic, M., Silva, I.T., Rommel, P.C., Bosque, D., *et al.* (2015). Plasmodium Infection Promotes Genomic Instability and AID-Dependent B Cell Lymphoma. Cell *162*, 727-737.

Rochford, R., Cannon, M.J., and Moormann, A.M. (2005). Endemic Burkitt's lymphoma: a polymicrobial disease? Nature reviews Microbiology *3*, 182-187.

Rowe, M., Rowe, D.T., Gregory, C.D., Young, L.S., Farrell, P.J., Rupani, H., and Rickinson, A.B. (1987). Differences in B cell growth phenotype reflect novel patterns of Epstein-Barr virus latent gene expression in Burkitt's lymphoma cells. The EMBO journal *6*, 2743-2751.

Salanti, A., Staalsoe, T., Lavstsen, T., Jensen, A.T., Sowa, M.P., Arnot, D.E., Hviid, L., and Theander, T.G. (2003). Selective upregulation of a single distinctly structured var gene in chondroitin sulphate A-adhering Plasmodium falciparum involved in pregnancy-associated malaria. Molecular microbiology *49*, 179-191.

Scherf, A., Hernandez-Rivas, R., Buffet, P., Bottius, E., Benatar, C., Pouvelle, B., Gysin, J., and Lanzer, M. (1998). Antigenic variation in malaria: in situ switching, relaxed and mutually exclusive transcription of var genes during intra-erythrocytic development in Plasmodium falciparum. The EMBO journal *17*, 5418-5426.

Seifert, M., Przekopowitz, M., Taudien, S., Lollies, A., Ronge, V., Drees, B., Lindemann, M., Hillen, U., Engler, H., Singer, B.B., *et al.* (2015). Functional capacities of human IgM memory B cells in early inflammatory responses and secondary germinal center reactions. Proceedings of the National Academy of Sciences of the United States of America *112*, E546-555.

Shaffer, A.L., 3rd, Young, R.M., and Staudt, L.M. (2012). Pathogenesis of human B cell lymphomas. Annual review of immunology *30*, 565-610.

Simone, O., Bejarano, M.T., Pierce, S.K., Antonaci, S., Wahlgren, M., Troye-Blomberg, M., and Donati, D. (2011). TLRs innate immunereceptors and Plasmodium falciparum erythrocyte membrane protein 1 (PfEMP1) CIDR1alpha-driven human polyclonal B-cell activation. Acta tropica *119*, 144-150.

Smith, J.D., Chitnis, C.E., Craig, A.G., Roberts, D.J., Hudson-Taylor, D.E., Peterson, D.S., Pinches, R., Newbold, C.I., and Miller, L.H. (1995). Switches in expression of Plasmodium falciparum var genes correlate with changes in antigenic and cytoadherent phenotypes of infected erythrocytes. Cell *82*, 101-110.

Snow, R.W., Guerra, C.A., Noor, A.M., Myint, H.Y., and Hay, S.I. (2005). The global distribution of clinical episodes of Plasmodium falciparum malaria. Nature *434*, 214-217.

Su, X.Z., Heatwole, V.M., Wertheimer, S.P., Guinet, F., Herrfeldt, J.A., Peterson, D.S., Ravetch, J.A., and Wellems, T.E. (1995). The large diverse gene family var encodes proteins involved in cytoadherence and antigenic variation of Plasmodium falciparum-infected erythrocytes. Cell *82*, 89-100.

Takizawa, M., Tolarova, H., Li, Z., Dubois, W., Lim, S., Callen, E., Franco, S., Mosaico, M., Feigenbaum, L., Alt, F.W., *et al.* (2008). AID expression levels determine the extent of cMyc oncogenic translocations and the incidence of B cell tumor development. The Journal of experimental medicine *205*, 1949-1957.

Thorley-Lawson, D.A. (2001). Epstein-Barr virus: exploiting the immune system. Nature reviews Immunology *1*, 75-82.

Thorley-Lawson, D.A., and Allday, M.J. (2008). The curious case of the tumour virus: 50 years of Burkitt's lymphoma. Nat Rev Micro *6*, 913-924.

Thorley-Lawson, D.A., and Gross, A. (2004). Persistence of the Epstein-Barr virus and the origins of associated lymphomas. The New England journal of medicine *350*, 1328-1337.

Torgbor, C., Awuah, P., Deitsch, K., Kalantari, P., Duca, K.A., and Thorley-Lawson, D.A. (2014). A multifactorial role for P. falciparum malaria in endemic Burkitt's lymphoma pathogenesis. PLoS pathogens *10*, e1004170.

Urban, B.C., Ferguson, D.J., Pain, A., Willcox, N., Plebanski, M., Austyn, J.M., and Roberts, D.J. (1999). Plasmodium falciparum-infected erythrocytes modulate the maturation of dendritic cells. Nature *400*, 73-77.

Urban, B.C., and Roberts, D.J. (2003). Inhibition of T cell function during malaria: implications for immunology and vaccinology. The Journal of experimental medicine *197*, 137-141.

Vereide, D.T., Seto, E., Chiu, Y.F., Hayes, M., Tagawa, T., Grundhoff, A., Hammerschmidt, W., and Sugden, B. (2014). Epstein-Barr virus maintains lymphomas via its miRNAs. Oncogene *33*, 1258-1264.

Westhoff Smith, D., and Sugden, B. (2013). Potential cellular functions of Epstein-Barr Nuclear Antigen 1 (EBNA1) of Epstein-Barr Virus. Viruses *5*, 226-240.

Whittle, H.C., Brown, J., Marsh, K., Greenwood, B.M., Seidelin, P., Tighe, H., and Wedderburn, L. (1984). T-cell control of Epstein-Barr virus-infected B cells is lost during P. falciparum malaria. Nature *312*, 449-450.

Wilmore, J.R., Asito, A.S., Wei, C., Piriou, E., Sumba, P.O., Sanz, I., and Rochford, R. (2015). AID expression in peripheral blood of children living in a malaria holoendemic region is associated with changes in B cell subsets and Epstein-Barr virus. International journal of cancer Journal international du cancer *136*, 1371-1380.

Wright, D.H. (1967). The epidemiology of Burkitt's tumor. Cancer research *27*, 2424-2438.

Wright, D.H. (1971). Burkitt's lymphoma: a review of the pathology, immunology, and possible etiologic factors. Pathology annual *6*, 337-363.

Wu, X., Darce, J.R., Chang, S.K., Nowakowski, G.S., and Jelinek, D.F. (2008). Alternative splicing regulates activation-induced cytidine deaminase (AID): implications for suppression of AID mutagenic activity in normal and malignant B cells. Blood *112*, 4675-4682.

Xu, Z., Pone, E.J., Al-Qahtani, A., Park, S.R., Zan, H., and Casali, P. (2007). Regulation of aicda expression and AID activity: relevance to somatic hypermutation and class switch DNA recombination. Critical reviews in immunology *27*, 367-397.

Yamane, A., Resch, W., Kuo, N., Kuchen, S., Li, Z., Sun, H.W., Robbiani, D.F., McBride, K., Nussenzweig, M.C., and Casellas, R. (2011). Deep-sequencing identification of the genomic targets of the cytidine deaminase AID and its cofactor RPA in B lymphocytes. Nature immunology *12*, 62-69.

Zindy, F., Eischen, C.M., Randle, D.H., Kamijo, T., Cleveland, J.L., Sherr, C.J., and Roussel, M.F. (1998). Myc signaling via the ARF tumor suppressor regulates p53-dependent apoptosis and immortalization. Genes & development *12*, 2424-2433.